

**Exploring the mode of action of novel antibacterial agents:  
Natural product antibiotics elansolids and peptide-conjugated  
daptomycin derivatives**

**Dissertation**  
zur Erlangung des Grades  
des Doktors der Naturwissenschaften  
der Naturwissenschaftlich-Technischen Fakultät  
der Universität des Saarlandes

von

**Sari Rasheed**

Saarbrücken

2022

Tag des Kolloquiums: 31. August 2022

Dekan: Prof. Dr. Jörn Eric Walter

Berichterstatter: Prof. Dr. Rolf Müller

Prof. Dr. Alexandra K. Kiemer

Vorsitz: Prof. Dr. Markus R. Meyer

Akad. Mitarbeiter: Dr. Michael Ring

Die vorliegende Arbeit wurde von November 2017 bis Januar 2022 unter Anleitung von Herrn Prof. Dr. Rolf Müller an Helmholtz-Institut für Pharmazeutische Forschung Saarland (HIPS) angefertigt.

## Acknowledgments

I would like to thank Prof. Dr. Rolf Müller for giving me the opportunity to join HIPS and be part of the team. I am thankful for his professional support and guidance.

I am also thankful for the supervision and valuable advice from Prof. Dr. Alexandra Kiemer.

I would like to extend my special thanks to Dr. Jennifer Herrmann for her assistance at every stage during my journey. Her experience and knowledge helped me improve at personal and professional level.

Furthermore, I would like to thank all the team members, colleagues, and friends at HIPS for their scientific and emotional support. Special thanks to Franziska Fries, Felix Deschner, Viktoria George, Anastasia Andreas, Yu Mi Park, Dr. Katarina Cirnski, Dr. Fabienne Hennessen, Janetta Coetzee, Timo Risch, Stefanie Neuber, Alexandra Amann, Dr. Asfandyar Sikandar, Dr. Emilia Oueis, Dr. Susanne Kirsch-Dahmen, Besnik Qallaku and Verena Qallaku.

I thank my family and friends for their continuous encouragement during my stay in Germany. Big thanks goes to my wife Lara for her motivation and patience throughout this journey.

Finally, I thank Laure, our daughter, for all the smiles during the stressful writing times.

## Abstract

The overuse and misuse of antibiotics, both, in clinical and agricultural setting is considered the most common cause of emergence of antimicrobial resistance (AMR). AMR represents a major threat to public health leading to life-threatening infections where the available treatments fail to cure and further leads to prolonged hospital stay and increase in healthcare costs. The alarming spread in resistance is unfortunately accompanied by a slow development of novel antibiotics. Nevertheless, different strategies are being established to deliver the next generation of antibiotics. Such strategies include natural product-guided drug discovery, synthetic development of antibiotics and improvement of efficacy of existing antibiotics by conjugation and employing combination therapy. The thesis work covers two important aspects in overcoming AMR; one focuses on biological evaluation, mode of resistance and mode of action elucidation, and characterization of a novel class of antibiotics produced by soil bacteria, the elansolids. The other focuses on structural modification of an already available antibiotic, daptomycin, by conjugation to a polycationic peptide, to compare its efficacy and study its effect in overcoming resistance *in vitro* and *in vivo*.

## **Zusammenfassung**

Der übermäßige und missbräuchliche Einsatz von Antibiotika, sowohl im klinischen Sektor als auch in der Landwirtschaft, gilt als häufigste Ursache für das Auftreten von Antibiotikaresistenzen (*antimicrobial resistance*, AMR). AMR stellt eine große Bedrohung für die öffentliche Gesundheit dar, indem sie zu lebensbedrohlichen Infektionen führt, die auf herkömmliche Behandlungen nicht mehr ansprechen. Dies wiederum führt zu verlängerten Krankenhausaufenthalten und höheren Kosten im Gesundheitswesen. Die besorgniserregende Ausbreitung von Resistenzen geht unglücklicherweise mit einer eher schleppenden Entwicklung neuer Antibiotika einher. Nichtsdestotrotz werden ständig neue Strategien erarbeitet, um neue Generationen von Antibiotika hervorzubringen. Diese Strategien umfassen insbesondere die Entdeckung von Wirkstoffen auf Grundlage von Naturstoffen, die synthetische Entwicklung von Antibiotika und die Optimierung der Wirksamkeit bestehender Antibiotika durch Konjugation- und Kombinationstherapie.

Diese Dissertation befasst sich mit zwei wichtigen Aspekten bei der Überwindung von AMR. Eine neue von Bodenbakterien stammende Antibiotikaklasse, die Elansolide, wird biologisch bewertet und ihr Resistenzmechanismus sowie ihre Wirkungsweise aufgeklärt. Ein weiterer Ansatz ist die strukturelle Veränderung des bereits verfügbaren Antibiotikums Daptomycin durch Konjugation mit einem polykationischen Peptid, mit dem Ziel die Wirksamkeit des Konjugats zu vergleichen und seine Wirkung bei der Überwindung von Antibiotikaresistenzen *in vitro* und *in vivo* untersuchen.

## Vorveröffentlichungen der Dissertation

Teile dieser Arbeit wurden vorab mit Genehmigung der Naturwissenschaftlich-Technischen Fakultät III, vertreten durch den Mentor der Arbeit, in folgenden Beiträgen veröffentlicht oder sind derzeit in Vorbereitung zur Veröffentlichung:

### Publications

Umstätter, F.<sup>†</sup>; **Rasheed, S.**<sup>†</sup>; Mühlberg, E.; HertleinT.; Domhan, C.; Klika, D.; Kleist, C.; Werner, J.; Zimmermann, S.; Müller, R.; Herrmann, J.; Mier W.; Uhl, P.

One Step Ahead of Bacteria: Daptomycin-Peptide Conjugates Acquire a Calcium-Independent Mechanism of Action. *Submitted manuscript.*

Megahed, S. H.<sup>†</sup>; **Rasheed, S.**<sup>†</sup>; Herrmann, J.; El-Hossary, E. M.; El-Shabrawy, Y. I.; Abadi, A. H.; Engel, M.; Müller, R.; Abdel-Halim, M.; Hamed, M. M.

Novel 2,4-Disubstituted Quinazoline Analogs as Antibacterial Agents with Improved Cytotoxicity Profile: Modification of the Benzenoid Part. *Bioorg. Med. Chem. Lett.* **2022**, 59, 128531. <https://doi.org/10.1016/j.bmcl.2022.128531>

Aboushady, D.<sup>†</sup>; **Rasheed, S.**<sup>†</sup>; Herrmann, J.; Maher, A.; El-Hossary, E. M.; Ibrahim, E. S.; Abadi, A. H.; Engel, M.; Müller, R.; Abdel-Halim, M.; Hamed, M.

M. Novel 2,4-Disubstituted Quinazoline Analogs as Antibacterial Agents with Improved Cytotoxicity Profile: Optimization of the 2,4-Substituents. *Bioorganic Chem.* **2021**, 117, 105422. <https://doi.org/10.1016/j.bioorg.2021.105422>

**Rasheed, S.**<sup>†</sup>; Fries, F.<sup>†</sup>; Müller, R.; Herrmann, J.

Zebrafish: An Attractive Model to Study *Staphylococcus aureus* Infection and Its Use as a Drug Discovery Tool. *Pharmaceuticals* **2021**, 14, 594. <https://doi.org/10.3390/ph14060594>

Frank, N. A.; Széles, M.; Akone, S. H.; **Rasheed, S.**; Hüttel, S.; Frewert, S.; Hamed, M. M.; Herrmann, J.; Schuler, S. M. M.; Hirsch, A. K. H.; Müller, R.

Expanding the Myxochelin Natural Product Family by Nicotinic Acid Containing Congeners. *Molecules* **2021**, 26, 4929. <https://doi.org/10.20944/preprints202107.0315.v1>

<sup>†</sup>Authors contributed equally to the work)

## Conference Contributions

**Rasheed, S.**; Fries, F.; Wilson, D.; Herrmann, J.; Müller, R. Elansolid A: Unique Antibiotic Targeting Small Ribosomal Subunit of *S. aureus*. **Poster Presentation**, 5<sup>th</sup> Interdisciplinary Course on Antibiotics and Resistance ICARe, October **2021**, Annecy, France.

**Rasheed, S.**; Herrmann, J.; Müller, R. Using Zebrafish as a Model for Tuberculosis to Test Potential Anti-Tubercular Natural Products. **Oral Presentation**, The International VAAM Workshop ‘Biology of Microorganisms Producing Natural Products’, September **2019**, Jena, Germany.

**Rasheed, S.**; Herrmann, J.; Cirnski, K.; Andreas, A.; Park, Y.; Müller, R. Using Zebrafish as an *in vivo* infection model to study the efficacy of novel antibacterial compounds. **Poster Presentation**, 7<sup>th</sup> Summer School on Infection Research of the HZI International Graduate School, May **2018**, Wernigerode, Germany.

**Rasheed, S.**; Herrmann, Andreas, A.; Park, Y.; Müller, R. Zebrafish as a Model in Anti-infective Drug Discovery at HIPS, **Poster Presentation**, HIPS 9<sup>th</sup> International Symposium, June 27-28, **2019**, Saarbrücken, Germany.

**Rasheed, S.**; Herrmann, J.; Müller, R. Zebrafish as a Model in Anti-infective Drug Discovery at HIPS, **Oral Presentation**, 8<sup>th</sup> Symposium of the Interdisciplinary Graduate School of Natural Products Research, July 25, **2019**, Saarbrücken, Germany.

## Table of Contents

<b>1</b>	<b>Introduction .....</b>	<b>1</b>
1.1	History of antibiotics .....	1
1.2	Mode of action of antibiotics and mechanisms of bacterial resistance .....	3
1.2.1	Antibiotics targeting the bacterial cell envelope .....	5
1.2.2	Antibiotics targeting DNA synthesis.....	7
1.2.3	Antibiotics targeting RNA synthesis.....	8
1.2.4	Antibiotics targeting protein synthesis.....	10
1.2.5	Antibiotics targeting folic acid metabolism .....	12
1.3	Approaches to overcome antimicrobial resistance .....	16
1.3.1	Overview of pre-clinical and clinical development of antibiotics.....	17
1.3.2	Natural-product-guided drug discovery.....	19
1.3.3	Antibiotics-conjugates drug development .....	20
1.4	Outline of the thesis.....	22
1.5	References .....	24
<b>2</b>	<b>Elansolid A2: A Unique Natural Product Antibiotic Targeting the Small Ribosomal Subunit and Inhibiting Translation in <i>S. aureus</i> .....</b>	<b>38</b>
2.1	Abstract .....	38
2.2	Introduction .....	39
2.3	Materials and Methods .....	43
2.3.1	Bacterial strains and antimicrobial susceptibility testing .....	43
2.3.2	Killing kinetics of elansolid A2 in <i>S. aureus</i> .....	43
2.3.3	Mutant generation and characterization .....	44
	Whole genome sequencing .....	44
	Mutation reversibility and mutant growth kinetics .....	45
	Assessment of metabolic activity with isothermal microcalorimetry .....	45
	Cross-resistance with reference antibiotics .....	46
	Checkerboard assay.....	46
	Surface Plasmon Resonance SPR .....	47
2.4	Results .....	49
2.4.1	Antimicrobial susceptibility testing.....	49
2.4.2	Killing kinetics of elansolid A2 in <i>S. aureus</i> .....	51
2.4.3	Mutant generation and characterization.....	52
	Whole genome sequence analysis .....	53
	Mutant growth kinetics .....	56
	Assessment of metabolic activity with isothermal microcalorimetry .....	58
	Cross-resistance studies with reference antibiotics.....	62

Checkerboard assay to study synergism of elansolid A2.....	63
Surface Plasmon Resonance SPR .....	64
2.5 Discussion .....	66
2.6 Conclusion.....	71
2.7 References .....	73
<b>3 Daptomycin-Peptide-Chimera are Active Against Multi-Resistant Pathogens and Acquire a Calcium-Independent Mechanism of Action.....</b>	<b>79</b>
3.1 Abstract .....	79
3.2 Introduction .....	80
3.3 Materials and Methods .....	88
3.3.1 Peptide synthesis .....	88
3.3.2 Daptomycin-conjugate synthesis.....	88
3.3.3 NMR studies.....	88
3.3.4 Ca <sup>2+</sup> ion-induced micelle formation by NMR .....	89
3.3.5 Bacterial strains and growth conditions .....	89
3.3.6 Antimicrobial susceptibility testing .....	89
3.3.7 Maximum tolerated concentration (MTC) in zebrafish embryos/larvae .....	90
3.3.8 Time-kill curves (TKC) and cell lysis monitoring .....	90
3.3.9 Measurement of total ATP over time .....	91
3.3.10 Scanning Electron Microscopy (SEM) .....	91
Sample preparation and fixation .....	91
Imaging .....	91
3.3.11 Bacterial membrane potential.....	92
3.3.12 In-vivo efficacy in zebrafish-DRSA model .....	92
3.4 Results .....	94
3.4.1 Peptide and daptomycin-conjugate synthesis.....	94
3.4.2 Antimicrobial susceptibility testing .....	95
3.4.3 MIC determination at different calcium concentrations .....	96
3.4.4 In vitro and in vivo toxicity assessment .....	99
3.4.5 Time-kill curves (TKC) and cell lysis monitoring .....	101
3.4.6 Measurement of total ATP over time .....	103
3.4.7 Scanning Electron Microscopy (SEM) .....	103
3.4.8 Bacterial membrane potential.....	104
3.4.9 In vivo efficacy in zebrafish-DRSA model .....	106
3.5 Discussion .....	108
3.6 Conclusion.....	112

3.7 Acknowledgements .....	112
3.8 Supplementary information.....	113
3.8.1 Antimicrobial susceptibility testing.....	113
3.8.2 In-vivo toxicity in zebrafish .....	114
3.9 References .....	115
<b>4 General Discussion and Conclusion.....</b>	<b>120</b>
4.1 Natural product antibiotics addressing unique targets .....	120
4.2 Modification of existing antibiotic classes to overcome AMR .....	123
4.3 Conclusion.....	125
4.4 References .....	127

## Chapter 1

### 1 Introduction

#### 1.1 History of antibiotics

Already thousands of years ago, moldy bread and soil have been reported in ancient civilizations as remedies<sup>1</sup>. In 1941, Selman Waksman then used the term ‘antibiotic’ to refer to any ‘small molecule made by a microbe to antagonize the growth of other microbes’<sup>2,3</sup>. The history of antibiotics started with salvarsan (arsphenamine or Ehrlich 606), that was the first synthetic antibiotic introduced by Paul Ehrlich in 1910<sup>4</sup>. The antibiotic was widely used until the 1940s and was known as the ‘magic bullet’ for the treatment of *Treponema pallidum*, the causative agent of syphilis<sup>5,6</sup>. Following the work of Ehrlich on the effect of dyes on bacterial staining, Gerhard Domagk and his colleagues discovered the sulfonamide prodrug prontosil in the year 1932<sup>2,5,7</sup>. The prodrug was tested in a murine model and cured infections with *Streptococcus pyogenes*<sup>5,7</sup>. The true turning point in history was with the discovery of penicillin in 1928 by Alexander Fleming, who noticed that the growth of *Staphylococcus aureus* on old culture plates was inhibited by the presence of a contaminating fungus<sup>8</sup>. Fourteen years later, the groundbreaking work by Howard Florey, Norman Heatley and Ernst Chain, led to the description, production, purification, and experimental use of penicillin<sup>8,9</sup>. And by the end of 1943, mass production of penicillin began in several countries where it was made available for public use<sup>9</sup>. The discovery of penicillin did not only change the course of medicine, but also had a tremendous effect during World War II, where thousands of wounded soldiers were treated<sup>10</sup>. The discovery of penicillin inspired Selman Waksman who investigated the impact of different bacterial species on each other as well as the production of antimicrobial compounds from soil bacteria<sup>11</sup>. Between 1940 and 1960, the work of Waksman initiated the ‘Golden Age’ of antibiotic discovery where various antibiotics produced by soil-dwelling

actinomycetes, including neomycin and streptomycin, that was used for the treatment of tuberculosis<sup>2,11</sup>. It is useful to note that more than 90% of antibiotics in clinical practice originate from the actinomycetes<sup>12</sup>. The increasing interest in studying soil bacteria led to the isolation of vancomycin from *Streptomyces orientalis* in 1952, however, its clinical use was soon abandoned in favor of other antibiotics that were more effective and less toxic<sup>13,14</sup>. Related to vancomycin, teicoplanin was isolated from *Actinoplanes teichomyceticus*, and belongs to the new glycopeptides class<sup>15</sup>. Following the discovery of penicillin, the  $\beta$ -lactam antibiotics, cephalosporins were discovered and developed in the 1960s, though, the work that led to their identification dates back to 1945 by Giuseppe Brotzu who isolated a fungus, *Cephalosporium acremonium* from sewer water in Sardinia, Italy<sup>5,13,16,17</sup>. Carbapenems represent another example of  $\beta$ -lactam antimicrobials derived from thienamycin, an antibiotic produced by the soil organism *Streptomyces cattleya*<sup>13,18</sup>. In the early 1980s, daptomycin was isolated from the soil bacterium *Streptomyces roseosporus*, by researchers at Eli Lilly, however, its development was halted at phase II due to skeletal muscle toxicity<sup>19</sup>. Daptomycin was approved by the Food and Drug Administration (FDA) in 2003 for the treatment of complex skin infections<sup>19–21</sup>. In the meantime, and due to the alarming resistance especially in Gram-negative pathogens, as well as the reduced drug development investments, old drugs have been reinvestigated. Colistin (polymyxin E) is one of the first antibiotics with significant activity against *Pseudomonas aeruginosa*, however, it was replaced by aminoglycosides in the 1970s because of neurotoxicity and nephrotoxicity<sup>22</sup>. In addition to discovering new  $\beta$ -lactamase inhibitors, an approach to combine an existing  $\beta$ -lactamase inhibitor together with an antibiotic has been developed. A timeline of antibiotic discovery is summarized in **Figure 1**.

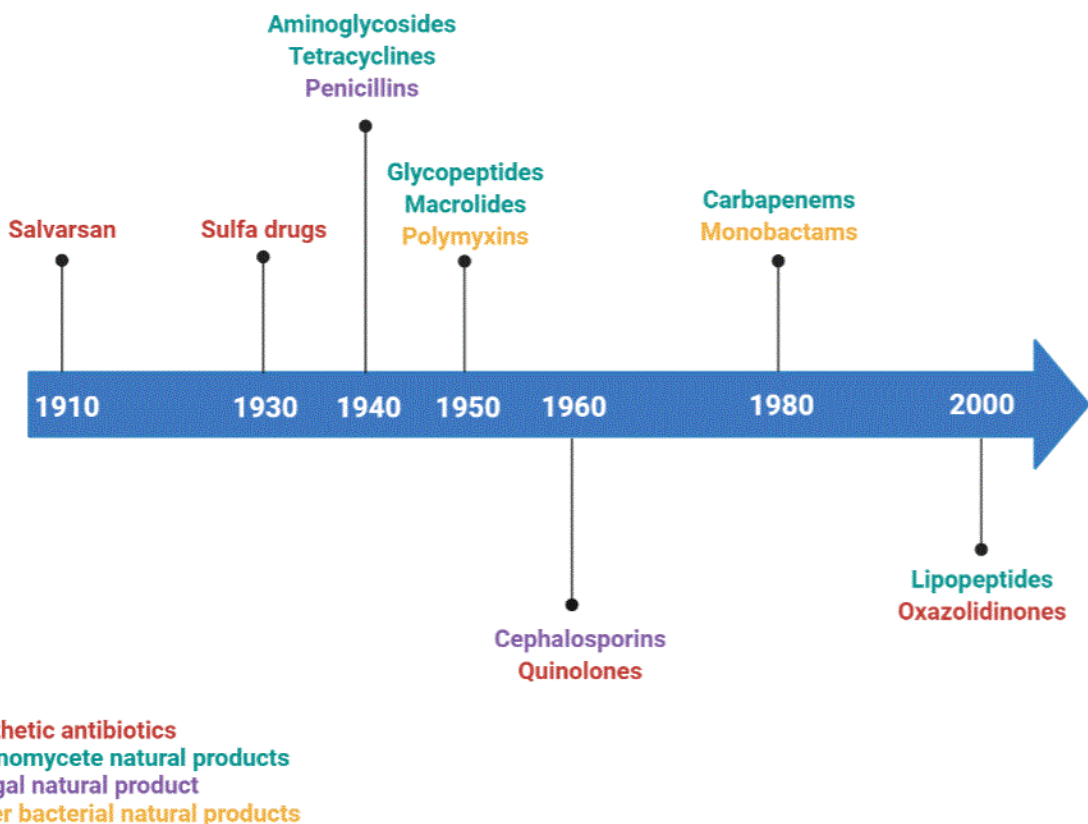


Figure 1: Discovery timeline of antibiotic classes

## 1.2 Mode of action of antibiotics and mechanisms of bacterial resistance

The introduction of antibiotics to treat infectious diseases has revolutionized the practice of medicine in the 20<sup>th</sup> century<sup>2</sup>. However, the misuse of these important compounds has resulted in the rapid development of antimicrobial resistance (AMR) presenting a major challenge in healthcare units, often resulting in treatment failure and increased mortality rates<sup>23,24</sup>.

Antibiotics exert their effect by targeting essential bacterial functions, systems, or cellular components, and can be classified based on their molecular structures, mode of action and spectrum of activity<sup>25</sup>. They can be also classified according to whether they kill cells (bactericidal drugs) or inhibit their growth (bacteriostatic drugs) and their route of administration (injection, oral or topical)<sup>24</sup>. Due to the extensive use of antibiotics, bacteria have gained several mechanisms to overcome the antibiotic effect and gain resistance. These mechanisms include decreased accumulation of antibiotics by reduced permeability or induced

efflux, antibiotic inactivation by modifying enzymes, target modification and acquisition of target by-pass systems<sup>26</sup>. In this chapter, antibiotic classification based on their mode of action as well as the main resistance mechanisms to antibiotic classes are discussed and summarized in **Figure 2** and **Table 1** respectively.

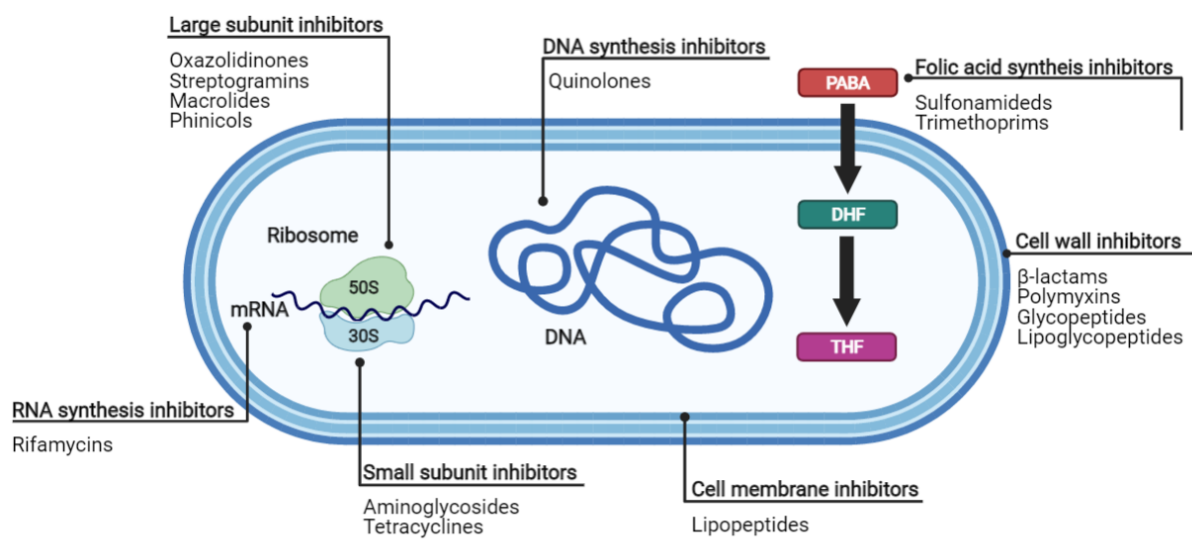


**Figure 2: Mechanism of action of major antibiotic classes targeting cell wall, cell membrane, replication, transcription, translation, and folic acid synthesis.**

### 1.2.1 Antibiotics targeting the bacterial cell envelope

Bacterial cells are surrounded by a cell wall made of peptidoglycan that provides strength and rigidity to the bacterial cell to withstand the high internal osmotic pressure. Gram-positive bacteria are usually enclosed by a thick peptidoglycan cell wall, in contrast, Gram-negative bacteria are surrounded by an additional outer membrane (OM)<sup>27</sup>. The outer leaflet of the outer membrane bilayer is composed of lipopolysaccharide (LPS) that prevents penetration by lipophilic antibiotics<sup>27,28</sup>.

Beta-lactams ( $\beta$ -lactams) and glycopeptides are antibiotic classes that interfere with cell wall synthesis.  $\beta$ -lactams (penicillin, cephalosporins and carbapenems) target penicillin binding proteins (PBPs) and block the cross-linking (transpeptidation) of peptidoglycan building blocks by penicilloylation of the PBP active site, which eventually leads to lysis of the cell<sup>29,30</sup>. The most effective mechanism of resistance among Gram-negative bacteria to  $\beta$ -lactams is via production of  $\beta$ -lactamases that hydrolyze the  $\beta$ -lactam ring.  $\beta$ -lactamases contain either serine residues (Ambler classes<sup>31</sup> A, C, D) and or metal ion (Zinc) (Ambler class B) in their active site<sup>31,32</sup>. Ambler class A enzymes are also referred as penicillinases and cause resistance to penicillins and third generation cephalosporins (e.g. ceftazidime, cefotaxime, ceftriaxone) and are inhibited by commercially available  $\beta$ -lactamase inhibitors (BLIs) such as clavulanic acid, sulbactam, or tazobactam<sup>33-35</sup>. Ambler class B  $\beta$ -lactamase are known as metallo- $\beta$ -lactamases (MBLs) and require zinc or heavy metals for catalysis. New Delhi MBL (NDM) are the most recently described carbapenemases and they were first reported in a *Klebsiella pneumoniae* isolate (NDM-1)<sup>36</sup>. Class C  $\beta$ -lactamases, also called cephalosporinases, include AmpC  $\beta$ -lactamases (AmpCs), and class D  $\beta$ -lactamases are oxacillin hydrolyzing enzymes (oxacillinases) that confer resistance to penicillin, cloxacillin, oxacillin, and methicillin<sup>37-39</sup>. Additional resistance mechanisms to  $\beta$ -lactam antibiotics include mutations in the target penicillin binding protein or active efflux of the drug out of the cell and modifications in cell wall porins that limit entry of drugs into the cell<sup>26</sup>.

Glycopeptides (e.g., vancomycin) and lipoglycopeptides (e.g., teicoplanin) inhibit peptidoglycan synthesis by binding to the D-alanyl-D-alanyl (D-Ala) dipeptide. This interaction inhibits the transglycosylation and/or transpeptidation steps of peptidoglycan synthesis. By inhibiting peptidoglycan maturation, glycopeptides weaken the peptidoglycan layers and make the bacterial cells prone to lysis<sup>40</sup>. Resistance to glycopeptides arises due to the synthesis of a modified precursor instead of D-Ala-D-Ala, that displays a decreased affinity for vancomycin and teicoplanin<sup>41,42</sup>. Eight acquired glycopeptide resistance types have been described in enterococci (VanA, VanB, VanD, VanE, VanG, VanL, VanM, and VanN) and one type of intrinsic resistance (VanC) in *E. gallinarum* and *E. casseliflavus*<sup>43</sup>. Change in the precursor to D-Ala-D-lactate (D-Lac) observed in VanA, VanB, VanD and VanM types, causes a high fold decrease in affinity for vancomycin, and a change to D-Ala-D-serine (D-Ser) reported in VanC, VanE, VanG, VanL and VanN causes lower levels of vancomycin resistance<sup>43-45</sup>. VanA is the most frequently observed type of resistance and is responsible for most of the human cases of VRE around the world<sup>46</sup>. The first vancomycin intermediate *S. aureus* (VISA) strain was reported in Japan in 1996<sup>47</sup>. Mutations in genes responsible for the biosynthesis of bacterial cell wall and/or mutations in the ribosomal gene *rpoB* are the most common genetic alterations associated with the VISA phenotype<sup>47,48</sup>.

Daptomycin is a lipopeptide that has an unique mode of action in interfering with the bacterial cell membrane<sup>21</sup>. The antibiotic complexes with calcium ions, binds and inserts itself into the cytoplasmic membrane and disrupts it, leading to the efflux of potassium and magnesium ions causing membrane depolarization and ultimately cell death<sup>49</sup>. Recent studies show that daptomycin interferes with fluid lipid microdomains, leading to delocalization of essential peripheral membrane proteins, such as the lipid II synthase MurG<sup>50,51</sup>. Several resistance mechanisms to overcome daptomycin have been proposed. The most common one involves the modification of the cell surface charge leading to the electrostatic ‘repulsion’ of the positively charged daptomycin-Ca<sup>2+</sup> complex from the cell membrane. Such mechanism has been

postulated in *Bacillus subtilis*, *Staphylococcus aureus*, and *Enterococcus faecium*<sup>52</sup>. Another resistance mechanism reported only in *Enterococcus faecalis*, known as ‘diversion’, involves changes in the membrane composition that leads to the diversion of the daptomycin from its binding site at the septum of bacterial cells<sup>53</sup>.

Polymyxins are cationic agents that bind to bacterial outer membrane with high affinity for the lipid moiety of lipopolysaccharide (LPS), leading to the disruption of membrane integrity<sup>54</sup>. The most important mechanism of resistance to polymyxins includes alterations of the bacterial outer membrane. Modification of lipid A phosphates in the lipopolysaccharide (LPS) moiety decreases surface negative charge and therefore reduces polymyxin binding to the modified membrane<sup>55</sup>.

### 1.2.2 Antibiotics targeting DNA synthesis

DNA replication is a rapid and highly accurate process that ensures the transmission of genetic instructions. Replication is divided into three steps: initiation, elongation, and termination, and is aided by many proteins and enzymes. Initiation occurs at specific nucleotide sequence called the origin of replication during which DNA gyrase (topoisomerase II) introduces superhelical twists in the bacterial DNA double-helix catalyzing the separation of daughter chromosomes. During elongation, the addition of nucleotides occurs, and new DNA strands are synthesized by DNA polymerase III. Once the complete chromosome has been replicated, termination of replication occurs. Following replication, the resulting complete, interconnected circular chromosomes are separated by topoisomerase IV, which introduces double-stranded breaks allowing separation into two daughter cells. Bacterial DNA gyrase and topoisomerase IV are distinctive from their eukaryotic counterparts, thus they serve as targets for quinolones<sup>56-58</sup>.

Quinolones antibiotics are active against both Gram-positive and Gram-negative bacteria and inhibit bacterial DNA synthesis through disrupting the enzymes topoisomerase IV and DNA gyrase<sup>59</sup>. The primary target is DNA gyrase in Gram-negative bacteria and generally

topoisomerase IV is the target in Gram-positive bacteria<sup>60</sup>. Fluoroquinolones (e.g., ciprofloxacin and ofloxacin) show a broader spectrum of activity and improved pharmacokinetics compared to the first-generation quinolones, and they inhibit bacterial growth by interacting with the enzyme-bound DNA complex to create conformational changes that lead to the inhibition of enzyme activity and ultimately resulting in rapid bacterial cell death<sup>61,62</sup>. Target modification, decreased permeability and increase in efflux activity are among the mechanisms of resistance to fluoroquinolones. The main resistance mechanism in all bacterial species has been associated with mutation in the *gyrA* or *gyrB* genes; the genes that encode for the two subunits of DNA gyrase<sup>63,64</sup>. Furthermore, resistance to quinolones can be due to under-expression of porins and over-expression of efflux pumps. This is achieved by mutation in multiple antibiotic resistance (*mar*) gene that leads to both over-expression of the AcrAB efflux pump and reduced expression of OmpF (outer membrane protein F) porin<sup>65</sup>. Another gene that contributes to resistance against quinolones is the *nfxB* gene, which causes alterations in expression of functional OmpF at the cell surface<sup>66,67</sup>.

### 1.2.3 Antibiotics targeting RNA synthesis

Transcription is divided into three main steps: initiation, elongation, and termination, and is mediated by DNA-dependent RNA polymerase (RNAP)<sup>68</sup>. The core enzyme consisting of five conserved subunits ( $\alpha_2\beta\beta'\omega$ ) is unable to recognize specific promoter sequences and initiate transcription, without assembly with one of several transcription factors, sigma ( $\sigma$ ) to form RNAP holoenzyme ( $\alpha_2\beta\beta'\omega\sigma$ )<sup>69,70</sup>. Transcription is initiated by the complex formation between the holoenzyme and the double-stranded DNA (dsDNA) sequence at the promoter region, followed by the unwinding of a short region of DNA within the RNAP-bound sequence. The polymerase will then incorporate ribonucleotides and forms phosphodiester bond between them. At this stage the  $\sigma$  factor dissociates and the RNAP undergoes global conformational change and departs from the promoter to resume elongation<sup>71,72</sup>. During elongation, the RNAP can transcribe DNA over long distances (>10,000 bp) without dissociation and release of RNA

product<sup>68</sup>. Finally, RNAP encounters a termination signal of RNA stem-loop “hairpin” followed by a segment of 8 to 10 nucleotides that encodes mostly uridine residues at the end of the released RNA<sup>73</sup>. This causes the release of the nascent transcript and the dissociation of the RNAP from the DNA template<sup>68,73</sup>. RNAP is vital for bacterial survival, and because it is distinct from its eukaryotic counterparts, it is an attractive target for antibiotics.

Drugs targeting RNAP can either disrupt its interactions with DNA, RNA or ribonucleoside triphosphates (NTPs) (e.g., rifamycins, sorangicin, microcin, myxopyronins, corallopyronin, ripostatin and squaramides), interfere with the movement of RNAP mobile elements during nucleotide addition cycle (NAC) (e.g., streptolydigin and salinamide), or disrupt RNAP interactions with the transcription factors<sup>74</sup>. The rifamycin antibacterial agents (e.g., rifampin, rifapentine, rifabutin, and rifamixin) and sorangicin bind with high affinity to DNA-bound RNAP and prevent extension of RNA strands RNAP and inhibit it<sup>75</sup>. Microcin prevents NTP uptake, thereby inhibiting abortive initiation and elongation. Myxopyronins, corallopyronin, ripostatin and squaramides prevent the  $\beta'$  clamp from opening, stabilize the  $\beta'$  clamp regions in a partly or fully closed conformation, and prevent template DNA from reaching the active site<sup>76-79</sup>. The predominant mode of resistance to rifamycins in *Mycobacterium tuberculosis* arises from mutations in the gene that encodes for RNA polymerase subunit  $\beta$  (*rpoB*) that result in a decreased affinity of the enzyme to the antibiotic<sup>80-82</sup>. Such mutations result in a decreased affinity of the enzyme to the antibiotic. Further studies hypothesized that resistance is due to the inactivation mechanism (ribosylation) of rifampicin observed in *Mycobacterium smegmatis* and efflux has been reported in *Mycobacterium smegmatis* and *Mycobacterium aurum*<sup>83,84</sup>.

### 1.2.4 Antibiotics targeting protein synthesis

The ribosome is a highly abundant and conserved macromolecular-protein synthesis machinery in the cell<sup>85</sup>. Bacterial 70S ribosome is composed of two highly conserved unequal ribonucleoprotein particles: small (30S) and large (50S) subunits<sup>86</sup>. The small ribosomal subunit decodes the genetic information from messenger RNA (mRNA) and the large subunit hosts the catalytic peptidyl transferase center (PTC), where amino acids attached to transfer RNAs (tRNAs) are linked into polypeptides<sup>85,86</sup>. Aided by several translation factors, the ribosome hosts protein synthesis consisting of initiation, elongation, termination and recycling<sup>87</sup>. Initiation requires the assembly of 70S ribosome with the initiator tRNA and start codon of the mRNA at the P-site, followed by elongation which involves the delivery of the aa-tRNA to the A-site by the assist of elongation factor Tu (EF-Tu) and the base-pairing between mRNA and tRNA, this allows the subsequent peptide bond formation to occur between the growing amino acids, later tRNA translocate from P-to E-site and from A-to P-site. Termination occurs when one of the stop codons (UAA, UAG or UGA) is encountered and are recognized by termination release factors (RF1 and RF2) that hydrolyze the peptidyl-tRNA bound to the P site and release the polypeptide chain from the ribosome. After ribosome disassembly, recycling of the components for the next round of initiation occurs<sup>88-92</sup>. Due to its importance in cell functions and since it is distinct from the eukaryotic counterpart, the ribosome and protein translation represent an attractive target for antibiotics.

Inhibitors of 30S ribosomal subunit include aminoglycosides and tetracyclines. Aminoglycosides (e.g., spectinomycin, neomycin B, gentamicin, paromomycin and kanamycin) bind to the small subunit causing the disruption of mRNA-decoding fidelity of the ribosome which, in turn, introduces mistakes during protein synthesis ultimately leading to the accumulation of miscoded proteins<sup>93</sup>. Bacterial resistance to aminoglycosides is challenging due to the large number and diversity of modifying enzymes. Three classes of modifying enzymes have been reported, and these include: aminoglycoside phosphotransferase (APH),

aminoglycoside acetyltransferases (AAC) and aminoglycoside nucleotidyltransferases (ANT)<sup>94</sup>. Spectinomycin is an aminoglycoside that impairs the movement of the small subunit head leading to the disruption in tRNA translocation. Tetracyclines cross the outer membrane of Gram-negative bacteria through the OmpF and OmpC porin channels and block the accumulation of aminoacyl-tRNA to the ribosome<sup>95-97</sup>. Resistance to tetracyclines is due to efflux, ribosomal protection proteins (RPPs), and enzymatic inactivation of the antibiotic. Tetracycline efflux proteins (Tet proteins) share amino acid structure with other efflux proteins involved in chloramphenicol and quinolone resistance<sup>97,98</sup>. RPPs bind to the ribosome, modifying its conformation, and thus, preventing tetracycline from binding to its target, thus releasing the ribosome from the inhibitory effects of the drug so that protein synthesis can proceed<sup>99,100</sup>. An additional mechanism of tetracycline resistance was reported in *E. coli* only when cells are growing aerobically, involves the *tetX* gene encoding a cytoplasmic protein which detoxifies tetracycline<sup>101,102</sup>.

Inhibitors of 50S ribosomal subunit include phenicols, macrolides, oxazolidinones and streptogramins. Phenicols (e.g., chloramphenicol) block the catalytic portion of the peptidyl transferase center, thus preventing binding of tRNA to the ribosome<sup>103</sup>. Chloramphenicol resistance is mainly due to the inactivation of the antibiotic by the enzyme chloramphenicol acetyltransferase (CAT) that converts it successively to 3-acetyl and 1,3-diacetyl derivatives<sup>104,105</sup>. Nonenzymatic chloramphenicol resistance has been observed in Gram-negative bacteria such as *Pseudomonas aeruginosa* and in members of *Enterobacteriaceae*. Such alternative mechanisms involve increased membrane permeability and porin deficiency that prevents the entry of the drug to the bacterial cell<sup>106,107</sup>. Macrolides (e.g., erythromycin) inhibit translation by blocking the progression of the peptide chain and interfere with the formation of long polypeptides, which causes a premature detachment of incomplete peptide chains from the ribosome<sup>103,108</sup>. The first mechanism of macrolide resistance described in *Escherichia coli* was due to posttranscriptional modification of the 23S rRNA by an adenine-

specific *N*-methyltransferase specified by a class of genes termed *erm* (erythromycin ribosome methylation)<sup>109,110</sup>. Recently, resistance by efflux was found to be clinically significant for Gram-positive and Gram-negative pathogens. The genes of efflux pumps can be either acquired, such as macrolide efflux gene (*mef*) encoded in *S. pneumoniae* and *S. pyogenes* by *mefE* and *mefA*, respectively, or carried intrinsically by macrolide-specific ABC-type efflux carrier (*macAB*) in *E. coli*<sup>111,112</sup>. Oxazolidinones (e.g., linezolid) bind to the 50S subunit, preventing complex formation with the 30S subunit and they block assembly of a functional translation initiation complex<sup>113,114</sup>. Most common resistance mechanism to linezolid is mediated by amplification of the 23S rRNA gene region corresponding to the peptidyl transferase site<sup>115</sup>. Another mechanism of resistance to linezolid based on nucleotide mutations for genes encoding for ribosomal proteins *rplC* (L3) and *rplD* (L4) has been reported in enterococci<sup>116</sup>. Streptogramins consist of 2 types of components: A and B, both of which inhibit the elongation step of translation. Streptogramin B shows a similar mode of action as macrolides, whereas streptogramin A blocks aminoacyl-tRNA (AA-tRNA) binding to the A site of ribosomes and peptide bond formation with peptidyl-tRNA (pep-tRNA) at the P site<sup>117</sup>. Both streptogramin groups act synergistically *in vivo*<sup>85</sup>. Resistance to streptogramin B components is due to either enzymatic modification of the drug (hydrolysis of the depsipeptidic ring), antibiotic efflux or modification of the target (methylation of the 23S rRNA). Acquired resistance to streptogramin A components is due to either antibiotic efflux or inactivation of the drug (acetylation of the hydroxyl group)<sup>118-121</sup>.

### 1.2.5 Antibiotics targeting folic acid metabolism

Many microorganisms possess the ability to synthesize folic acid derivatives de novo, initially forming dihydrofolate<sup>122</sup>. The folate biosynthesis in bacteria starts with the synthesis of the pterin ring, which is catalyzed by GTP cyclohydrolase I (GTPCHI), followed by the transfers of the pyrophosphate from ATP to DHMP catalyzed by 7,8-hydroxymethyl-7,8-dihydropterin pyrophosphokinase (HPPK), which produce 6-hydroxymethyl-7,8-dihydropterin

pyrophosphate (DHPPP). The latter is the substrate of dihydropteroate synthase (DHPS), that further performs the condensation with pABA to produce 7,8-dihydropteroate. Dihydrofolate synthase (DHFS) and folylpoly- $\gamma$ -glutamate synthetase (FPGS) add glutamates to the 7,8-dihydropteroate, producing dihydrofolate and its derivatives. The last step of the pathway is catalyzed by dihydrofolate reductase (DHFR), which catalyzes the reduction of dihydrofolate to tetrahydrofolate using NADPH as a cofactor<sup>123</sup>.

DHFR and DHPS are the most studied enzyme of the folate pathway<sup>123</sup>. Sulfonamides inhibit dihydropteroate synthase (DHPS) by competing with the natural substrate *p*-amino-benzoic acid and trimethoprim acts at a later stage of folic acid synthesis and inhibits the enzyme dihydrofolate reductase (DHFR) by competing with its normal substrate, dihydrofolate<sup>124–126</sup>. Since trimethoprim targets a later step in the same enzymic pathway as sulfonamides, they act synergistically, and has been successfully developed in the combination drug co-trimoxazole<sup>124</sup>. A variety of resistance mechanisms responsible for either intrinsic or acquired resistance to trimethoprim, sulfonamides, or trimethoprim-sulfonamide combinations have been studied. Bacterial resistance mechanisms to trimethoprim involve low cell permeability/efflux, alternative metabolic pathways (bacteria lose their ability to synthesize thymidylate and can circumvent the need for DHFR by using exogenous thymidine), production of a resistant chromosomal DHFR enzyme, overproduction of a chromosomal DHR (with low affinity to trimethoprim), and production of a plasmid-mediated resistant DHFR enzyme<sup>125–127</sup>. Bacterial resistance to sulfonamides is due to low cell permeability/efflux, production of insensitive DHPS enzyme (with low affinity to sulfonamide), over production of DHPS natural substrate *p*-aminobenzoic acid (competes with sulfonamides to the enzyme active site) and plasmid-mediated production of additional sulfonamide-resistant DHPS enzyme<sup>123–125,127</sup>. Resistance to the combination of trimethoprim-sulfonamide has developed rapidly, although the relevance of such resistance to the combined agents is less than that of each drug alone<sup>128</sup>.

**Table 1: Resistance mechanisms of various antibiotics**

<b>Target</b>	<b>Antibiotic class</b>	<b>Resistance type</b>	<b>Resistance mechanism</b>
Cell wall	Beta-lactams	Inactivating enzymes	Production of $\beta$ -lactamases that hydrolyze the $\beta$ -lactam ring
		Target modification	Mutations in the target penicillin binding protein (PBP)
		Decreased uptake/efflux pumps	Acquisition of new PBPs with decreased affinity for the drug Active efflux of the drug out of the cell and modifications in cell wall porins
	Glycopeptides	Target modification	Synthesis of D-Ala-D-Lac/-Ser instead of D-Ala-D-Ala
	Polymyxins	Target modification	Modification of lipid A phosphates in lipopolysaccharide (LPS) moiety
Cell membrane	Lipopeptide	Target modification	Modification of the cell surface charge leading to the electrostatic repulsion of daptomycin from the cell membrane Changes in the membrane composition via the alteration of membrane metabolism
DNA synthesis	Quinolones	Target modification	Mutation in the genes that encode for DNA gyrase ( <i>gyrA</i> or <i>gyrB</i> ) Mutations in topoisomerase IV
		Decreased uptake/efflux pumps	Down regulation of the expression of outer membrane protein F (OmpF) Overexpression of the AcrAB multidrug efflux pump
RNA synthesis	Rifamycins	Target modification Inactivating enzymes Efflux pumps	Mutations in the gene that encodes for RNA polymerase subunit $\beta$ ( <i>rpoB</i> ) inactivation of rifampicin by ribosylation

Protein synthesis	Aminoglycosides	Inactivating enzymes	Production of modifying enzymes (phosphotransferase, acetyltransferases and nucleotidyltransferase)
	Tetracyclines	Target modification	Production of ribosomal protection proteins (RPPs) which prevents tetracycline from binding
		Efflux pumps	Synthesis of tetracycline efflux proteins (Tet proteins)
		Inactivating enzymes	Expression of gene <i>TetX</i> encoding a cytoplasmic protein which detoxifies tetracycline (reported in <i>E. coli</i> )
	Phenicols	Inactivating enzymes	Synthesis of chloramphenicol acetyltransferase (CAT) which inactivates the antibiotic
		Decreased uptake	Porin deficiency
	Macrolides	Target modification	Posttranscriptional modification of the 23S rRNA
		Efflux pump	Macrolide efflux gene ( <i>mef</i> ) and macrolide-specific ABC-type efflux carrier ( <i>macAB</i> )
	Oxazolidinones	Target modification	Amplification of the 23S rRNA gene region
	Streptogramins	Inactivating enzymes	Acetylation of the hydroxyl group of streptogramin A
		Target modification	Hydrolysis of the depsipeptidic ring of streptogramin B
			Methylation of the 23S rRNA (streptogramin B)
Folic acid synthesis	Trimethoprim	Target by-pass	Loss of ability to synthesize thymidylate and circumvent the need for DHFR by using exogenous thymidine
		Target modification	Production of resistant chromosomal DHFR enzyme
		Decreased uptake/efflux pumps	
	Sulfonamide	Target by-pass	Over production of <i>p</i> -aminobenzoic acid that competes with sulfonamides to the DHPS
		Target modification	Production of insensitive DHPS enzyme
		Decreased uptake/efflux pumps	

### 1.3 Approaches to overcome antimicrobial resistance

The global emergence of antimicrobial-resistant pathogens has alarmingly escalated, leading to life-threatening infections, where the available treatments will fail to cure. According to the World Health Organization (WHO) priority pathogen list (summarized in **Table 2**), twelve species of bacteria are resistant to almost all available antibiotics<sup>129</sup>. This alarming spread in resistance is unfortunately accompanied by a slow development of novel antibiotics, however, different strategies with a well-constructed roadmap are being investigated to deliver the next generation of antibiotics<sup>130</sup>. Such strategies include (but are not limited to) natural product-guided drug discovery, synthetic development of antibiotics and improvement of efficacy of existing antibiotics by conjugation and combination. In this chapter, an overview of most recent reports on antibiotics discovery pipeline from WHO and Pew Charitable Trusts is summarized, and a focus on strategies as well as discoveries from recent literature is presented.

**Table 2: WHO priority pathogens list<sup>131</sup>**

**Priority 1: Critical**

*Acinetobacter baumannii*, carbapenem resistant

*Pseudomonas aeruginosa*, carbapenem-resistant

*Enterobacteriaceae*, carbapenem-resistant, third generation cephalosporin-resistant

**Priority 2: High**

*Enterococcus faecium*, vancomycin-resistant

*Staphylococcus aureus*, methicillin-resistant (MRSA), vancomycin-intermediate and -resistant (VISA-VRSA)

*Helicobacter pylori*, clarithromycin-resistant

*Campylobacter* spp., fluoroquinolone-resistant

*Salmonella* spp., fluoroquinolone-resistant

*Neisseria gonorrhoeae*, third generation cephalosporin-resistant, fluoroquinolone-resistant

**Priority 3: Medium**

*Streptococcus pneumoniae*, penicillin-non-susceptible

*Haemophilus influenzae*, ampicillin-resistant

*Shigella* spp., fluoroquinolone-resistant

### 1.3.1 Overview of pre-clinical and clinical development of antibiotics

In 2019, WHO published a global review of the preclinical antibacterial pipeline, based on publicly available data mainly collected through a WHO data call on 252 agents in preclinical development from 145 institutions worldwide. From the total reported agents, 83% (n = 209) are direct-acting curative treating agents, including 69% (n = 144) small and 31% (n = 65) large molecules. Most agents (19.8%) in the preclinical pipeline target cell wall synthesis (22% are  $\beta$ -lactam/ $\beta$ -lactamase inhibitor combinations), followed by those that have direct membrane effect (14.3%), and protein synthesis (8.3%)<sup>129</sup>. In summary, the pre-clinical pipeline shows a number of innovative and diverse compounds. However, it would require a long period of time to reach the market, as they are still in very early stages of development. Additionally, the number of candidates in the preclinical pipeline is inadequate to provide the needed innovative therapeutics for WHO priority pathogens list. There is a need for a large size of preclinical pipeline to ensure that a few will eventually reach the market. Moreover, there is a very few agents in development that target critical Gram-negative bacteria that present the most critical priority. Thus, it is vital to further invest in the discovery and development of new antibacterial treatments that overcome the challenge of drug-resistant bacterial infections.

Another report by WHO in 2019 indicated that there are 50 antibiotics in the clinical pipeline. Only 64% of them (n = 32) target the WHO priority pathogens, 37.5% of which (n = 12) have activity against at least one of the critical Gram-negative pathogens. In summary, most of the agents in the clinical pipeline are derivatives of existing classes and less innovative than the ones in pre-clinical pipeline. On the other hand, the anti-tuberculosis and *Clostridium difficile* antibacterial clinical pipeline is more innovative than that of the WHO priority pathogens<sup>132</sup>. Given the fact that only a small fraction of approved antibiotics over the past few years represents new compound classes, there is a crucial need for development of new therapeutic agents with innovative chemistry and novel modes of action<sup>130</sup>.

According to the Pew Charitable Trusts, there are around 43 new potential antibiotics in clinical development for the US market as of December 2020<sup>133</sup>. Of these antibiotics in development, 35% are in phase I clinical trials, 30% in phase II and phase III, and 5% has new drug applications. Majority (62%) of the submitted candidates belong to known NP classes and the rest (38%) are synthetic. At least 44% of the antibiotics in clinical development target infections caused by Gram-negative ESKAPE pathogens (*Klebsiella pneumoniae*, *Acinetobacter baumannii*, *Pseudomonas aeruginosa* and *Enterobacter* spp.) and at least 35% of the candidates have potential activity against carbapenem-resistant/extended spectrum  $\beta$ -lactamase (ESBL)-producing Enterobacteriaceae, *A. baumannii*, and *P. aeruginosa*<sup>2,133–135</sup>.

In the WHO report of antibacterial agents in preclinical development, most of the projects were led by commercial institutions, followed by academic institutions and foundations, where 93% of the commercial institutions are small and medium-sized<sup>129</sup>. Similarly, the Pew Charitable Trusts data showed that over 95% of the products in development are explored by small companies, where more than 70% are considered pre-revenue companies (have no products on the market that they previously developed, commercialized, and marketed)<sup>134</sup>. Such numbers show that large pharmaceutical companies show no or little interest in funding early antibiotic research and, particularly, new classes of compounds, which is due to the low return on investment in this area of early stage drug discovery<sup>129,130</sup>. Additionally, developing entirely new scaffolds is more costly than for derivatives of established classes. In order to ensure a dynamic and collaborative discovery pipeline, efforts are needed to bridge the gap between academia and industry to exchange skills and expertise in order to transform hits into potential drug products<sup>130</sup>. Another challenge is the limited funding especially for small and medium-sized enterprises<sup>130,136</sup>.

### 1.3.2 Natural-product-guided drug discovery

In the search for new antimicrobial agents and anti-infective drugs, natural products (NPs) represent the best hope for the generation of such novel agents. NPs comprise a large family of distinct, novel, complex and diverse chemical entities that originate from bacterial, fungal, plant, and marine sources<sup>137</sup>. Ever since the discovery of penicillin, more than 23,000 NPs have been characterized, most of which were produced by the family *Actinomycetaceae*, specifically, most of them (75%) were produced by a single genus, *Streptomyces*<sup>136,137</sup>. Around 50 % of drugs that were newly introduced into the market between 1985 and 2005 were NPs or NP-inspired products (NP-derivatives, semi-synthetic, synthetic compounds based on NP pharmacophores)<sup>136,138</sup>. More recently, in 2013 around 40% of the total NCEs approved by the US Food and Drug administration (FDA) were NP or NP-related compounds<sup>139</sup>. Furthermore, in a recent review, a total of 163 antibacterial agents were approved between 1981 and 2019, 55% of which were unaltered NP or NP derivatives and 22% were synthetic<sup>138</sup>.

A promising number of novel NPs are currently under investigation in preclinical studies. Some examples are discussed hereafter. Odilorhabdins (ODLs) represent a new class of modified peptide antibiotics produced by the enzymes of the non-ribosomal peptide synthetase (NRPS) gene cluster of the nematode-symbiotic bacterium *Xenorhabdus nematophila*<sup>140</sup>. ODLs demonstrated *in vitro* and *in vivo* activity against several Gram-positive and Gram-negative bacterial pathogens, including carbapenem-resistant *Enterobacteriaceae* (CRE). Mode of action studies showed that ODLs interacts with the 16S rRNA and with the anticodon loop of the A-site tRNA in the small ribosomal subunit<sup>140</sup>. Cystobactamids are novel class of NPs isolated from *Cystobacter* sp. and demonstrated a strong inhibitory effect against several Gram-positive and Gram-negative pathogens especially against *E. coli* and *A. baumannii*<sup>141</sup>. The molecular targets of cystobactamids were identified as bacterial type topoisomerases type IIA, namely DNA gyrase and topoisomerase IV<sup>141,142</sup>. Another interesting NP compound is Corallopyronin, obtained from myxobacterial strain *Corallococcus coralloides*, that targets

DNA-dependent RNA polymerase (RNAP) of Gram-positive bacteria, including rifampicin-resistant *S. aureus*<sup>143,144</sup>. Streptomyces-derived griseimycins represent an important example of drug discovery from soil bacteria. The antibiotic showed a superb activity against *M. tuberculosis*, both *in vitro* and *in vivo*, by inhibiting the DNA polymerase sliding clamp DnaN<sup>145</sup>. The examples presented above shows that NPs remain the best source for discovering novel compounds with novel and unique targets that can lead to effective agents to fight pathogens and overcome antimicrobial resistance. Such discovery has been evolving over the past decades aided by major advances in the field, as development of analytical methods, target-based approaches, combinatorial chemistry, genetic engineering, bioinformatics, transcriptomics, proteomics, and metabolomics<sup>137</sup>.

### 1.3.3 Antibiotics-conjugates drug development

The development of new classes of antibiotics from natural products is time and money consuming and accompanied with commercial risks, therefore, new strategies to improve the antibacterial efficacy of existing antibiotics and to overcome their toxic effects have been implemented. Antibiotic conjugation aims at addressing difficult-to-treat bacterial infections, such as intracellular infections. Antibiotics-peptide conjugates (APCs) typically contain an antibiotic, a linker, and a peptide, that would enhance uptake, distribution, metabolism and reduce cytotoxicity, and hemolysis<sup>146,147</sup>. Among the most prominent and successful examples of antibiotic conjugation strategies, are those with iron(III)-chelators, known as siderophores<sup>148,149</sup>. Bacteria secret siderophores to solubilize and import iron from the extracellular environment, as well as from competing organisms. Studies have shown that siderophore–antibiotic conjugates can be actively transported into the bacterial cell using siderophore iron uptake pathways, an approach termed the ‘Trojan horse’<sup>150</sup>. Cefiderocol (Fetroja®, Fetcroja®) is the first siderophore cephalosporin approved for the treatment of Gram-negative bacterial infections, including complicated urinary tract infections (cUTIs), hospital-acquired pneumonia (HAP) and ventilator-acquired pneumonia (VAP)<sup>151</sup>. Cefiderocol is active

against all four Ambler classes of  $\beta$ -lactamases and exhibits superb activity against many Gram-negative pathogens, including multidrug resistant strains<sup>152</sup>. Another conjugation strategy includes the linkage of antibiotics to antimicrobial peptides (AMPs), which are a membrane-active peptides belonging to a novel class of antimicrobials<sup>153</sup>. AMPs have been conjugated to antibiotics such as vancomycin, levofloxacin, chloramphenicol and neomycin, in order to increase their antibacterial efficacy<sup>154–157</sup>. Unlike AMP, cell-penetrating peptides (CPPs) have been studied as a technique to reach intracellular targets, infiltrating them without lysing<sup>158</sup>. CCPs can be either co-administered with antibiotics such as vancomycin, amoxicillin and norfloxacin, or conjugated to them<sup>159</sup>. CCP-vancomycin conjugates have been recently studied to treat intracellular vancomycin-resistant *S. aureus* and enterococci, and kanamycin conjugated to CCP demonstrated an interesting *in vitro* activity in clearing of intracellular *Mycobacterium tuberculosis* within macrophages and significant *in vivo* reduction of *Salmonella* in the *Caenorhabditis elegans* model<sup>160,161</sup>. Further promising examples include antibody–antibiotic conjugation (AAC) which has proven useful in the treatment of intracellular infections. An example of such conjugation is that of an anti-*Staphylococcus aureus* antibody conjugated to dmDNA31 (4-dimethylamino piperidino-hydroxybenzoxazino rifamycin) targeting intracellular *S. aureus*, has now completed phase I clinical trials<sup>158,162</sup>. In another antibody-antibiotic conjugation example to target *P. aeruginosa*, an antibody was linked to several photosensitizers which release singlet oxygen and trigger death in nearby cells, upon irradiation with light<sup>163</sup>. Many other novel conjugates have been explored including host defense peptides (HDPs), which are small cationic peptides that constitute the nonspecific innate immune system,<sup>164,165</sup>. More recently, polycationic peptides (e.g. hexa-arginine) were conjugated to vancomycin and the most active conjugate showed a 1000-fold increased antimicrobial activity, and preliminary data showed a distinct mode of action from cell wall inhibition<sup>166</sup>.

## 1.4 Outline of the thesis

The thesis work is divided into two parts, both describing the characterizing antibacterial modes-of-action of two distinct compound classes overcoming AMR. The first part covers the in-depth characterization of the antibiotic activity of the bacterial natural product elansolid A2 and provide insights into its target and mode-of-resistance in *S. aureus*. The second part describes the conjugation of daptomycin to a polycationic peptide, studies its activity, and compares it to daptomycin.

Elansolids biosynthetically belong to the group of type I *trans*-polyketides and comprise a group of secondary metabolites isolated as two atropisomers A1 and A2 from the gliding bacterium *Chitinophaga sancti*<sup>167</sup>. The two-atropisomeric elansolids differ in their biological activity, where elansolid A2 shows antibiotic activity against Gram-positive bacteria, while elansolid A1 is weakly active. The focus of this project is to study the biological activity of elansolid A2 on a broad panel of bacteria and to discover its mode of action as well as its mode of resistance in *S. aureus* by generating mutants, characterizing them, and exploring the genes involved in resistance by whole genome sequencing. Target validation will be carried out by several molecular and biophysical assays.

Modifications of existing drugs represent a strategy to shorten the drug development process and enhance the antibacterial efficiency of antibiotics. Previous studies with vancomycin conjugation to polycationic peptide revealed that such an approach is feasible to obtain highly active derivatives<sup>166</sup>. Daptomycin, the first-in-class cyclic lipopeptide antibiotic, is primarily used for the treatment of vancomycin-resistant *Enterococcus* spp. (VRE) and Methicillin-resistant *S. aureus* (MRSA)<sup>168</sup>. Daptomycin-conjugated to various peptide sequences differing in net charge obtained by solid phase peptide synthesis by our collaborators. The aim of this project was to assess the activity of the conjugates on daptomycin sensitive and resistant *S. aureus* strains (DSSA and DRSA), study the structure-activity relationship (SAR) of the

novel conjugates, and characterize and compare the lead conjugate DAP-R6 to daptomycin *in vitro* and *in vivo*. Scanning electron microscopy (SEM) is carried out to differentiate the cell morphology of daptomycin- and conjugate-treated bacteria.

## 1.5 References

- (1) Haas, L. F. Papyrus of Ebers and Smith. *Journal of Neurology, Neurosurgery & Psychiatry* **1999**, *67* (5), 578–578. <https://doi.org/10.1136/jnnp.67.5.578>.
- (2) Hutchings, M. I.; Truman, A. W.; Wilkinson, B. Antibiotics: Past, Present and Future. *Current Opinion in Microbiology* **2019**, *51*, 72–80. <https://doi.org/10.1016/j.mib.2019.10.008>.
- (3) Clardy, J.; Fischbach, M.; Currie, C. The Natural History of Antibiotics. *Curr Biol* **2009**, *19* (11), R437–R441. <https://doi.org/10.1016/j.cub.2009.04.001>.
- (4) Lloyd, N. C.; Morgan, H. W.; Nicholson, B. K.; Ronimus, R. S. The Composition of Ehrlich's Salvarsan: Resolution of a Century-Old Debate. *Angewandte Chemie International Edition* **2005**, *44* (6), 941–944. <https://doi.org/10.1002/anie.200461471>.
- (5) Zaffiri, L.; Gardner, J.; Toledo-Pereyra, L. H. History of Antibiotics. From Salvarsan to Cephalosporins. *Journal of Investigative Surgery* **2012**, *25* (2), 67–77. <https://doi.org/10.3109/08941939.2012.664099>.
- (6) Riethmiller, S. From Atoxyl to Salvarsan: Searching for the Magic Bullet. *Chemotherapy* **2005**, *51* (5), 234–242. <https://doi.org/10.1159/000087453>.
- (7) Iyer, H. V. History Revisited—Prontosil Red. *The Journal of Emergency Medicine* **2008**, *35* (2), 209–210. <https://doi.org/10.1016/j.jemermed.2007.07.064>.
- (8) Gaynes, R. The Discovery of Penicillin—New Insights After More Than 75 Years of Clinical Use. *Emerg Infect Dis* **2017**, *23* (5), 849–853. <https://doi.org/10.3201/eid2305.161556>.
- (9) Chain, E.; Florey, H. W.; Gardner, A. D.; Heatley, N. G.; Jennings, M. A.; Orr-Ewing, J.; Sanders, A. G. PENICILLIN AS A CHEMOTHERAPEUTIC AGENT. *The Lancet* **1940**, *236* (6104), 226–228. <https://doi.org/10.5555/uri:pii:S0140673601087281>.
- (10) Alexander Fleming Discovery and Development of Penicillin - Landmark <https://www.acs.org/content/acs/en/education/whatischemistry/landmarks/flemingpenicillin.html> (accessed 2021-12-29).
- (11) Waksman, S. A.; Schatz, A.; Reynolds, D. M. Production of Antibiotic Substances by Actinomycetes\*†. *Annals of the New York Academy of Sciences* **2010**, *1213* (1), 112–124. <https://doi.org/10.1111/j.1749-6632.2010.05861.x>.
- (12) Martens, E.; Demain, A. L. The Antibiotic Resistance Crisis, with a Focus on the United States. *J Antimicrob Chemotherapy* **2017**, *70* (5), 520–526. <https://doi.org/10.1038/ja.2017.30>.
- (13) Gould, K. Antibiotics: From Prehistory to the Present Day. *Journal of Antimicrobial Chemotherapy* **2016**, *71* (3), 572–575. <https://doi.org/10.1093/jac/dkv484>.
- (14) Levine, D. P. Vancomycin: A History. *Clinical Infectious Diseases* **2006**, *42* (Supplement\_1), S5–S12. <https://doi.org/10.1086/491709>.
- (15) Greenwood, D. Microbiological Properties of Teicoplanin. *Journal of Antimicrobial Chemotherapy* **1988**, *21* (suppl\_A), 1–13. [https://doi.org/10.1093/jac/21.suppl\\_A.1](https://doi.org/10.1093/jac/21.suppl_A.1).
- (16) Abraham, E. P. Cephalosporins 1945–1986. *Drugs* **1987**, *34* (2), 1–14. <https://doi.org/10.2165/00003495-198700342-00003>.
- (17) Drawz, S. M.; Bonomo, R. A. Three Decades of  $\beta$ -Lactamase Inhibitors. *Clinical Microbiology Reviews* **2010**, *23* (1), 160–201. <https://doi.org/10.1128/CMR.00037-09>.
- (18) Doi, Y.; Chambers, H. F. 22 Other  $\beta$ -Lactam Antibiotics. 1.
- (19) Tally, F. P.; Zeckel, M.; Wasilewski, M. M.; Carini, C.; Berman, C. L.; Drusano, G. L.; Oleson JR, F. B. Daptomycin: A Novel Agent for Gram-Positive Infections. *Expert Opinion on Investigational Drugs* **1999**, *8* (8), 1223–1238. <https://doi.org/10.1517/13543784.8.8.1223>.
- (20) Eisenstein, B. I.; Oleson, F. B., Jr; Baltz, R. H. Daptomycin: From the Mountain to the Clinic, with Essential Help from Francis Tally, MD. *Clinical Infectious Diseases* **2010**, *50* (Supplement\_1), S10–S15. <https://doi.org/10.1086/647938>.

(21) Tedesco, K. L.; Rybak, M. J. Daptomycin. *Pharmacotherapy: The Journal of Human Pharmacology and Drug Therapy* **2004**, *24* (1), 41–57. <https://doi.org/10.1592/phco.24.1.41.34802>.

(22) Nation, R. L.; Li, J. Colistin in the 21st Century. *Curr Opin Infect Dis* **2009**, *22* (6), 535–543. <https://doi.org/10.1097/QCO.0b013e328332e672>.

(23) Tenover, F. C. Mechanisms of Antimicrobial Resistance in Bacteria. *The American Journal of Medicine* **2006**, *119* (6, Supplement 1), S3–S10. <https://doi.org/10.1016/j.amjmed.2006.03.011>.

(24) Prescott, J. F. The Resistance Tsunami, Antimicrobial Stewardship, and the Golden Age of Microbiology. *Veterinary Microbiology* **2014**, *171* (3–4), 273–278. <https://doi.org/10.1016/j.vetmic.2014.02.035>.

(25) Etebu, E.; Arikekpar, I. Antibiotics: Classification and Mechanisms of Action with Emphasis on Molecular Perspectives. *12*.

(26) Sefton, A. M. Mechanisms of Antimicrobial Resistance. *Drugs* **2002**, *62* (4), 557–566. <https://doi.org/10.2165/00003495-200262040-00001>.

(27) Nikaido, H. Prevention of Drug Access to Bacterial Targets: Permeability Barriers and Active Efflux. *Science* **1994**, *264* (5157), 382–388. <https://doi.org/10.1126/science.8153625>.

(28) Kimura, K.; Bugg, T. D. H. Recent Advances in Antimicrobial Nucleoside Antibiotics Targeting Cell Wall Biosynthesis. *Nat. Prod. Rep.* **2003**, *20* (2), 252–273. <https://doi.org/10.1039/b202149h>.

(29) Penicillins and Cephalosporins Are Active Site-Directed Acylating Agents: Evidence in Support of the Substrate Analogue Hypothesis. *Phil. Trans. R. Soc. Lond. B* **1980**, *289* (1036), 257–271. <https://doi.org/10.1098/rstb.1980.0044>.

(30) Tomasz, A. The Mechanism of the Irreversible Antimicrobial Effects of Penicillins: How the Beta-Lactam Antibiotics Kill and Lyse Bacteria. *Annu. Rev. Microbiol.* **1979**, *33* (1), 113–137. <https://doi.org/10.1146/annurev.mi.33.100179.000553>.

(31) Ambler, R. P.; Baddiley, J.; Abraham, E. P. The Structure of  $\beta$ -Lactamases. *Philosophical Transactions of the Royal Society of London. B, Biological Sciences* **1980**, *289* (1036), 321–331. <https://doi.org/10.1098/rstb.1980.0049>.

(32) Garau, G.; Bebrone, C.; Anne, C.; Galleni, M.; Frère, J.-M.; Dideberg, O. A Metallo- $\beta$ -Lactamase Enzyme in Action: Crystal Structures of the Monozinc Carbapenemase CphA and Its Complex with Biapenem. *Journal of Molecular Biology* **2005**, *345* (4), 785–795. <https://doi.org/10.1016/j.jmb.2004.10.070>.

(33) Bonnet, R. Growing Group of Extended-Spectrum  $\beta$ -Lactamases: The CTX-M Enzymes. *Antimicrob Agents Chemother* **2004**, *48* (1), 1–14. <https://doi.org/10.1128/AAC.48.1.1-14.2004>.

(34) Shamsuddin, I.; Shawai, S. A. MOJDDT-03-00080. *2019*. <https://doi.org/10.15406/mojddt.2019.03.00080>.

(35) Papp-Wallace, K. M.; Bethel, C. R.; Distler, A. M.; Kasuboski, C.; Taracila, M.; Bonomo, R. A. Inhibitor Resistance in the KPC-2  $\beta$ -Lactamase, a Preeminent Property of This Class A  $\beta$ -Lactamase. *Antimicrobial Agents and Chemotherapy* **2010**, *54* (2), 890–897. <https://doi.org/10.1128/AAC.00693-09>.

(36) Yong, D.; Toleman, M. A.; Giske, C. G.; Cho, H. S.; Sundman, K.; Lee, K.; Walsh, T. R. Characterization of a New Metallo- $\beta$ -Lactamase Gene, BlaNDM-1, and a Novel Erythromycin Esterase Gene Carried on a Unique Genetic Structure in *Klebsiella pneumoniae* Sequence Type 14 from India. *Antimicrobial Agents and Chemotherapy* **2009**, *53* (12), 5046–5054. <https://doi.org/10.1128/AAC.00774-09>.

(37) Chia, J. H.; Siu, L. K.; Su, L. H.; Lin, H. S.; Kuo, A. J.; Lee, M. H.; Wu, T. L. Emergence of Carbapenem-Resistant *Escherichia Coli* in Taiwan: Resistance Due to Combined

CMY-2 Production and Porin Deficiency. *Journal of Chemotherapy* **2009**, *21* (6), 621–626. <https://doi.org/10.1179/joc.2009.21.6.621>.

(38) Medeiros, A. A.; Cohenford, M.; Jacoby, G. A. Five Novel Plasmid-Determined Beta-Lactamases. *Antimicrobial Agents and Chemotherapy* **1985**, *27* (5), 715–719. <https://doi.org/10.1128/AAC.27.5.715>.

(39) Naas, T.; Nordmann, P. OXA-Type -Lactamases. *Current pharmaceutical design* **1999**, *5*, 865–880.

(40) Kahne, D.; Leimkuhler, C.; Lu, W.; Walsh, C. Glycopeptide and Lipoglycopeptide Antibiotics. *Chem. Rev.* **2005**, *105* (2), 425–448. <https://doi.org/10.1021/cr030103a>.

(41) Mc Dermott, P. F.; Walker, R. D.; White, D. G. Antimicrobials: Modes of Action and Mechanisms of Resistance. *Int J Toxicol* **2003**, *22* (2), 135–143. <https://doi.org/10.1080/10915810305089>.

(42) Leclercq, R.; Courvalin, P. Resistance to Glycopeptides in Enterococci. *Clinical Infectious Diseases* **1997**, *24* (4), 545–554.

(43) Vancomycin Resistance in Gram-Positive Cocci | Clinical Infectious Diseases | Oxford Academic [https://academic.oup.com/cid/article/42/Supplement\\_1/S25/275393?login=true](https://academic.oup.com/cid/article/42/Supplement_1/S25/275393?login=true) (accessed 2021 -12 -30).

(44) Boyd, D. A.; Willey, B. M.; Fawcett, D.; Gillani, N.; Mulvey, M. R. Molecular Characterization of Enterococcus Faecalis N06-0364 with Low-Level Vancomycin Resistance Harboring a Novel d-Ala-d-Ser Gene Cluster, VanL. *Antimicrobial Agents and Chemotherapy* **2008**. <https://doi.org/10.1128/AAC.01516-07>.

(45) O'Driscoll, T.; Crank, C. W. Vancomycin-Resistant Enterococcal Infections: Epidemiology, Clinical Manifestations, and Optimal Management. *Infect Drug Resist* **2015**, *8*, 217–230. <https://doi.org/10.2147/IDR.S54125>.

(46) Schouten, M. A.; Willems, R. J. L.; Kraak, W. A. G.; Top, J.; Hoogkamp-Korstanje, J. A. A.; Voss, A. Molecular Analysis of Tn1546-Like Elements in Vancomycin-Resistant Enterococci Isolated from Patients in Europe Shows Geographic Transposon Type Clustering. *Antimicrobial Agents and Chemotherapy* **2001**, *45* (3), 986–989. <https://doi.org/10.1128/AAC.45.3.986-989.2001>.

(47) Hiramatsu, K.; Hanakia, H.; Inob, T.; Yabutab, K.; Oguric, T.; Tenoverd, F. C. Journal of Antimicrobial Chemotherapy (1997) *40*, 135–146 Methicillin-Resistant Staphylococcus Aureus.

(48) Gardete, S.; Tomasz, A. Mechanisms of Vancomycin Resistance in *Staphylococcus Aureus*. *J Clin Invest* **2014**, *124* (7), 2836–2840. <https://doi.org/10.1172/JCI68834>.

(49) Silverman, J. A.; Perlmutter, N. G.; Shapiro, H. M. Correlation of Daptomycin Bactericidal Activity and Membrane Depolarization in *Staphylococcus Aureus*. *Antimicrobial Agents and Chemotherapy* **2003**, *47* (8), 2538–2544. <https://doi.org/10.1128/AAC.47.8.2538-2544.2003>.

(50) Müller, A.; Wenzel, M.; Strahl, H.; Grein, F.; Saaki, T. N. V.; Kohl, B.; Siersma, T.; Bandow, J. E.; Sahl, H.-G.; Schneider, T.; Hamoen, L. W. Daptomycin Inhibits Cell Envelope Synthesis by Interfering with Fluid Membrane Microdomains. *PNAS* **2016**, *113* (45), E7077–E7086. <https://doi.org/10.1073/pnas.1611173113>.

(51) Grein, F.; Müller, A.; Scherer, K. M.; Liu, X.; Ludwig, K. C.; Klöckner, A.; Strach, M.; Sahl, H.-G.; Kubitscheck, U.; Schneider, T. Ca2+-Daptomycin Targets Cell Wall Biosynthesis by Forming a Tripartite Complex with Undecaprenyl-Coupled Intermediates and Membrane Lipids. *Nat Commun* **2020**, *11* (1), 1455. <https://doi.org/10.1038/s41467-020-15257-1>.

(52) Tran, T. T.; Munita, J. M.; Arias, C. A. Mechanisms of Drug Resistance: Daptomycin Resistance. *Ann N Y Acad Sci* **2015**, *1354*, 32–53. <https://doi.org/10.1111/nyas.12948>.

(53) Tran, T. T.; Panesso, D.; Mishra, N. N.; Mileykovskaya, E.; Guan, Z.; Munita, J. M.; Reyes, J.; Diaz, L.; Weinstock, G. M.; Murray, B. E.; Shamoo, Y.; Dowhan, W.; Bayer, A. S.; Arias, C. A. Daptomycin-Resistant *Enterococcus Faecalis* Diverts the Antibiotic Molecule from the Division Septum and Remodels Cell Membrane Phospholipids. *mBio* **4** (4), e00281-13. <https://doi.org/10.1128/mBio.00281-13>.

(54) Landman, D.; Georgescu, C.; Martin, D. A.; Quale, J. Polymyxins Revisited. *Clinical Microbiology Reviews* **2008**, *21* (3), 449–465. <https://doi.org/10.1128/CMR.00006-08>.

(55) Kline, T.; Trent, M. S.; Stead, C. M.; Lee, M. S.; Sousa, M. C.; Felise, H. B.; Nguyen, H. V.; Miller, S. I. Synthesis of and Evaluation of Lipid A Modification by 4-Substituted 4-Deoxy Arabinose Analogs as Potential Inhibitors of Bacterial Polymyxin Resistance. *Bioorganic & Medicinal Chemistry Letters* **2008**, *18* (4), 1507–1510. <https://doi.org/10.1016/j.bmcl.2007.12.061>.

(56) Trojanowski, D.; Hołówka, J.; Zakrzewska-Czerwińska, J. Where and When Bacterial Chromosome Replication Starts: A Single Cell Perspective. *Frontiers in Microbiology* **2018**, *9*, 2819. <https://doi.org/10.3389/fmicb.2018.02819>.

(57) Gross, J. D. DNA Replication in Bacteria With 6 Figures. In *Current Topics in Microbiology and Immunology*; Arber, W., Braun, W., Haas, R., Henle, W., Hofsneider, P. H., Jerne, N. K., Koldovský, P., Koprowski, H., Maaløe, O., Rott, R., Schweiger, H. G., Sela, M., Syruček, L., Vogt, P. K., Wecker, E., Eds.; Current Topics in Microbiology and Immunology; Springer: Berlin, Heidelberg, 1972; pp 39–74. [https://doi.org/10.1007/978-3-642-65297-4\\_2](https://doi.org/10.1007/978-3-642-65297-4_2).

(58) Oakley, A. J. A Structural View of Bacterial DNA Replication. *Protein Science* **2019**, *28* (6), 990–1004. <https://doi.org/10.1002/pro.3615>.

(59) M. Pham, T. D.; M. Ziora, Z.; T. Blaskovich, M. A. Quinolone Antibiotics. *MedChemComm* **2019**, *10* (10), 1719–1739. <https://doi.org/10.1039/C9MD00120D>.

(60) Cheng, G.; Hao, H.; Dai, M.; Liu, Z.; Yuan, Z. Antibacterial Action of Quinolones: From Target to Network. *European Journal of Medicinal Chemistry* **2013**, *66*, 555–562. <https://doi.org/10.1016/j.ejmech.2013.01.057>.

(61) Blondeau, J. M. Fluoroquinolones: Mechanism of Action, Classification, and Development of Resistance. *Survey of Ophthalmology* **2004**, *49* (2, Supplement 2), S73–S78. <https://doi.org/10.1016/j.survophthal.2004.01.005>.

(62) Kampranis, S. C.; Maxwell, A. Conformational Changes in DNA Gyrase Revealed by Limited Proteolysis \*. *Journal of Biological Chemistry* **1998**, *273* (35), 22606–22614. <https://doi.org/10.1074/jbc.273.35.22606>.

(63) Neu, H. C. Bacterial Resistance to Fluoroquinolones. *Reviews of Infectious Diseases* **1988**, *10* (Supplement\_1), S57–S63. [https://doi.org/10.1093/clinids/10.Supplement\\_1.S57](https://doi.org/10.1093/clinids/10.Supplement_1.S57).

(64) Acar, J. F.; Goldstein, F. W. Trends in Bacterial Resistance to Fluoroquinolones. *Clinical Infectious Diseases* **1997**, *24* (Supplement\_1), S67–S73. [https://doi.org/10.1093/clinids/24.Supplement\\_1.S67](https://doi.org/10.1093/clinids/24.Supplement_1.S67).

(65) Goldman, J. D.; White, D. G.; Levy, S. B. Multiple Antibiotic Resistance (Mar) Locus Protects *Escherichia Coli* from Rapid Cell Killing by Fluoroquinolones. *Antimicrobial Agents and Chemotherapy* **1996**. <https://doi.org/10.1128/AAC.40.5.1266>.

(66) Hooper, D. C.; Wolfson, J. S.; Souza, K. S.; Tung, C.; McHugh, G. L.; Swartz, M. N. Genetic and Biochemical Characterization of Norfloxacin Resistance in *Escherichia Coli*. *Antimicrobial Agents and Chemotherapy* **1986**. <https://doi.org/10.1128/AAC.29.4.639>.

(67) Correia, S.; Poeta, P.; Hébraud, M.; Capelo, J. L.; Igrelas, G. 2017. Mechanisms of Quinolone Action and Resistance: Where Do We Stand? *Journal of Medical Microbiology* **66** (5), 551–559. <https://doi.org/10.1099/jmm.0.000475>.

(68) Lee, J.; Borukhov, S. Bacterial RNA Polymerase-DNA Interaction—The Driving Force of Gene Expression and the Target for Drug Action. *Frontiers in Molecular Biosciences* **2016**, *3*, 73. <https://doi.org/10.3389/fmolb.2016.00073>.

(69) Murakami, K. S.; Darst, S. A. Bacterial RNA Polymerases: The Whole Story. *Current Opinion in Structural Biology* **2003**, *13* (1), 31–39. [https://doi.org/10.1016/S0959-440X\(02\)00005-2](https://doi.org/10.1016/S0959-440X(02)00005-2).

(70) Decker, K. B.; Hinton, D. M. Transcription Regulation at the Core: Similarities Among Bacterial, Archaeal, and Eukaryotic RNA Polymerases. *Annual Review of Microbiology* **2013**, *67* (1), 113–139. <https://doi.org/10.1146/annurev-micro-092412-155756>.

(71) Saecker, R. M.; Record, M. T.; deHaseth, P. L. Mechanism of Bacterial Transcription Initiation: RNA Polymerase - Promoter Binding, Isomerization to Initiation-Competent Open Complexes, and Initiation of RNA Synthesis. *Journal of Molecular Biology* **2011**, *412* (5), 754–771. <https://doi.org/10.1016/j.jmb.2011.01.018>.

(72) Amster-Choder, O. Transcriptional Regulation. In *Encyclopedia of Microbiology (Third Edition)*; Schaechter, M., Ed.; Academic Press: Oxford, 2009; pp 501–516. <https://doi.org/10.1016/B978-012373944-5.00105-X>.

(73) Yarnell, W. S.; Roberts, J. W. Mechanism of Intrinsic Transcription Termination and Antitermination. *Science* **1999**. <https://doi.org/10.1126/science.284.5414.611>.

(74) Ma, C.; Yang, X.; Lewis, P. J. Bacterial Transcription as a Target for Antibacterial Drug Development. *Microbiology and Molecular Biology Reviews* **2016**. <https://doi.org/10.1128/MMBR.00055-15>.

(75) Srivastava, A.; Talaue, M.; Liu, S.; Degen, D.; Ebright, R. Y.; Sineva, E.; Chakraborty, A.; Druzhinin, S. Y.; Chatterjee, S.; Mukhopadhyay, J.; Ebright, Y. W.; Zozula, A.; Shen, J.; Sengupta, S.; Niedfeldt, R. R.; Xin, C.; Kaneko, T.; Irschik, H.; Jansen, R.; Donadio, S.; Connell, N.; Ebright, R. H. New Target for Inhibition of Bacterial RNA Polymerase: ‘Switch Region.’ *Current Opinion in Microbiology* **2011**, *14* (5), 532–543. <https://doi.org/10.1016/j.mib.2011.07.030>.

(76) Structural basis for substrate loading in bacterial RNA polymerase | Nature <https://www.nature.com/articles/nature05931> (accessed 2021-12-31).

(77) Transcription inhibition by the depsipeptide antibiotic salinamide A | eLife <https://elifesciences.org/articles/2451> (accessed 2021-12-31).

(78) Adelman, K.; Yuzenkova, J.; La Porta, A.; Zenkin, N.; Lee, J.; Lis, J. T.; Borukhov, S.; Wang, M. D.; Severinov, K. Molecular Mechanism of Transcription Inhibition by Peptide Antibiotic Microcin J25. *Molecular Cell* **2004**, *14* (6), 753–762. <https://doi.org/10.1016/j.molcel.2004.05.017>.

(79) Mukhopadhyay, J.; Das, K.; Ismail, S.; Koppstein, D.; Jang, M.; Hudson, B.; Sarafianos, S.; Tuske, S.; Patel, J.; Jansen, R.; Irschik, H.; Arnold, E.; Ebright, R. H. The RNA Polymerase “Switch Region” Is a Target for Inhibitors. *Cell* **2008**, *135* (2), 295–307. <https://doi.org/10.1016/j.cell.2008.09.033>.

(80) Telenti, A.; Imboden, P.; Marchesi, F.; Matter, L.; Schopfer, K.; Bodmer, T.; Lowrie, D.; Colston, M. J.; Cole, S. Detection of Rifampicin-Resistance Mutations in *Mycobacterium Tuberculosis*. *The Lancet* **1993**, *341* (8846), 647–651. [https://doi.org/10.1016/0140-6736\(93\)90417-F](https://doi.org/10.1016/0140-6736(93)90417-F).

(81) Ramaswamy, S.; Musser, J. M. Molecular Genetic Basis of Antimicrobial Agent Resistance In *Mycobacterium Tuberculosis*: 1998 Update. *Tubercle and Lung Disease* **1998**, *79* (1), 3–29. <https://doi.org/10.1054/tuld.1998.0002>.

(82) Taniguchi, H.; Aramaki, H.; Nikaido, Y.; Mizuguchi, Yasuo; Nakamura, M.; Koga, T.; Yoshida, S. Rifampicin Resistance and Mutation of the *RpoB* Gene in *Mycobacterium Tuberculosis*. *FEMS Microbiology Letters* **1996**, *144* (1), 103–108. <https://doi.org/10.1111/j.1574-6968.1996.tb08515.x>.

(83) Dabbs, E. R.; Yazawa, K.; Mikami, Y.; Miyaji, M.; Morisaki, N.; Iwasaki, S.; Furihata, K. Ribosylation by Mycobacterial Strains as a New Mechanism of Rifampin Inactivation. *Antimicrob Agents Chemother* **1995**, *39* (4), 1007–1009. <https://doi.org/10.1128/AAC.39.4.1007>.

(84) Piddock, L. J. V.; Williams, K. J.; Ricci, V. Accumulation of Rifampicin by *Mycobacterium Aurum*, *Mycobacterium Smegmatis* and *Mycobacterium Tuberculosis*. *Journal of Antimicrobial Chemotherapy* **2000**, *45* (2), 159–165. <https://doi.org/10.1093/jac/45.2.159>.

(85) Polikanov, Y. S.; Aleksashin, N. A.; Beckert, B.; Wilson, D. N. The Mechanisms of Action of Ribosome-Targeting Peptide Antibiotics. *Frontiers in Molecular Biosciences* **2018**, *5*, 48. <https://doi.org/10.3389/fmolsb.2018.00048>.

(86) Arenz, S.; Wilson, D. N. Bacterial Protein Synthesis as a Target for Antibiotic Inhibition. *Cold Spring Harb Perspect Med* **2016**, *6* (9), a025361. <https://doi.org/10.1101/cshperspect.a025361>.

(87) McCoy, L. S.; Xie, Y.; Tor, Y. Antibiotics That Target Protein Synthesis. *WIREs RNA* **2011**, *2* (2), 209–232. <https://doi.org/10.1002/wrna.60>.

(88) Wilson, D. N. Ribosome-Targeting Antibiotics and Mechanisms of Bacterial Resistance. *Nat Rev Microbiol* **2014**, *12* (1), 35–48. <https://doi.org/10.1038/nrmicro3155>.

(89) Polikanov, Y. S.; Aleksashin, N. A.; Beckert, B.; Wilson, D. N. The Mechanisms of Action of Ribosome-Targeting Peptide Antibiotics. *Frontiers in Molecular Biosciences* **2018**, *5*, 48. <https://doi.org/10.3389/fmolsb.2018.00048>.

(90) Schmeing, T. M.; Ramakrishnan, V. What Recent Ribosome Structures Have Revealed about the Mechanism of Translation. *Nature* **2009**, *461* (7268), 1234–1242. <https://doi.org/10.1038/nature08403>.

(91) Voorhees, R. M.; Ramakrishnan, V. Structural Basis of the Translational Elongation Cycle. *Annu. Rev. Biochem.* **2013**, *82* (1), 203–236. <https://doi.org/10.1146/annurev-biochem-113009-092313>.

(92) Karimi, R.; Pavlov, M. Y.; Buckingham, R. H.; Ehrenberg, M. Novel Roles for Classical Factors at the Interface between Translation Termination and Initiation. *Molecular Cell* **1999**, *3* (5), 601–609. [https://doi.org/10.1016/S1097-2765\(00\)80353-6](https://doi.org/10.1016/S1097-2765(00)80353-6).

(93) Giuliodori, A. M.; Spurio, R.; Milón, P.; Fabbretti, A. Antibiotics Targeting the 30S Ribosomal Subunit: A Lesson from Nature to Find and Develop New Drugs. *Current Topics in Medicinal Chemistry* **2018**, *18* (24), 2080–2096. <https://doi.org/10.2174/1568026618666181025092546>.

(94) Wright, G. D. Aminoglycoside-Modifying Enzymes. *Current Opinion in Microbiology* **1999**, *2* (5), 499–503. [https://doi.org/10.1016/S1369-5274\(99\)00007-7](https://doi.org/10.1016/S1369-5274(99)00007-7).

(95) Borovinskaya, M. A.; Shoji, S.; Holton, J. M.; Fredrick, K.; Cate, J. H. D. A Steric Block in Translation Caused by the Antibiotic Spectinomycin. *ACS Chem Biol* **2007**, *2* (8), 545–552. <https://doi.org/10.1021/cb700100n>.

(96) Suarez, G.; Nathans, D. Inhibition of Aminoacyl-SRNA Binding to Ribosomes by Tetracycline. *Biochemical and Biophysical Research Communications* **1965**, *18* (5), 743–750. [https://doi.org/10.1016/0006-291X\(65\)90848-X](https://doi.org/10.1016/0006-291X(65)90848-X).

(97) Chopra, I.; Roberts, M. Tetracycline Antibiotics: Mode of Action, Applications, Molecular Biology, and Epidemiology of Bacterial Resistance. *Microbiol Mol Biol Rev* **2001**, *65* (2), 232–260. <https://doi.org/10.1128/MMBR.65.2.232-260.2001>.

(98) Levy, S. B. Active Efflux Mechanisms for Antimicrobial Resistance. *Antimicrob Agents Chemother* **1992**, *36* (4), 695–703. <https://doi.org/10.1128/AAC.36.4.695>.

(99) Connell, S. R.; Tracz, D. M.; Nierhaus, K. H.; Taylor, D. E. Ribosomal Protection Proteins and Their Mechanism of Tetracycline Resistance. *Antimicrob Agents*

*Chemother* **2003**, *47* (12), 3675–3681. <https://doi.org/10.1128/AAC.47.12.3675-3681.2003>.

(100) Trieber, C. A.; Burkhardt, N.; Nierhaus, K. H.; Taylor, D. E. Ribosomal Protection from Tetracycline Mediated by Tet(O): Tet(O) Interaction with Ribosomes Is GTP-Dependent. *Biological Chemistry* **1998**, *379* (7). <https://doi.org/10.1515/bchm.1998.379.7.847>.

(101) Speer, B. S.; Salyers, A. A. Novel Aerobic Tetracycline Resistance Gene That Chemically Modifies Tetracycline. *J Bacteriol* **1989**, *171* (1), 148–153.

(102) Speer, B. S.; Bedzyk, L.; Salyers, A. A. Evidence That a Novel Tetracycline Resistance Gene Found on Two *Bacteroides* Transposons Encodes an NADP-Requiring Oxidoreductase. *Journal of Bacteriology* **1991**, *173* (1), 176–183. <https://doi.org/10.1128/jb.173.1.176-183.1991>.

(103) Vannuffel, P.; Cocito, C. Mechanism of Action of Streptogramins and Macrolides. *Drugs* **1996**, *51* (1), 20–30. <https://doi.org/10.2165/00003495-199600511-00006>.

(104) Trieu-Cuot, P.; de Cespédès, G.; Bentorcha, F.; Delbos, F.; Gaspar, E.; Horaud, T. Study of Heterogeneity of Chloramphenicol Acetyltransferase (CAT) Genes in Streptococci and Enterococci by Polymerase Chain Reaction: Characterization of a New CAT Determinant. *Antimicrobial Agents and Chemotherapy* **1993**, *37* (12), 2593–2598. <https://doi.org/10.1128/AAC.37.12.2593>.

(105) Shaw, W. V. Chloramphenicol Acetyltransferase: Enzymology and Molecular Biology. *CRC Crit Rev Biochem* **1983**, *14* (1), 1–46. <https://doi.org/10.3109/10409238309102789>.

(106) Dorman, C. J.; Foster, T. J. Nonenzymatic Chloramphenicol Resistance Determinants Specified by Plasmids R26 and R55-1 in *Escherichia Coli* K-12 Do Not Confer High-Level Resistance to Fluorinated Analogs. *Antimicrob Agents Chemother* **1982**, *22* (5), 912–914. <https://doi.org/10.1128/AAC.22.5.912>.

(107) Bissonnette, L.; Champetier, S.; Buisson, J. P.; Roy, P. H. Characterization of the Nonenzymatic Chloramphenicol Resistance (CmlA) Gene of the In4 Integron of Tn1696: Similarity of the Product to Transmembrane Transport Proteins. *Journal of Bacteriology* **1991**, *173* (14), 4493–4502. <https://doi.org/10.1128/jb.173.14.4493-4502.1991>.

(108) Gaynor, M.; Mankin, A. S. Macrolide Antibiotics: Binding Site, Mechanism of Action, Resistance. *Current Topics in Medicinal Chemistry* **2003**, *3* (9), 949–960. <https://doi.org/10.2174/1568026033452159>.

(109) Weisblum, B. Erythromycin Resistance by Ribosome Modification. *Antimicrob Agents Chemother* **1995**, *39* (3), 577–585. <https://doi.org/10.1128/AAC.39.3.577>.

(110) Roberts, M. C.; Sutcliffe, J.; Courvalin, P.; Jensen, L. B.; Rood, J.; Seppala, H. Nomenclature for Macrolide and Macrolide-Lincosamide-Streptogramin B Resistance Determinants. *Antimicrobial Agents and Chemotherapy* **1999**, *43* (12), 2823–2830. <https://doi.org/10.1128/AAC.43.12.2823>.

(111) Zhong, P.; Shortridge, V. D. The Role of Efflux in Macrolide Resistance. *Drug Resistance Updates* **2000**, *3* (6), 325–329. <https://doi.org/10.1054/drup.2000.0175>.

(112) Kobayashi, N.; Nishino, K.; Yamaguchi, A. Novel Macrolide-Specific ABC-Type Efflux Transporter In *Escherichia Coli*. *Journal of Bacteriology* **2001**, *183* (19), 5639–5644. <https://doi.org/10.1128/JB.183.19.5639-5644.2001>.

(113) Perry, C. M.; Jarvis, B. Linezolid. *Drugs* **2001**, *61* (4), 525–551. <https://doi.org/10.2165/00003495-200161040-00008>.

(114) Livermore, D. M. Linezolid in Vitro : Mechanism and Antibacterial Spectrum. *Journal of Antimicrobial Chemotherapy* **2003**, *51* (suppl\_2), ii9–ii16. <https://doi.org/10.1093/jac/dkg249>.

(115) Bender, J. K.; Cattoir, V.; Hegstad, K.; Sadowy, E.; Coque, T. M.; Westh, H.; Hammerum, A. M.; Schaffer, K.; Burns, K.; Murchan, S.; Novais, C.; Freitas, A. R.; Peixe, L.; Del Grosso, M.; Pantosti, A.; Werner, G. Update on Prevalence and Mechanisms of Resistance to Linezolid, Tigecycline and Daptomycin in Enterococci in Europe: Towards a Common Nomenclature. *Drug Resistance Updates* **2018**, *40*, 25–39. <https://doi.org/10.1016/j.drup.2018.10.002>.

(116) Chen, H.; Wu, W.; Ni, M.; Liu, Y.; Zhang, J.; Xia, F.; He, W.; Wang, Q.; Wang, Z.; Cao, B.; Wang, H. Linezolid-Resistant Clinical Isolates of Enterococci and *Staphylococcus Cohnii* from a Multicentre Study in China: Molecular Epidemiology and Resistance Mechanisms. *International Journal of Antimicrobial Agents* **2013**, *42* (4), 317–321. <https://doi.org/10.1016/j.ijantimicag.2013.06.008>.

(117) Bonfiglio, G.; Furneri, P. M. Novel Streptogramin Antibiotics. *Expert Opinion on Investigational Drugs* **2001**, *10* (2), 185–198. <https://doi.org/10.1517/13543784.10.2.185>.

(118) Rende-Fournier, R.; Leclercq, R.; Galimand, M.; Duval, J.; Courvalin, P. Identification of the SatA Gene Encoding a Streptogramin A Acetyltransferase in *Enterococcus Faecium* BM4145. *Antimicrob Agents Chemother* **1993**, *37* (10), 2119–2125. <https://doi.org/10.1128/AAC.37.10.2119>.

(119) Simjee, S.; McDermott, P. F.; Wagner, D. D.; White, D. G. Variation within the Vat(E) Allele of *Enterococcus Faecium* Isolates from Retail Poultry Samples. *Antimicrobial Agents and Chemotherapy* **2001**, *45* (10), 2931–2932. <https://doi.org/10.1128/AAC.45.10.2931-2932.2001>.

(120) MICROBIAL ACETYLATION OF M FACTOR OF VIRGINIAMYCIN [https://www.jstage.jst.go.jp/article/antibiotics1968/29/12/29\\_12\\_1297/\\_article](https://www.jstage.jst.go.jp/article/antibiotics1968/29/12/29_12_1297/_article) (accessed 2021-11-14).

(121) Weisblum, B. Inducible Resistance to Macrolides, Lincosamides and Streptogramin Type B Antibiotics: The Resistance Phenotype, Its Biological Diversity, and Structural Elements That Regulate Expression--a Review. *J Antimicrob Chemother* **1985**, *16 Suppl A*, 63–90. [https://doi.org/10.1093/jac/16.suppl\\_a.63](https://doi.org/10.1093/jac/16.suppl_a.63).

(122) Bermingham, A.; Derrick, J. P. The Folic Acid Biosynthesis Pathway in Bacteria: Evaluation of Potential for Antibacterial Drug Discovery. *Bioessays* **2002**, *24* (7), 637–648. <https://doi.org/10.1002/bies.10114>.

(123) Bertacine Dias, M. V.; Santos, J. C.; Libreros-Zúñiga, G. A.; Ribeiro, J. A.; Chavez-Pacheco, S. M. Folate Biosynthesis Pathway: Mechanisms and Insights into Drug Design for Infectious Diseases. *Future Medicinal Chemistry* **2018**, *10* (8), 935–959. <https://doi.org/10.4155/fmc-2017-0168>.

(124) Sköld, O. Sulfonamides and Trimethoprim. *Expert Review of Anti-infective Therapy* **2010**, *8* (1), 1–6. <https://doi.org/10.1586/eri.09.117>.

(125) Huovinen, P.; Sundström, L.; Swedberg, G.; Sköld, O. Trimethoprim and Sulfonamide Resistance. *Antimicrob Agents Chemother* **1995**, *39* (2), 279–289. <https://doi.org/10.1128/AAC.39.2.279>.

(126) Huovinen, P. Trimethoprim Resistance. *ANTIMICROB AGENTS CHEMOTHER* **1987**, *31*, 6.

(127) Then, R. L. Mechanisms of Resistance to Trimethoprim, the Sulfonamides, and Trimethoprim-Sulfamethoxazole. *Clinical Infectious Diseases* **1982**, *4* (2), 261–269. <https://doi.org/10.1093/clinids/4.2.261>.

(128) Eliopoulos, G. M.; Huovinen, P. Resistance to Trimethoprim-Sulfamethoxazole. *Clinical Infectious Diseases* **2001**, *32* (11), 1608–1614. <https://doi.org/10.1086/320532>.

(129) World Health Organization. *Antibacterial Agents in Preclinical Development: An Open Access Database*; WHO/EMP/IAU/2019.12; World Health Organization, 2019.

(130) Miethke, M.; Pieroni, M.; Weber, T.; Brönstrup, M.; Hammann, P.; Halby, L.; Arimondo, P. B.; Glaser, P.; Aigle, B.; Bode, H. B.; Moreira, R.; Li, Y.; Luzhetskyy, A.; Medema, M. H.; Pernodet, J.-L.; Stadler, M.; Tormo, J. R.; Genilloud, O.; Truman, A. W.; Weissman, K. J.; Takano, E.; Sabatini, S.; Stegmann, E.; Brötz-Oesterhelt, H.; Wohlleben, W.; Seemann, M.; Empting, M.; Hirsch, A. K. H.; Loretz, B.; Lehr, C.-M.; Titz, A.; Herrmann, J.; Jaeger, T.; Alt, S.; Hesterkamp, T.; Winterhalter, M.; Schiefer, A.; Pfarr, K.; Hoerauf, A.; Graz, H.; Graz, M.; Lindvall, M.; Ramurthy, S.; Karlén, A.; van Dongen, M.; Petkovic, H.; Keller, A.; Peyrane, F.; Donadio, S.; Fraisse, L.; Piddock, L. J. V.; Gilbert, I. H.; Moser, H. E.; Müller, R. Towards the Sustainable Discovery and Development of New Antibiotics. *Nat Rev Chem* **2021**, 5 (10), 726–749. <https://doi.org/10.1038/s41570-021-00313-1>.

(131) World Health Organization. *Prioritization of Pathogens to Guide Discovery, Research and Development of New Antibiotics for Drug-Resistant Bacterial Infections, Including Tuberculosis*; WHO/EMP/IAU/2017.12; World Health Organization, 2017.

(132) 2019 antibacterial agents in clinical development: an analysis of the antibacterial clinical development pipeline <https://www.who.int/publications-detail-redirect/9789240000193> (accessed 2021-11-15).

(133) Antibiotics Currently in Global Clinical Development <http://pew.org/1YkUFkT> (accessed 2022-01-02).

(134) Tracking the Global Pipeline of Antibiotics in Development, March 2021 <https://pew.org/30pDy96> (accessed 2022-01-02).

(135) Kim, W.; Krause, K.; Zimmerman, Z.; Outterson, K. Improving Data Sharing to Increase the Efficiency of Antibiotic R&D. *Nat Rev Drug Discov* **2021**, 20 (1), 1–2. <https://doi.org/10.1038/d41573-020-00185-y>.

(136) Demain, A. L. Importance of Microbial Natural Products and the Need to Revitalize Their Discovery. *Journal of Industrial Microbiology and Biotechnology* **2014**, 41 (2), 185–201. <https://doi.org/10.1007/s10295-013-1325-z>.

(137) Katz, L.; Baltz, R. H. Natural Product Discovery: Past, Present, and Future. *Journal of Industrial Microbiology and Biotechnology* **2016**, 43 (2–3), 155–176. <https://doi.org/10.1007/s10295-015-1723-5>.

(138) Newman, D. J.; Cragg, G. M.; Snader, K. M. Natural Products as Sources of New Drugs over the Period 1981–2002. *J. Nat. Prod.* **2003**, 66 (7), 1022–1037. <https://doi.org/10.1021/np0300961>.

(139) Kinch, M. S.; Haynesworth, A.; Kinch, S. L.; Hoyer, D. An Overview of FDA-Approved New Molecular Entities: 1827–2013. *Drug Discovery Today* **2014**, 19 (8), 1033–1039. <https://doi.org/10.1016/j.drudis.2014.03.018>.

(140) Pantel, L.; Florin, T.; Dobosz-Bartoszek, M.; Racine, E.; Sarciaux, M.; Serri, M.; Houard, J.; Campagne, J.-M.; de Figueiredo, R. M.; Midrier, C.; Gaudriault, S.; Givaudan, A.; Lanois, A.; Forst, S.; Aumelas, A.; Cotteaux-Lautard, C.; Bolla, J.-M.; Vingsbo Lundberg, C.; Huseby, D. L.; Hughes, D.; Villain-Guillot, P.; Mankin, A. S.; Polikanov, Y. S.; Gualtieri, M. Odilorhabdins, Antibacterial Agents That Cause Miscoding by Binding at a New Ribosomal Site. *Molecular Cell* **2018**, 70 (1), 83–94.e7. <https://doi.org/10.1016/j.molcel.2018.03.001>.

(141) Baumann, S.; Herrmann, J.; Raju, R.; Steinmetz, H.; Mohr, K. I.; Hüttel, S.; Harmrolfs, K.; Stadler, M.; Müller, R. Cystobactamids: Myxobacterial Topoisomerase Inhibitors Exhibiting Potent Antibacterial Activity. *Angew. Chem. Int. Ed.* **2014**, 53 (52), 14605–14609. <https://doi.org/10.1002/anie.201409964>.

(142) Elgaher, W. A. M.; Hamed, M. M.; Baumann, S.; Herrmann, J.; Siebenbürger, L.; Krull, J.; Cirnski, K.; Kirschning, A.; Brönstrup, M.; Müller, R.; Hartmann, R. W. Cystobactamid 507: Concise Synthesis, Mode of Action, and Optimization toward

More Potent Antibiotics. *Chemistry – A European Journal* **2020**, *26* (32), 7219–7225. <https://doi.org/10.1002/chem.202000117>.

(143) Schäberle, T. F.; Schiefer, A.; Schmitz, A.; König, G. M.; Hoerauf, A.; Pfarr, K. Corallopyronin A – A Promising Antibiotic for Treatment of Filariasis. *International Journal of Medical Microbiology* **2014**, *304* (1), 72–78. <https://doi.org/10.1016/j.ijmm.2013.08.010>.

(144) O'Neill, A.; Oliva, B.; Storey, C.; Hoyle, A.; Fishwick, C.; Chopra, I. RNA Polymerase Inhibitors with Activity against Rifampin-Resistant Mutants of *Staphylococcus Aureus*. *Antimicrobial Agents and Chemotherapy* **2000**, *44* (11), 3163–3166. <https://doi.org/10.1128/AAC.44.11.3163-3166.2000>.

(145) Kling, A.; Lukat, P.; Almeida, D. V.; Bauer, A.; Fontaine, E.; Sordello, S.; Zaburannyi, N.; Herrmann, J.; Wenzel, S. C.; König, C.; Ammerman, N. C.; Barrio, M. B.; Borchers, K.; Bordon-Pallier, F.; Brönstrup, M.; Courtemanche, G.; Gerlitz, M.; Geslin, M.; Hammann, P.; Heinz, D. W.; Hoffmann, H.; Klieber, S.; Kohlmann, M.; Kurz, M.; Lair, C.; Matter, H.; Nuermberger, E.; Tyagi, S.; Fraisse, L.; Grosset, J. H.; Lagrange, S.; Müller, R. Antibiotics. Targeting DnaN for Tuberculosis Therapy Using Novel Griselimycins. *Science* **2015**, *348* (6239), 1106–1112. <https://doi.org/10.1126/science.aaa4690>.

(146) David, A. A.; Park, S. E.; Parang, K.; Tiwari, R. K. Antibiotics-Peptide Conjugates Against Multidrug-Resistant Bacterial Pathogens. *Current Topics in Medicinal Chemistry* **2018**, *18* (22), 1926–1936. <https://doi.org/10.2174/1568026619666181129141524>.

(147) Mariathasan, S.; Tan, M.-W. Antibody–Antibiotic Conjugates: A Novel Therapeutic Platform against Bacterial Infections. *Trends in Molecular Medicine* **2017**, *23* (2), 135–149. <https://doi.org/10.1016/j.molmed.2016.12.008>.

(148) Wencewicz, T. A.; Long, T. E.; Möllmann, U.; Miller, M. J. Trihydroxamate Siderophore–Fluoroquinolone Conjugates Are Selective Sideromycin Antibiotics That Target *Staphylococcus Aureus*. *Bioconjugate Chem.* **2013**, *24* (3), 473–486. <https://doi.org/10.1021/bc300610f>.

(149) Challis, G. L.; Hopwood, D. A. Synergy and Contingency as Driving Forces for the Evolution of Multiple Secondary Metabolite Production by *Streptomyces* Species. *PNAS* **2003**, *100* (suppl 2), 14555–14561. <https://doi.org/10.1073/pnas.1934677100>.

(150) Studies and Syntheses of Siderophores, Microbial Iron Chelators, ...: Ingenta Connect <https://www.ingentaconnect.com/content/ben/cmc/2000/00000007/00000002/art00002> (accessed 2022-01-07).

(151) Golan, Y. Empiric Therapy for Hospital-Acquired, Gram-Negative Complicated Intra-Abdominal Infection and Complicated Urinary Tract Infections: A Systematic Literature Review of Current and Emerging Treatment Options. *BMC Infect Dis* **2015**, *15* (1), 313. <https://doi.org/10.1186/s12879-015-1054-1>.

(152) Syed, Y. Y. Cefiderocol: A Review in Serious Gram-Negative Bacterial Infections. *Drugs* **2021**, *81* (13), 1559–1571. <https://doi.org/10.1007/s40265-021-01580-4>.

(153) Reinhardt, A.; Neundorf, I. Design and Application of Antimicrobial Peptide Conjugates. *International Journal of Molecular Sciences* **2016**, *17* (5), 701. <https://doi.org/10.3390/ijms17050701>.

(154) Arnusch, C. J.; Pieters, R. J.; Breukink, E. Enhanced Membrane Pore Formation through High-Affinity Targeted Antimicrobial Peptides. *PLOS ONE* **2012**, *7* (6), e39768. <https://doi.org/10.1371/journal.pone.0039768>.

(155) Abdul Ghaffar, K.; M. Hussein, W.; G. Khalil, Z.; J. Capon, R.; Skwarczynski, M.; Toth, I. Levofloxacin and Indolicidin for Combination Antimicrobial Therapy. *Current Drug Delivery* **2015**, *12* (1), 108–114.

(156) Chen, H.; Liu, C.; Chen, D.; Madrid, K.; Peng, S.; Dong, X.; Zhang, M.; Gu, Y. Bacteria-Targeting Conjugates Based on Antimicrobial Peptide for Bacteria Diagnosis and Therapy. *Mol. Pharmaceutics* **2015**, *12* (7), 2505–2516. <https://doi.org/10.1021/acs.molpharmaceut.5b00053>.

(157) Synthesis and antibacterial activity of amphiphilic lysine-ligated neomycin B conjugates - ScienceDirect [https://www.sciencedirect.com/science/article/pii/S0008621511000279?casa\\_token=L\\_PjXewELnqMAAAAA:9lTZW7Y-JGGG\\_hcCCg0C08pCgShBQjtbtcLf\\_vVW9iDe4pQLHxNMxq5cjgMEkn-o7aZrkSxWg](https://www.sciencedirect.com/science/article/pii/S0008621511000279?casa_token=L_PjXewELnqMAAAAA:9lTZW7Y-JGGG_hcCCg0C08pCgShBQjtbtcLf_vVW9iDe4pQLHxNMxq5cjgMEkn-o7aZrkSxWg) (accessed 2021-11-16).

(158) Cheng, A. V.; Wuest, W. M. Signed, Sealed, Delivered: Conjugate and Prodrug Strategies as Targeted Delivery Vectors for Antibiotics. *ACS Infect. Dis.* **2019**, *5* (6), 816–828. <https://doi.org/10.1021/acsinfecdis.9b00019>.

(159) Randhawa, H. K.; Gautam, A.; Sharma, M.; Bhatia, R.; Varshney, G. C.; Raghava, G. P. S.; Nandanwar, H. Cell-Penetrating Peptide and Antibiotic Combination Therapy: A Potential Alternative to Combat Drug Resistance in Methicillin-Resistant *Staphylococcus Aureus*. *Appl Microbiol Biotechnol* **2016**, *100* (9), 4073–4083. <https://doi.org/10.1007/s00253-016-7329-7>.

(160) Jiang, Y.; Han, M.; Bo, Y.; Feng, Y.; Li, W.; Wu, J. R.; Song, Z.; Zhao, Z.; Tan, Z.; Chen, Y.; Xue, T.; Fu, Z.; Kuo, S. H.; Lau, G. W.; Luijten, E.; Cheng, J. “Metaphilic” Cell-Penetrating Polypeptide-Vancomycin Conjugate Efficiently Eradicates Intracellular Bacteria via a Dual Mechanism. *ACS Cent. Sci.* **2020**, *6* (12), 2267–2276. <https://doi.org/10.1021/acscentsci.0c00893>.

(161) Brezden, A.; Mohamed, M. F.; Nepal, M.; Harwood, J. S.; Kuriakose, J.; Seleem, M. N.; Chmielewski, J. Dual Targeting of Intracellular Pathogenic Bacteria with a Cleavable Conjugate of Kanamycin and an Antibacterial Cell-Penetrating Peptide. *J. Am. Chem. Soc.* **2016**, *138* (34), 10945–10949. <https://doi.org/10.1021/jacs.6b04831>.

(162) Lehar, S. M.; Pillow, T.; Xu, M.; Staben, L.; Kajihara, K. K.; Vandlen, R.; DePalatis, L.; Raab, H.; Hazenbos, W. L.; Hiroshi Morisaki, J.; Kim, J.; Park, S.; Darwish, M.; Lee, B.-C.; Hernandez, H.; Loyet, K. M.; Lupardus, P.; Fong, R.; Yan, D.; Chalouni, C.; Luis, E.; Khalfin, Y.; Plise, E.; Cheong, J.; Lyssikatos, J. P.; Strandh, M.; Koefoed, K.; Andersen, P. S.; Flygare, J. A.; Wah Tan, M.; Brown, E. J.; Mariathasan, S. Novel Antibody–Antibiotic Conjugate Eliminates Intracellular *S. Aureus*. *Nature* **2015**, *527* (7578), 323–328. <https://doi.org/10.1038/nature16057>.

(163) Berthiaume, F.; Reiken, S. R.; Toner, M.; Tompkins, R. G.; Yarmush, M. L. Antibody-Targeted Photolysis of Bacteria In Vivo. *Nat Biotechnol* **1994**, *12* (7), 703–706. <https://doi.org/10.1038/nbt0794-703>.

(164) Yeung, A. T. Y.; Gellatly, S. L.; Hancock, R. E. W. Multifunctional Cationic Host Defence Peptides and Their Clinical Applications. *Cell. Mol. Life Sci.* **2011**, *68* (13), 2161. <https://doi.org/10.1007/s00018-011-0710-x>.

(165) Desgranges, S.; Ruddle, C. C.; Burke, L. P.; McFadden, T. M.; O’Brien, J. E.; Fitzgerald-Hughes, D.; Humphreys, H.; Smyth, T. P.; Devocelle, M.  $\beta$ -Lactam-Host Defence Peptide Conjugates as Antibiotic Prodrug Candidates Targeting Resistant Bacteria. *RSC Adv.* **2012**, *2* (6), 2480. <https://doi.org/10.1039/c2ra01351g>.

(166) Umstätter, F.; Domhan, C.; Hertlein, T.; Ohlsen, K.; Mühlberg, E.; Kleist, C.; Zimmermann, S.; Beijer, B.; Klika, K. D.; Haberkorn, U.; Mier, W.; Uhl, P. Vancomycin Resistance Is Overcome by Conjugation of Polycationic Peptides. *Angewandte Chemie International Edition* **2020**, *59* (23), 8823–8827. <https://doi.org/10.1002/anie.202002727>.

(167) Steinmetz, H.; Gerth, K.; Jansen, R.; Schläger, N.; Dehn, R.; Reinecke, S.; Kirschning, A.; Müller, R. Elansolid A, a Unique Macrolide Antibiotic from Chitinophaga Sancti

Isolated as Two Stable Atropisomers. *Angewandte Chemie International Edition* **2011**, *50* (2), 532–536. <https://doi.org/10.1002/anie.201005226>.

(168) Markwart, R.; Willrich, N.; Eckmanns, T.; Werner, G.; Ayobami, O. Low Proportion of Linezolid and Daptomycin Resistance Among Bloodborne Vancomycin-Resistant Enterococcus Faecium and Methicillin-Resistant *Staphylococcus Aureus* Infections in Europe. *Frontiers in Microbiology* **2021**, *12*, 1379. <https://doi.org/10.3389/fmicb.2021.664199>.

## Chapter 2

# Elansolid A2: A Unique Natural Product Antibiotic Targeting the Small Ribosomal Subunit and Inhibiting Translation in *S. aureus*

(Manuscript in preparation)

Sari Rasheed<sup>[a,b]</sup>, Franziska Fries<sup>[a,b,c]</sup>, Jennifer Herrmann<sup>[a,b]</sup>, Daniel Wilson<sup>[d]</sup> and Rolf Müller<sup>\*[a,b,c]</sup>

---

- [a] S. Rasheed, F. Fries, Dr. J. Herrmann, Prof. Dr. R. Müller\*  
Helmholtz Institute for Pharmaceutical Research Saarland (HIPS), Helmholtz Centre for Infection Research (HZI), Saarland University, Saarbrücken, Germany
- [b] S. Rasheed, F. Fries, Dr. J. Herrmann, Prof. Dr. R. Müller  
German Centre for Infection Research (DZIF), Braunschweig, Germany
- [c] F. Fries, Prof. Dr. R. Müller  
Department of Pharmacy, Saarland University, Saarbrücken, Germany
- [d] Prof. Dr. D. Wilson  
Institute for Biochemistry and Molecular Biology, University of Hamburg, Hamburg, Germany

---

## Contributions to the presented work

### Author's contribution

The author significantly contributed to the conception of this study, designed, and performed experiments, evaluated, and interpreted resulting data. The author performed the biological evaluation experiments, generated mutants, and characterized them. Furthermore, the author conducted DNA-extraction and analyzed the whole genome sequencing of the mutants, performed Surface Plasmon Resonance (SPR) measurements, cross-resistance, and synergy assessments. The author contributed significantly to conceiving and writing this manuscript.

### Contribution by others

F. Fries performed time-kill experiments, synergy assessments and DNA-extraction. J. Herrmann contributed to the experimental design of the study and performed proofreading of this chapter. D. Wilson Performed *in vitro* translation inhibition assay and toe-printing experiments. R. Müller was responsible for the conception of the project and performed the proofreading of this chapter.

## 2 Elansolid A2: A Unique Natural Product Antibiotic Targeting the Small Ribosomal Subunit and Inhibiting Translation in *S. aureus*

### 2.1 Abstract

Elansolids are secondary metabolites produced by the gliding bacterium *Chitinophaga sancti*. Elansolid A2, an atropisomer of elansolid A1 showed a remarkable activity against Gram-positive bacteria, specifically against Methicillin-resistant *Staphylococcus aureus* (MRSA). Given the promising activity of this interesting class of novel antibiotics, we further investigate the antibacterial effect of elansolid A2 using a broader panel of bacteria. In addition to its good activity against MRSA, elansolid A2 exhibited promising minimum inhibitory concentrations (MICs) of 1 and 4  $\mu\text{g/mL}$  against daptomycin-resistant *S. aureus* and penicillin-resistant *Streptococcus pneumoniae* (PRSP), respectively. Importantly, characterization of *in vitro* selected elansolid-resistant mutants of *S. aureus* enabled the identification of the target of elansolids. Whole genome sequencing of these mutants revealed mutations in two genes, *rpsG* and *rpsK*, encoding for two small subunit ribosomal proteins, S7 and S11. *In vitro* translation inhibition assays and toeprinting experiments further confirmed that elansolid A2 traps the ribosome with the initiator tRNA in the P-site preventing the elongation step. Importantly, elansolid-resistant *S. aureus* mutants carrying mutations in *rpsG* and *rpsK* do not show cross-resistance to common 30S and 50S ribosomal subunit inhibitors, which confirms a unique target site of elansolids on the ribosome. Elansolid A2 exerts its inhibitory effect through a bactericidal mode of action and the natural product displays a synergistic effect with 50S ribosomal inhibitors such as erythromycin, chloramphenicol, and linezolid.

## 2.2 Introduction

To tackle the alarming rise of antimicrobial resistance (AMR), there is an urgent need for the development of novel antibiotics with unique chemistry and distinct mechanisms of action. Natural products (NPs) have been historically known as an attractive source for drug discovery in infection research<sup>1</sup>. NPs originate from bacterial, fungal, plant, and marine sources, comprising an enormously broad scope of distinct and chemically complex entities. Furthermore, NPs possess a wide range of biological activities against pathogenic bacteria by addressing diverse targets<sup>2</sup>. Screening of Actinomycetes species from soil samples by Waksman et al. in the 1940s followed by campaigns by companies such as Eli Lilly for bacterial strains from soil collections from all over the world, opened the door for pharmaceutical companies to begin extensive screening for isolating secondary metabolites from soil bacteria<sup>3</sup>. Almost 80% of vital antimicrobial classes including tetracyclines, macrolides and aminoglycosides have been isolated from soil bacteria<sup>4,5</sup>. Given their pharmaceutical value, secondary metabolites produced by soil bacteria remain an attractive target for researchers in their efforts to discover novel antimicrobial agents.

Elansolids (chemical structures in **Figure 1**) comprise a group of secondary metabolites isolated from the filamentous, chitinolytic, gliding bacterium *Chitinophaga sancti*, and they belong to the group of *trans*-polyketides type I<sup>6,7</sup>. Elansolid A was isolated as two separable atropisomers A1 and A2, where elansolid A2 shows antibiotic activity against Gram positive bacteria, unlike elansolid A1 which is weakly active<sup>6</sup>. Atropisomerism arises in many common scaffolds in drug discovery and is defined as a dynamic type of axial chirality that refers to the restricted rotation of a single bond<sup>8-10</sup>. In reverse to elansolid A2, in elansolid A1, at C6 the methylene protons are oriented to the outside of the lactone ring and at C7 the secondary alcohol is folded in the lactone ring<sup>6</sup>. Additionally, elansolid A3, B1 and B2 bearing the unusual *p*-quinone methide unit were isolated from the fermentation extract<sup>6,11</sup>. Elansolid C1 was obtained

by addition of anthranilic acid to a crude fermentation extract containing the macrolide elansolid A2 and under mild acidic conditions, a Grob-type fragmentation of elansolid A3 led to the *p*-hydroxy styryl isomer elansolid D<sup>12,13</sup>. Elansolid A2 showed promising activity against Gram-positive bacteria specifically against Methicillin-resistant *S. aureus*, and against efflux-deficient *E. coli* *ΔtolC* in combination with the membrane-permeabilizing peptide polymyxin B nonapeptide (PMBN), which suggests that the antibiotic might address a broad-spectrum target while activity against Gram-negative bacteria is hampered by insufficient uptake and efflux<sup>14</sup>.

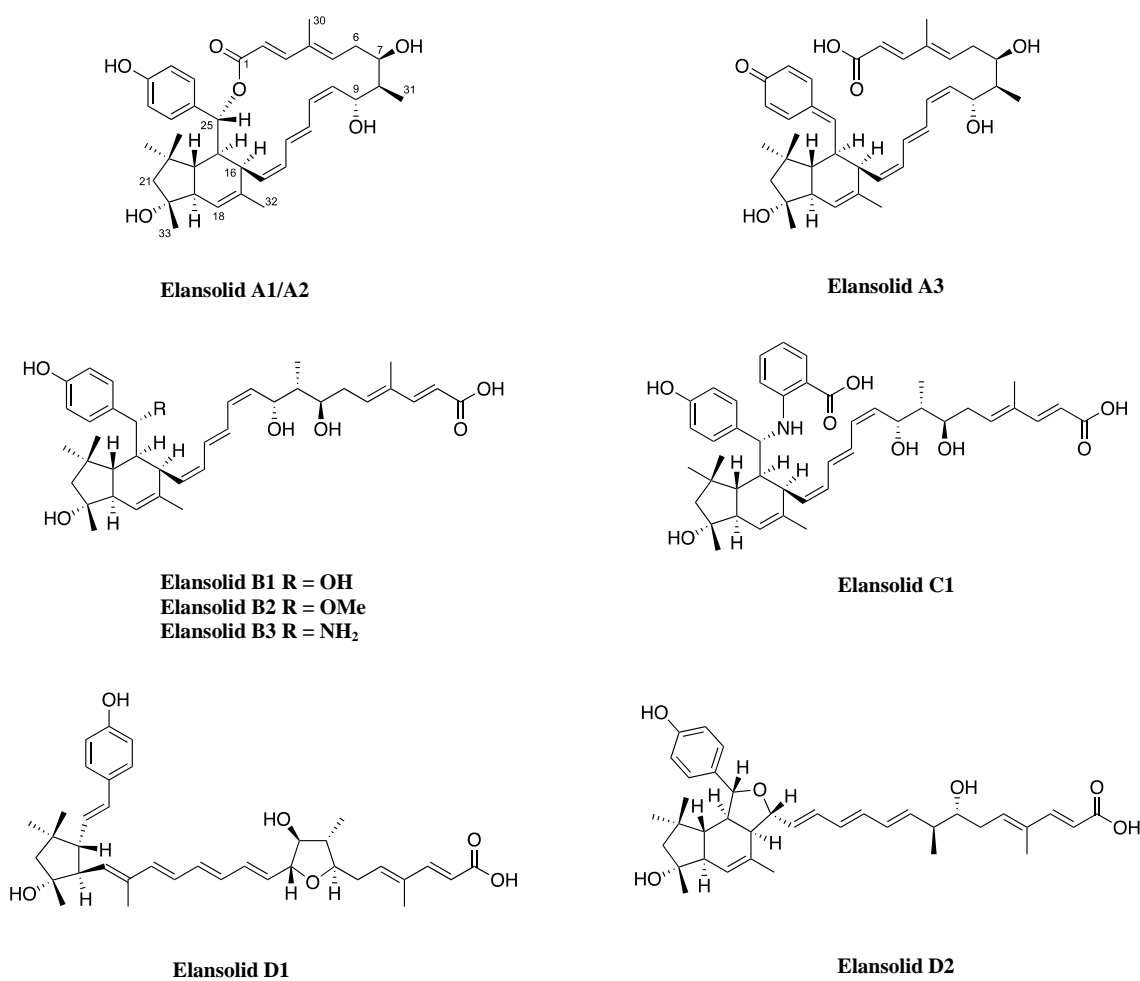


**Figure 1: Chemical structures of elansolids (A1-A3, B1-B3, C1, D1 and D2)**

Ever since the introduction of antibiotics, drugs targeting the ribosomes have been an important subject of numerous studies<sup>15</sup>. Ribosomes are among the most conserved macromolecular organelles in the bacterial cell, having an essential role in protein biosynthesis<sup>16</sup>. The bacterial 70S ribosome is composed of two unequal subunits, the small (30S) and large (50S) subunits that associate during translation. The small (30S) subunit contains 16S rRNA and ~ 20 proteins, while the large (50S) subunit contains 23S rRNA, 5S rRNA, and over 30 proteins<sup>17</sup>. Protein synthesis (summarized in **Figure 2**) is divided into four steps: initiation, elongation, termination, and recycling. Given their pivotal role in protein synthesis, ribosomes represent an attractive target for antibiotics for the treatment of infectious diseases. Several antibiotics targeting the ribosome and interfering with protein synthesis have been developed and many are in clinical application, with e.g. linezolid being used to treat infections caused by hard-to-treat vancomycin-resistant *Enterococcus* spp., (VRE)<sup>18</sup>.

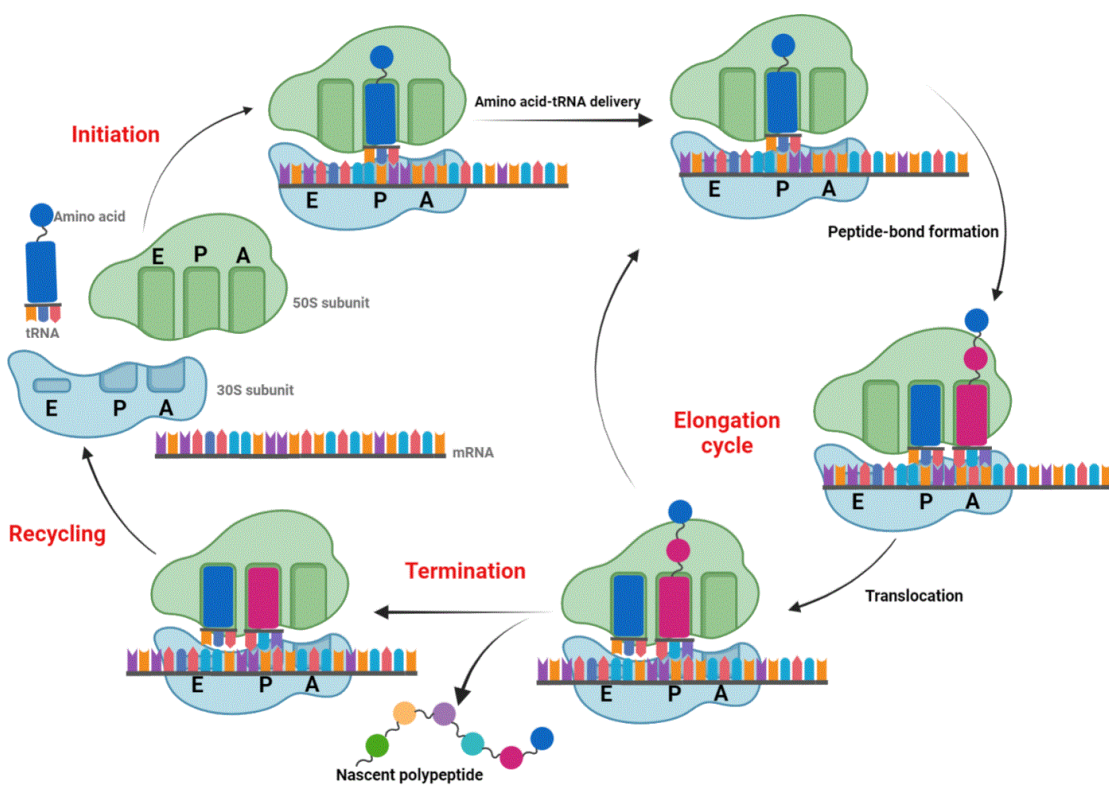


**Figure 2: proteins synthesis cycle.** Translation is mainly divided to four steps: initiation, elongation, termination, and recycling. Initiation occurs by the assembly of 30S and a 50S ribosomal subunits with the initiator tRNA and start codon of the mRNA positioned at the P-site. Elongation cycle encompasses the delivery of the aminoacylated-tRNA (aa-tRNA) to the A-site of the ribosome, followed by the base-pairing between mRNA and tRNA, allowing the peptide bond formation to occur between the growing amino acids and later, tRNA translocating from P-to E-site and from A-to P-site. Termination and recycling lead to release of the polypeptide chain and the dissociation of the 70S ribosome, followed by recycling of the translation components.

Herein, we aim to study the mode of action, mode of resistance as well as killing kinetics and biological activity of elansolid A2 against a panel of Gram-positive and Gram-negative pathogens. We generated elansolid-resistant *S. aureus* mutants and characterized them to assess their growth kinetics, metabolic activity, and to study the genes involved in resistance by performing whole genome sequence analysis. Intriguingly, elansolid-resistant mutants acquired point mutations in genes encoding for small ribosomal subunit-proteins. We further confirmed the target of elansolid is protein biosynthesis by *in vitro* translation inhibition assays and toeprinting experiments that proved the position in which elansolid traps the ribosomes. Mutants' characterization revealed no cross-resistance to a selection of 30S and 50S ribosomal subunit inhibitors, which confirms a unique target of the antibiotic.

## 2.3 Materials and Methods

### 2.3.1 Bacterial strains and antimicrobial susceptibility testing

All bacterial were handled under conditions recommended by the depositor. *S. aureus* strains Newman, Mu50 and N315 were obtained from the stock collection of the Institute of Medical Microbiology, Zurich, Switzerland, and kindly provided by Brigitte Berger-Bächi. *S. aureus* HG001 and the corresponding HG001 daptomycin-resistant DAP<sup>R</sup> mutant (Müller et al., 2017)<sup>19</sup> were provided by Prof. Dr. Tanja Schneider (University Hospital Bonn).

Experiments with all bacterial strains were conducted in Mueller Hinton II Broth (Cation-Adjusted) (BD BBL) (MHBII) and Mueller Hinton II Broth supplemented to 50 mg/L Ca<sup>2+</sup> (MHBII-Ca<sup>2+</sup>) for daptomycin-resistant *S. aureus* strain according to the guidelines of Clinical and Laboratory Standards Institute (CLSI). Experiments with mycobacteria (*M. marinum*, *M. smegmatis* and *M. tuberculosis*) were conducted in Middlebrook 7H9 broth base (Sigma-Aldrich) supplemented with 10% Oleic Acid-Dextrose-Catalase (OADC).

Minimal inhibitory concentrations (MICs) were determined by standard broth microdilution (BMD) based on 2-fold serial dilutions of tested compounds according to guidelines of the Clinical & Laboratory Standards Institute (CLSI). Briefly, 75 µl/well of bacterial suspension at  $\sim 4 \times 10^5$  CFU/mL were added to a 96-well plate, along with 75 µl of compounds in serial dilution (0.03-64 µg/mL). The plates were then incubated at ambient temperature, and the lowest concentration at which no growth was observed by visual observation was considered as the MIC. For *M. marinum* and *M. tuberculosis*, a final suspension of  $1 \times 10^5$  CFU/mL were used in the assay and the plates were incubated at 30 °C and 37 °C for 4 and 7 days respectively.

### 2.3.2 Killing kinetics of elansolid A2 in *S. aureus*

TKCs were performed using early logarithmic phase of growth of *S. aureus* strain Newman. Briefly, an overnight culture of *S. aureus* Newman was incubated in MHBII, overnight at 37 °C. The culture was diluted 1:10 and incubated for one hour at 37 °C. Compound solutions

were prepared with 4- and 8-fold MIC of Elansolid A2 (Final concentration of DMSO in assay did not exceed 1%). The bacterial culture was diluted to an Optical Density (OD<sub>600</sub>) of 0.04 (~1 x 10<sup>7</sup> CFU/mL) and the bacteria were either left untreated or treated with elansolid A2 at 4-fold and 8-fold MIC, respectively. Samples were incubated at 37 °C and 180 rpm over the whole course of the experiment. At specified time points (0, 10, 20, 30, 45, 60, 90 min, 2 h, 3 h, 4 h, 5 h, 6 h and 24 h), OD<sub>600</sub> was measured, and cultures were plated on Tryptic Soy agar (TSA) (Millipore-Merck). CFU (colony-forming unit) counts were determined after 24 hours of incubation at 37 °C.

### 2.3.3 Mutant generation and characterization

Resistant colonies to elansolid A2 were generated and characterized. Briefly, OD<sub>600</sub> early logarithmic phase of growth of *S. aureus* Newman overnight-cultures was adjusted to 10 (~5 x 10<sup>9</sup> CFU/mL). 200 µL of the culture was confluently streaked on selective Tryptic Soy agar (TSA) (Millipore-Merck) containing 2- and 4-fold MIC of elansolid A2 to have ~1 x 10<sup>9</sup> CFU/plate. A culture was streaked on non-selective TSA (without elansolid A2) and served as a control for the growth of the wild type (wt.) *S. aureus* strain. Plates were incubated at 37 °C for 24 hours. Frequency of resistance was determined, resistant colonies were randomly selected, and MIC was determined. Resistant colonies that showed a shift in MIC to > 64 µg/mL were then selected as resistant mutants and these were further tested. Ten resistant colonies were selected, and for simplicity were given the abbreviation 'M', standing for mutant and a random number (1-10) e.g., M1 for mutant number 1.

### Whole genome sequencing

Genomic DNA extraction of the mutants was performed by phenol-chloroform with lysostaphin. DNA concentration and purity were measured by NanoDrop (Thermo Scientific™ NanoDrop 2000). Genomic DNA of different variants and one control *S. aureus* Newman strain was sequenced using Illumina Paired-End technology on the MiSeq instrument at the Helmholtz

Centre for Infection Research (Braunschweig, Germany). Raw data were imported into the Geneious 9.1.337 software package and trimmed of low-quality parts with an error probability threshold of 0.05. It was aligned against the *S. aureus* reference sequence. Assembly files were then converted to consensus sequences by the ‘Generate consensus sequence’ option in the Geneious software and ‘Highest quality’ consensus calling option. Resulting consensus sequences were aligned to each other and to the reference genome sequence by the ‘progressiveMauve’ algorithm of the MAUVE whole-genome sequence alignment tool.

### **Mutation reversibility and mutant growth kinetics**

Generated *S. aureus* mutants were characterized to study the reversibility of their elansolid-resistant phenotype and fitness cost. Mutants (M1-M8) and the respective wild-type (wt) strain were cultured in MHBII media without selective pressure and the culture was sub-cultivated 1:10<sup>5</sup> daily for 10 passages. MIC testing for the sub-cultivated cultures was performed to assess whether the mutants revert to the elansolid-sensitive wild type phenotype.

To study and compare the growth kinetics of the mutans (M1-M8) to the wild type (wt) strain of *S. aureus*, OD<sub>600</sub> of overnight cultures was adjusted to 0.1 (~1 x 10<sup>7</sup> CFU/mL) in fresh MHBII and the growth kinetics were assessed by measuring OD<sub>600</sub> on plate reader (Tecan Infinite M200Pro). The same experiment was performed under antibiotic pressure incubating the mutants (M1-M10) as well as the wild type strain with supra-MIC of 64 µg/mL of elansolid A2.

### **Assessment of metabolic activity with isothermal microcalorimetry**

To measure the metabolic activity of elansolid A2 mutants in the absence and presence of elansolid A2 pressure, the calScreener microcalorimeter (Symcel, Stockholm, Sweden) was used. Briefly, early logarithmic phase of growth of *S. aureus* of overnight cultures was adjusted to OD<sub>600</sub> of 0.01 (~1 x 10<sup>6</sup> CFU/mL). 100 µL of mutants (M1-M8) and wild type *S. aureus* strain were transferred to plastic inserts, then placed in titanium vials and tightened with

titanium lids using torque wrench, set to 40 cNm force. Similar approach was done for the mutants grown with supra-MIC of 64  $\mu$ g/mL elansolid A2. After instrument calibration, the heat flow was measured at 37 °C for 48 hrs. The ‘baseline’ and ‘main’ sections of the heat flow curves for the samples were defined and data were analyzed using the web based Symcel Calorimetry analysis application ([https://symcel.shinyapps.io/symcel\\_calorimetricgrowth/](https://symcel.shinyapps.io/symcel_calorimetricgrowth/)).

### **Cross-resistance with reference antibiotics**

To study the cross resistance of elansolid A2 with different antibiotics that target the ribosomes and cell wall synthesis, MIC testing with the elansolid-resistant mutants (M1-M8) and wild type *S. aureus* Newman was performed. Minimal inhibitory concentrations (MICs) were determined by standard broth microdilution (BMD) based on 2-fold serial dilutions of tested antibiotics (0.03-64  $\mu$ g/mL) according to guidelines of the Clinical & Laboratory Standards Institute (CLSI) (section 4.1). Antibiotics tested included: 30S ribosomal subunit inhibitors (Tetracyclin, Spectinomycin, Kanamycin and Gentamicin) and 50S ribosomal subunit inhibitors (Erythromycin, linezolid, and Chloramphenicol) and cell wall synthesis inhibitors (vancomycin and ampicillin). MIC of the mutants was determined against the panel of antibiotics to study any shift in MIC as compared to the wild type. All antibiotics used were purchased from Sigma-Aldrich and dissolved according to the manufacture’s recommendation.

### **Checkerboard assay**

The assay was used to evaluate synergism (or antagonism) between elansolid A2 and several antibiotics. Briefly, a 2-fold serial dilution of elansolid A2 (0.09-192  $\mu$ g/mL) in MHBII was prepared in a 96-well microtiter plate (panel A) with a volume of 100  $\mu$ L/well. Another 96-well plate (panel B) was used for the 2-fold serial dilution in MHBII of different antibiotics (30S ribosomal subunit inhibitors (tetracyclin, spectinomycin, kanamycin and gentamicin) and 50S ribosomal subunit inhibitors (Erythromycin, linezolid, and Chloramphenicol) and cell wall synthesis (vancomycin and ampicillin), respectively, with final 50  $\mu$ L/well. For each antibiotic,

the selected concentration ranges depended on previously determined MICs. After dilution, 50  $\mu$ L were transferred from wells of panel A and dispensed in the corresponding wells of panel B (final 100  $\mu$ L volume). 50  $\mu$ L of bacterial suspension of *S. aureus* Newman were added to the plate to achieve  $\sim 10^5$  CFU/mL (final volume 150  $\mu$ L/well). The plates were incubated at 37 °C for 24 hrs. and wells were observed for turbidity and OD<sub>600</sub> was measured. MIC of each of elansolid A2 (from panel A) and panel B (antibiotic) alone as well as the combination wells were observed. Each test was performed at least in duplicate and included a growth control without addition of any antibiotic. Fractional Inhibitory Concentration Index (FICI) of the combination of the two compounds in each row was calculated by the formula<sup>20</sup>:

$$\sum \text{FICI} = \text{FIC}_{\text{ElanA2}} + \text{FIC}_{\text{Antibiotic}}$$

$$= \frac{\text{MIC}_{\text{ElanA2 in combination}}}{\text{MIC}_{\text{ElanA2 alone}}} + \frac{\text{MIC}_{\text{Antibiotic in combination}}}{\text{MIC}_{\text{Antibiotic alone}}}$$

We refer to the FICI interpretation proposed by Odds, 2003<sup>20</sup> : FICI  $\leq 0.5$  synergy, FICI  $> 4$  antagonism and  $1 \leq \text{FIC} \leq 4$  indifference.

### Surface Plasmon Resonance SPR

To confirm the elansolid target, we studied the interaction of elansolid A2 with two ribosomal proteins S7 and S11 and determined the equilibrium dissociation constant (KD) by SPR. SPR analyses were performed on a Biacore X100 system (GE Healthcare). Recombinant *E. coli* 30S ribosomal protein S7 (*rpsG*) and S11 (*rpsK*) were purchased from 2BScientific (Oxfordshire). S7 and S11 proteins were diluted to 50  $\mu$ g/mL in 10 mM sodium acetate buffer (pH 4.5) and immobilized on CM5 sensor chips (Biacore) by standard amine coupling for 200 sec to reach  $\sim 3000$  response units (RU). All measurements were performed in duplicate. Increasing concentrations of elansolid A2 were injected over the immobilized S7 or S11 proteins: 50, 100, 200, 400 and 800  $\mu$ M. Binding interactions were monitored at 25 °C with a flow rate 30  $\mu$ L/min

in HBS-EP/5% DMSO as running buffer. The theoretical maximal RU (Rmax) for S7 and S11 was determined to be 74 and 100 RU, respectively, as calculated by the formula:

$$R_{max} = \frac{\text{Molecular weight (MW) Analyte}}{\text{Molecular weight (MW) Ligand}} \times \text{immobilized ligand density (RU)} \times \text{Stoichiometric ratio}$$

The MW of S7 and S11 protein is 23,900 and 17700 Da, respectively. The MW values for elansolid A2 is 589 Da. The stoichiometric ratio for all interactions were assumed to be 1. the K<sub>D</sub> values were calculated from the response data fitted to a model (the classical Langmuir binding model) using the Biacore X100 evaluation software 2.0.1.

## 2.4 Results

### 2.4.1 Antimicrobial susceptibility testing

Elansolid A2 was tested against a panel of Gram-positive and Gram-negative pathogens as well as *Mycobacterium* spp. The natural product showed good antimicrobial activity with an MIC of 4  $\mu\text{g}/\text{mL}$  with *S. aureus* Newman and no apparent cross-resistance in methicillin-resistant, vancomycin intermediate and daptomycin-resistant *S. aureus* strains. Other Gram-positive strains such as *S. carnosus*, *Micrococcus luteus* and penicillin-resistant *Streptococcus pneumoniae* were also sensitive towards elansolids with MICs in the range of 1-8  $\mu\text{g}/\text{mL}$ . Interestingly, *Bacillus subtilis* (MIC 32  $\mu\text{g}/\text{mL}$ ) and *Enterococcus* spp. (MIC 64  $\mu\text{g}/\text{mL}$ ) displayed reduced susceptibility. Gram-negative strains of the test panel were non-susceptible (*E. coli*, *P. aeruginosa* and *A. baumannii*) but a very weak activity was observed against an efflux-deficient *E. coli*  $\Delta tolC$  strain (MIC 64  $\mu\text{g}/\text{mL}$ ). Elansolid A2 did not show any inhibitory effect against the tested mycobacterial strains; *M. smegmatis*, *M. tuberculosis*, and *M. marinum* (MIC > 64  $\mu\text{g}/\text{mL}$ ). All data are summarized in **Table 1**. Given the importance as often multi-drug resistant nosocomial pathogen and as a member of the ESKAPE group, *S. aureus* - being particularly sensitive towards treatment with elansolid A2 - was chosen as model organisms to elucidate the mechanism of action of elansolids.

**Table 1: Antimicrobial susceptibility testing of elansolid A2**

Organism	Strain	MIC [µg/mL] of Elansolid A2
<i>Staphylococcus aureus</i>	Newman	4
	N315 (MRSA)	8
	Mu50 (VISA/MRSA)	4
	HG001 (wt)	4
	HG001(DRSA)	1
<i>Staphylococcus carnosus</i>	DSM20501	8
<i>Bacillus subtilis</i>	DSM10	32
<i>Micrococcus luteus</i>	DSM1790	1
<i>Streptococcus pneumoniae</i>	DSM 20566 (wt)	8
	DSM 11865 (PRSP)	8
<i>Enterococcus faecalis</i>	DSM20478	64
	DSM12956 (VRE)	64
<i>Enterococcus faecium</i>	DSM20477	64
	ATCC51559 (VRE)	64
<i>Pseudomonas aeruginosa</i>	PA14	> 64
<i>Acinetobacter baumannii</i>	DSM30008	> 64
<i>Escherichia coli</i>	DSM1116	> 64
	ΔtolC efflux-deficient	32-64
<i>Mycobacterium marinum</i>	Strain M	> 64
<i>Mycobacterium smegmatis</i>	mc <sup>2</sup> 155	> 64
<i>Mycobacterium tuberculosis</i>	H37 Ra	> 64

#### 2.4.2 Killing kinetics of elansolid A2 in *S. aureus*

To decipher the mode of action of elansolid A2, time-kill curves were recorded to monitor bacterial growth and death (Figure 3). For this, exponential phase *S. aureus* was treated with elansolid A2 at 2- and 4-fold MIC, and samples for counting of colony-forming units (CFUs) were taken at time points depicted in Figure 3. Over the course of the experiment (24 h), CFU/mL of the untreated control increased by ca. 1.5-log. Killing kinetics against *S. aureus* showed a reduction in number of viable cells directly after 15 minutes of treatment with 8 and 16  $\mu$ g/mL elansolid A2, respectively. A 3-log reduction of viable cell count, which is typically used to define a bactericidal mode of action, was achieved after approximately 2.5 h (4x MIC) and 4 h (2x MIC), respectively. Importantly, no regrowth of bacteria was recorded after 24 hours for neither of the two concentrations. Taken together, this kinetic profile indicates that elansolid A2 shows a bactericidal effect against *S. aureus* as defined as a reduction greater than 99.9% ( $> 3 \log_{10}$  units) of the total count in the original inoculum<sup>29</sup>.

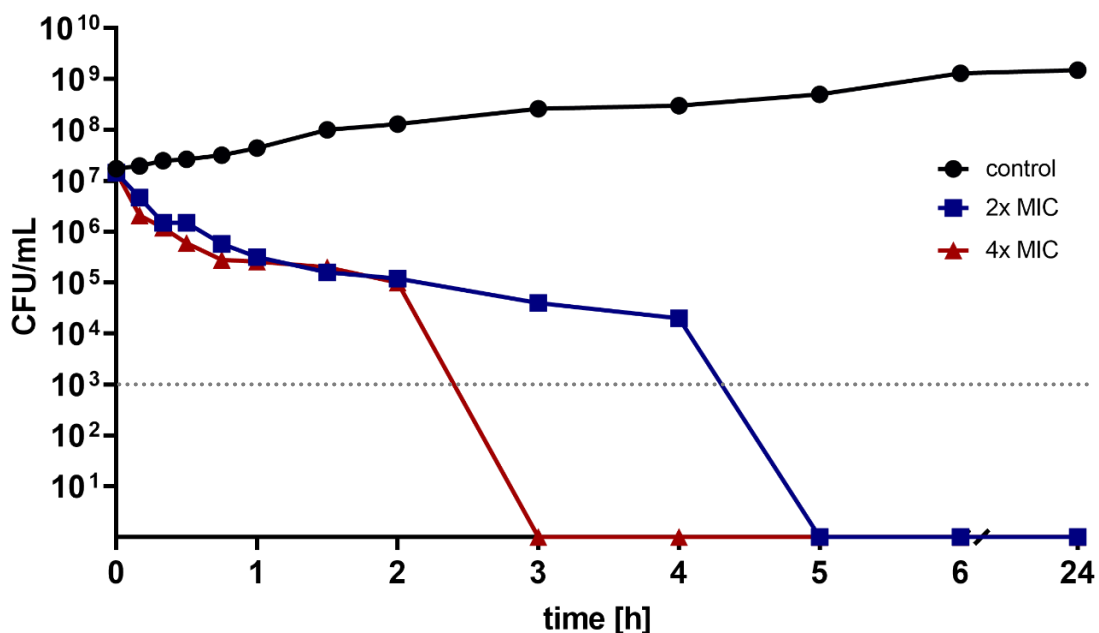


**Figure 3: Time-kill kinetics of elansolid A2 against *S. aureus* Newman.** 2- and 4-fold MIC (MIC = 4  $\mu$ g/mL) of elansolid A2 eradicated more than 99.9% of the total count in the original inoculum verifying a bactericidal activity. A 3-log reduction of viable cell count, which is typically used to define a bactericidal mode of action, was achieved after approximately 2.5 h (4x MIC) and 4 h (2x MIC), respectively. Dotted line represents limit of detection (LoD)

### 2.4.3 Mutant generation and characterization

The frequency at which resistant mutants appear *in vitro* is often used as an indicator of the overall mutation frequency in bacteria and the likelihood and time frame of resistant strains evolving after the introduction of an antibiotic into clinics. The frequency of resistance to elansolid A2 in *S. aureus* was high with a value of  $\sim 1 \times 10^{-7}$  at 4-fold MIC. For the mutant characterization, random ten colonies were picked from an agar plate containing elansolid A2 at 4-fold MIC (16  $\mu$ g/mL). The isolated colonies were then re-tested for MIC with elansolid A2 to confirm their resistant phenotype and the level of resistance. All colonies showed a shift in MIC to a value greater than 64  $\mu$ g/mL compared to an MIC of 4  $\mu$ g/mL with the wild type ( $> 16$ -fold shift). To study whether elansolid A2-resistance in *S. aureus* is reversible, the resistant mutants were grown without antibiotic pressure for several passages with daily 1:10<sup>5</sup> dilution into fresh growth medium. MIC was tested after 3 and 10 passages, respectively (data summarized in **Table 2**). MIC assessment showed that none of the mutants reverted to wild type level (MIC of 4  $\mu$ g/mL). These data suggest that the mutation is stabilized in the bacterial populations where antibiotic selective pressure is absent. Such stability might be due to the development of cost-free resistance mutations<sup>21</sup>.

**Table 2: MIC data of wild type (wt) and elansolid mutants (M1-M8) originally and after serial passages without selective pressure.**

## Whole genome sequence analysis

Having isolated elansolid A2-resistant *S. aureus*, whole genome sequencing was applied to identify mutations responsible for this phenotype. Intriguingly, point mutations in two 30S ribosomal genes, *rpsK* or *rpsG*, were found. Most of the variants developed mutations in *rpsK*, encoding for the tertiary binding protein **S11** (proline is replaced by alanine at position 60; P60A) situated on the platform of the 30S ribosomal subunit<sup>22-24</sup>. Only one mutant (M3) harbored a point mutation in *rpsG* encoding for the primary binding protein **S7** (proline is replaced by serine at position 88; P88S) located in the head of the 30S subunit (data summarized in Figure 4)<sup>23-25</sup>.

Protein	Structure	Gene	Organism	Sequence
				... 81 <b>88</b> 95 ...
			<i>S. aureus</i> reference strain	...GGSNYQV <b>P</b> VEVRPER...
			<i>S. aureus</i> Newman WT	...GGSNYQV <b>P</b> VEVRPER...
			M1, M2, M4-M8	...GGSNYQV <b>P</b> VEVRPER...
			M3	...GGSNYQV <b>S</b> VEVRPER...
<b>S7</b>		<i>rpsG</i>	<i>Escherichia coli</i>	...GGSTYQV <b>P</b> VEVRPVR...
			<i>Mycobacterium tuberculosis</i>	...GGATYQV <b>P</b> VEVRPDR...
			<i>Streptococcus pneumoniae</i>	...GGSNYQV <b>P</b> VEVRPER...
			<i>Thermus thermophilus</i>	...GGANYQV <b>P</b> MEVSPRR...
Protein	Structure	Gene	Organism	Sequence
				... 51 <b>60</b> 65 ...
			<i>S. aureus</i> reference strain	...GFKGSKK <b>STP</b> FAAQM...
			<i>S. aureus</i> Newman WT	...GFKGSKK <b>STP</b> FAAQM...
			M1, M2, M4-M8	...GFKGSKK <b>STP</b> AFAAQ...
			M3	...GFKGSKK <b>STP</b> FAAQM...
<b>S11</b>		<i>rpsK</i>	<i>Escherichia coli</i>	...GFRGSRK <b>STP</b> FAAQV...
			<i>Mycobacterium tuberculosis</i>	...GFKGSKK <b>STP</b> FAAQM...
			<i>Streptococcus pneumoniae</i>	...GFKGSRK <b>STP</b> FAAQM...
			<i>Thermus thermophilus</i>	...GYKGSRK <b>GT</b> YAAQL...

**Figure 4: Sequence of S7 (*rpsG*) and S11 (*rpsK*) ribosomal proteins of *S. aureus* reference strain, wildtype, and mutants M1-M8 in addition to a selection of bacteria.** S7 protein sequence of mutant M3 shows a replacement of proline by serine in residue 88 marked in red (P88S), with no mutation in S11 protein. S11 protein sequence of mutants M1, M2, M3-M8 shows a replacement of proline by alanine in residue 60 marked in red (P60A), with no mutation in S7 protein. Protein structures of S7 and S11 are presented in yellow and brown respectively. Residue highlighted in grey represent proline as a conserved amino acid in position 88 and 60 for S7 and S11 respectively, in reference *S. aureus* strain as well as other bacteria and mycobacteria. *S. aureus* reference strain NCTC8325/PS47 and *S. aureus* Newman strain as a wildtype. *Escherichia coli* (strain K12), *Mycobacterium tuberculosis* (strain ATCC25618/H37Rv), *Streptococcus pneumoniae* (strain ATCCBAA-255/R6), and *Thermus thermophilus* (strain ATCC27634/DSM 579/HB8). Sequences are obtained from Sequences from the Swiss-Prot protein database ([us.expasy.org/sprot](http://us.expasy.org/sprot))

The head and platform (**Figure 5-A**) of the small ribosomal subunit undergo a series of conformational changes and move along each other during translation. These conformational changes are affected by S7-S11(**Figure 5-A**) interaction during protein synthesis<sup>23</sup>. Both mutations in elansolid variants show a replacement of proline in the protein sequences. Unlike other proteinogenic amino acids, proline contains a secondary amino group as part of a pyrrolidine residue, a feature that highly restricts its conformational flexibility. Furthermore, proline can exist in both the *cis* and *trans* conformation in polypeptides conferring the amino acid an important role in protein folding, and is often found at the end of  $\alpha$  helix, in turns or loops<sup>26</sup>. Ribosomal proteins S7 and S11 interact via 148-155 region and the region encompassing residues 55–63 respectively. In elansolid mutants, mutation in S11 is located in residue 60 which is involved in the interaction with S7, however, mutation in S7 occurs in residue 88 which is not in the interaction region but in close proximity (**Figure 5-B**). The exchange of proline in either S7 or S11 in the mutants might change the conformation of the proteins and thus, hinder elansolid A2 from binding. We propose that elansolid A2 binds to the S7-S11 interface and prevents the interaction within the 30S subunit and further affects the dynamics of the ribosome. Crystal structures show that S7-S11 interaction aids in the formation of the exit channel, through which mRNA passes<sup>27</sup>. It was also observed that the C-terminal region of S7 could be cross-linked to the Shine-Dalgarno region of mRNA<sup>28</sup>. Further, it was demonstrated that the C-terminal domain of S7 contacts the anticodon of the tRNA bound to the E-site<sup>29</sup>. Moreover, cryo-electron microscopy (Cryo-EM) images suggest that translation initiation factor (IF3) binds to S7 and S11<sup>30</sup>. All the above-mentioned studies underline the importance of S7-S11 protein-protein interactions observed during the formation of a functional ribosome and their contribution to ribosome dynamics.

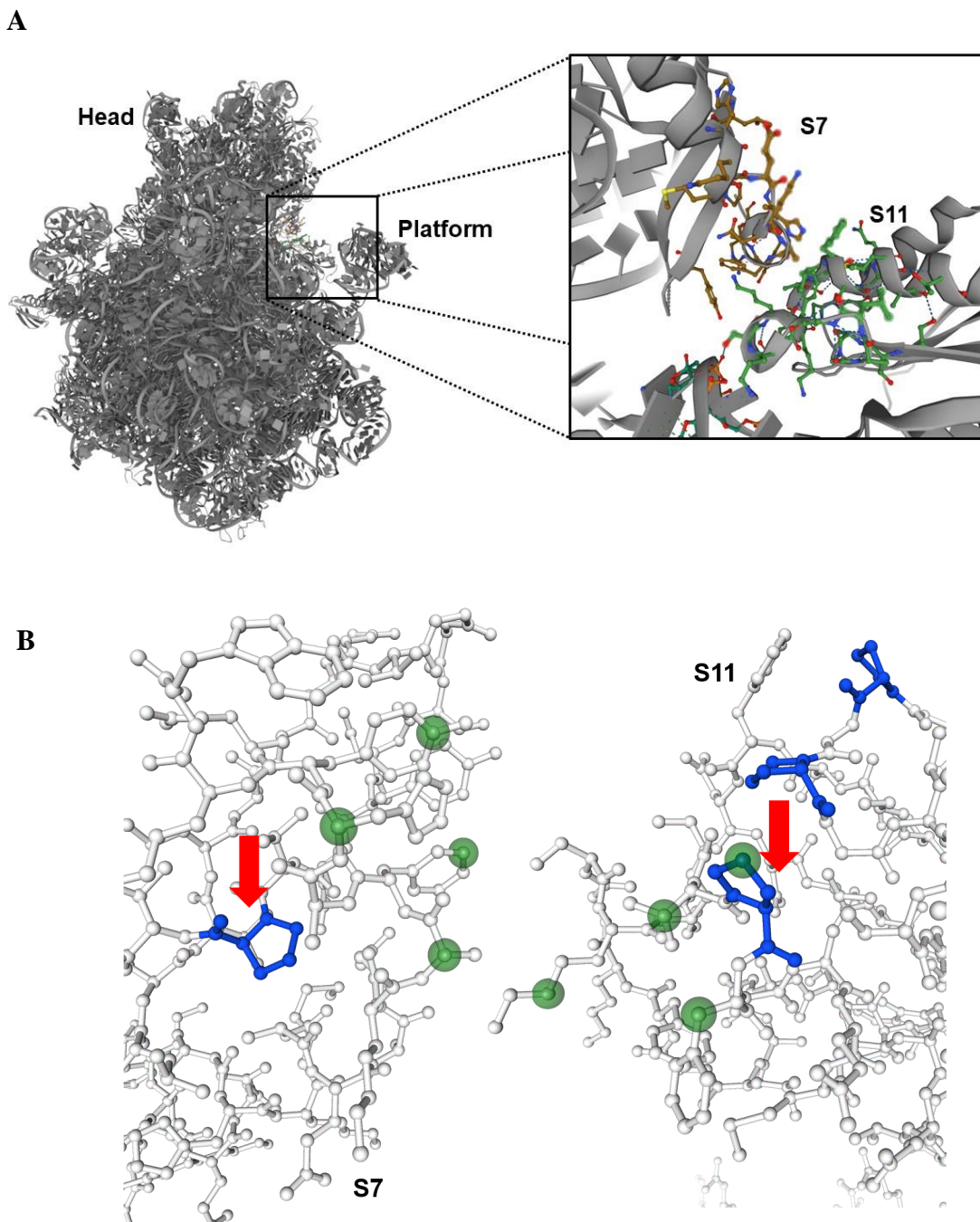


**Figure 5: Interaction between ribosomal proteins S7 and S11 in the 30S subunit.** (A) Crystallographic structure of the 30S ribosomal subunit of *S. aureus* showing the head and the platform. Zoomed picture displaying the interaction between S7 and S11 in brown and green respectively. (B) Ball-stick structure of S7 and S11 ribosomal proteins showing the residues involved in the binding in green. Structures in blue represent proline and the red arrow shows the position of the mutation observed in elansolid mutants. *Crystallographic structure of the 30S ribosome is obtained from the Swiss-Prot protein database ([us.expasy.org/sprot](http://us.expasy.org/sprot))*

### Mutant growth kinetics

To further investigate whether resistance to elansolid A2 in *S. aureus* influences the growth kinetics of the bacteria and their ability to replicate, we assessed Optical Density (OD<sub>600</sub>) values over time. As already suggested by the observed non-reversible resistance phenotype, we did not identify apparent differences in growth kinetics for the mutants compared to the wild type (**Figure 6-A**). However, we also assessed the growth kinetics of individual mutants under antibiotic pressure. For this, mutants as well as the wild type *S. aureus* strain were cultured with 64 µg/mL elansolid A2 (16-fold MIC, *S. aureus* wild type) (**Figure 6-B**). Intriguingly, although all isolated mutants are per definition resistant, as assessed in end-point MIC determination, we found one mutant (M3) with a mutation in S7 (*rpsG*) to exhibit a significantly slower growth rate in the presence of elansolid A2. We hypothesize that mutation in *rpsG* is least favored as it does not induce the same level of resistance and might have a more dramatic effect on the bacterial growth than the mutation in *rpsK*.

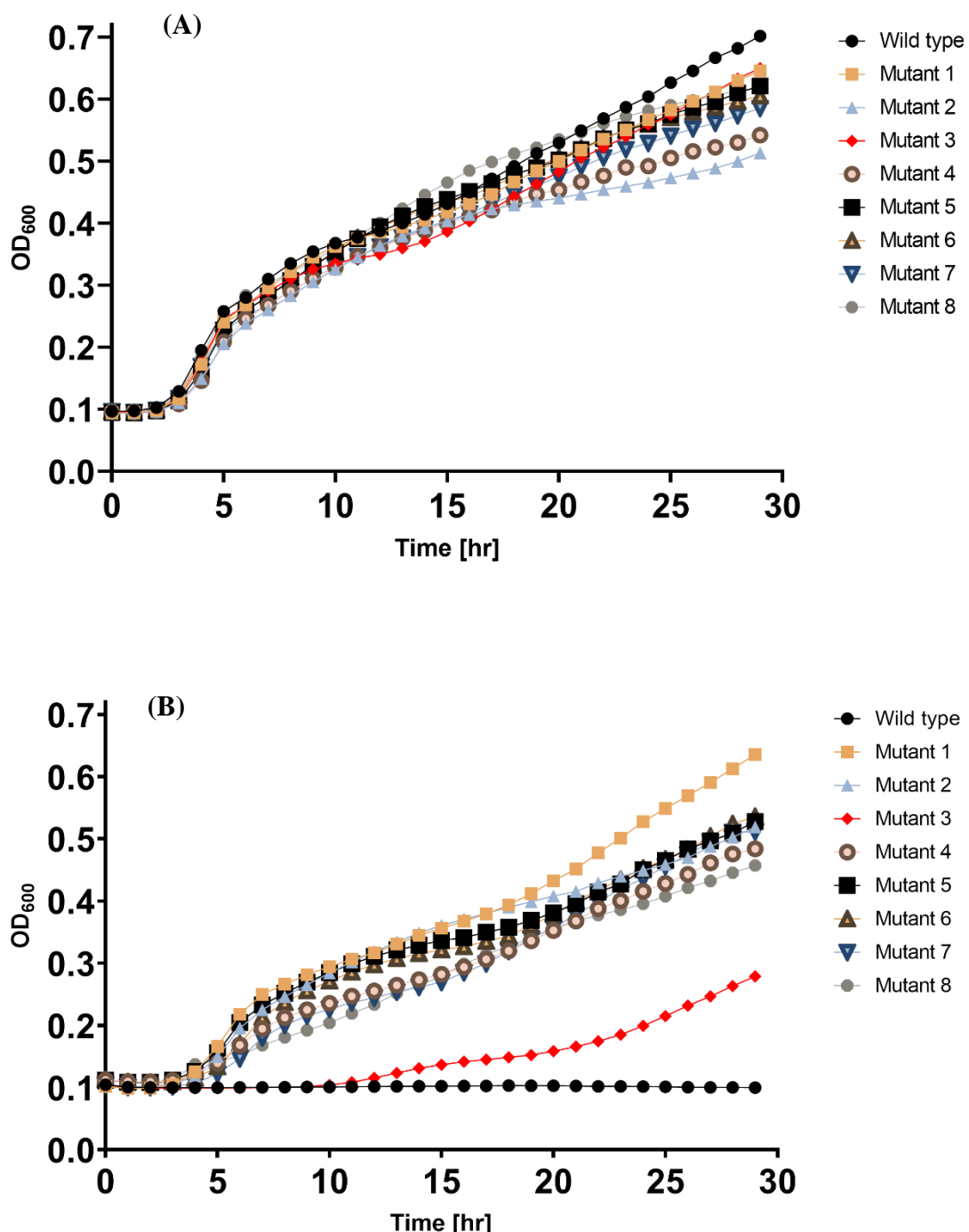


**Figure 6: Growth kinetics as a measurement of optical density over time.** OD<sub>600</sub> of *S. aureus* wild type strain and mutants assessed over 30 hrs for (A) untreated samples and (B) treated with 64 µg/mL elansolid A2. Unlike others, the variant expressing the mutation in *rpsG* encoding for S7 protein showed a slow and delayed growth kinetic in the presence of elansolid A2.

### Assessment of metabolic activity with isothermal microcalorimetry

In an orthogonal assay, the fitness of mutants in the absence and presence of elansolid A2 was evaluated on the level of the microcalorimeter calScreener™ (Symcel, Sweden). The latter allows the measurement of the total metabolic activity by the direct measurement of heat release from biological specimens. The data were analyzed using CalView software (Symcel) and presented as heat flow thermograms. **Figure 7** represents the heat flow profile of *S. aureus* wt and mutants (M1-M8), untreated and treated with 64 µg/mL, as a detection of bacterial activity. M3 harboring the mutation in *rpsG* (S7) showed ~5-fold increase in heat flow compared to other mutants harboring mutation in *rpsK* (S11), both, when untreated and treated with 64 µg/mL elansolid A2. Furthermore, when treated with elansolid A2, M3 showed a significant shift in lag and exponential phase (shift from 8 to 12 h), a longer stationary phase that lasts from 18 to 26 h (shift from 2 to 8 h) and a high heat flow. These data suggest that M3 has a different metabolic activity than other mutants. The metabolic rate of the elansolid A2-treated wildtype (**Figure 8**) was low since elansolid A2 exerts its antibiotic effect preventing most energy release of the sample. All mutants except for the variant M3 expressing the mutation in S7 (*rpsG*) showed a normal metabolic rate for treated and untreated samples. However, M3 showed a peak in metabolic rate, ~4-fold higher than other mutants. Such increase in metabolic rate demonstrates that the bacteria is undergoing a high metabolic activity which can be explained e.g., by a large energetic burden (fitness cost) for the mutant harboring *rpsG* mutation to survive.

The measurement of heat release as a representation of metabolic activity of M3 is in line with the slow growth kinetics of this mutant compared to other mutants. These data further prove that the S7 mutation might influence the bacteria in a more dramatic way than other mutations in S11 proteins. This is reflected by the low incidence of such mutation, a slow growth rate and a high metabolic rate. We speculate that mutation in the S7 protein of the 30S ribosomal subunit has a severe impact on the cell, given the importance of S7 in cross-linkage to the Shine-

Dalgarno region of mRNA and the contact to anticodon tRNA in the E-site during protein synthesis<sup>28,29</sup>.

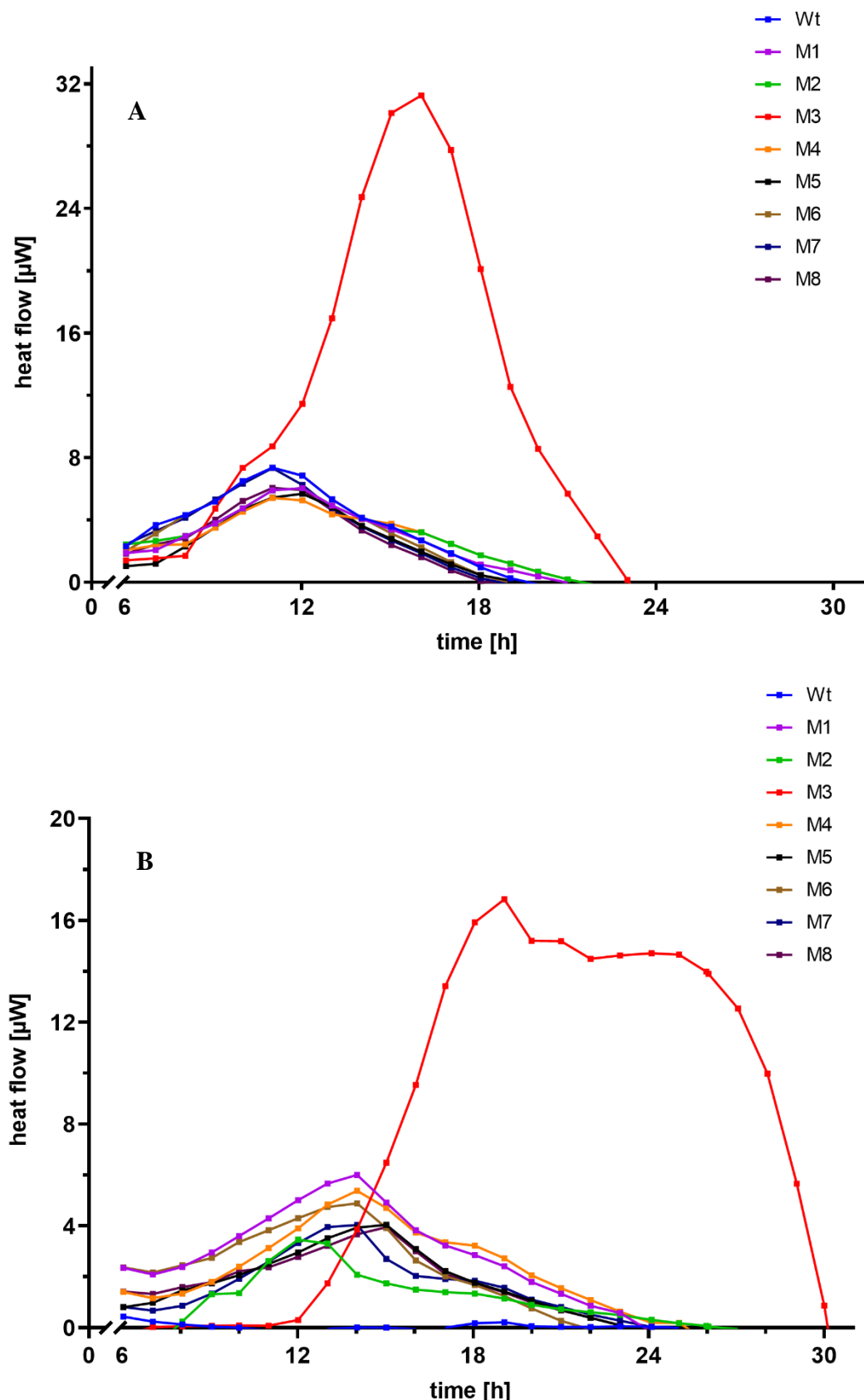


**Figure 7: Thermograms presented as heat flow vs. time for *S. aureus* wild type (wt) and mutants (M1-M8). (A) untreated wt and M1, M2, M4-M8 samples show a normal heat flow, unlike M3 that shows a higher peak in heat flow. (B) unlike other mutants, treatment with 64  $\mu\text{g/mL}$  of elansolid A2 shows a shift in lag and exponential phase, high peak of heat flow and a longer stationary phase in M3.**

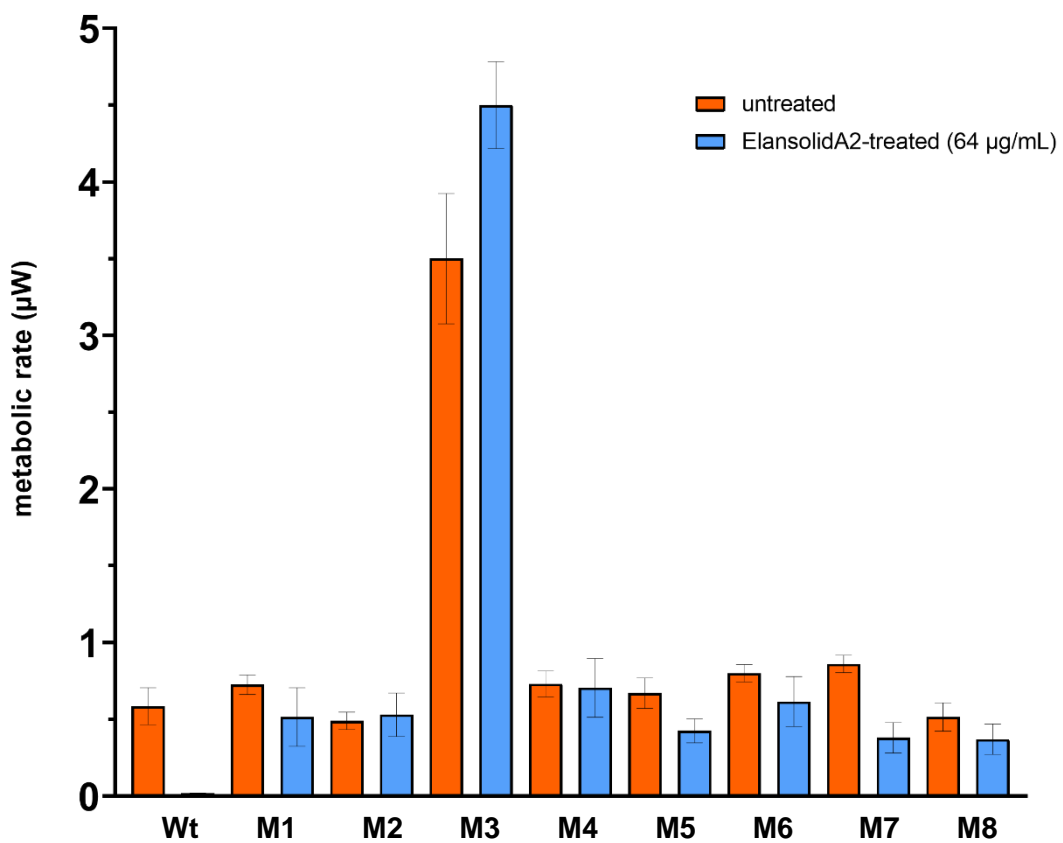


**Figure 8: Metabolic rate of *S. aureus* wildtype and mutants untreated and treated with elansolid A2.** M3 shows a high metabolic rate as measured compared to the other mutations (M1, M2, M4-M8) both when treated with elansolid A2 and when kept untreated.

## Cross-resistance studies with reference antibiotics

To study cross-resistance between elansolid A2 and other antibiotics, mainly those targeting protein biosynthesis, susceptibility profiles of mutants were generated and summarized in

**Table 3.** All mutants showed MIC values greater than 64 µg/mL for elansolid A2 as seen before, but they remained susceptible to all the other tested antibiotics, hence, no cross-resistance could be observed with neither 30S ribosomal subunit inhibitors (kanamycin, gentamicin, tetracycline, and linezolid) nor 50S ribosomal subunit inhibitors (linezolid, erythromycin, chloramphenicol) or antibiotics inhibiting cell wall synthesis (ampicillin and vancomycin). This further supports the assumption that elansolid A2 has a distinct mode of action in targeting the ribosome.

**Table 3: Susceptibility of elansolid A2 resistant *S. aureus* strains to a panel of ribosomal inhibitors.**

### Checkerboard assay to study synergism of elansolid A2

Assuming that antibiotics targeting the same cellular process through a different mechanism might exert synergistic activity (e.g., seen with the combination of folate synthesis inhibitors trimethoprim and sulfamethoxazole) checkerboard assays were performed to investigate interactions between elansolid A2 and a panel of antibiotics that target different sites of the ribosome<sup>31</sup>. Such an assay can help to decide if a specified combination of two antibiotics is useful (synergism) for antimicrobial therapy. On the other hand, antagonism can result from competition for target sites providing details on the mode of action of the respective antibiotic<sup>32</sup>.

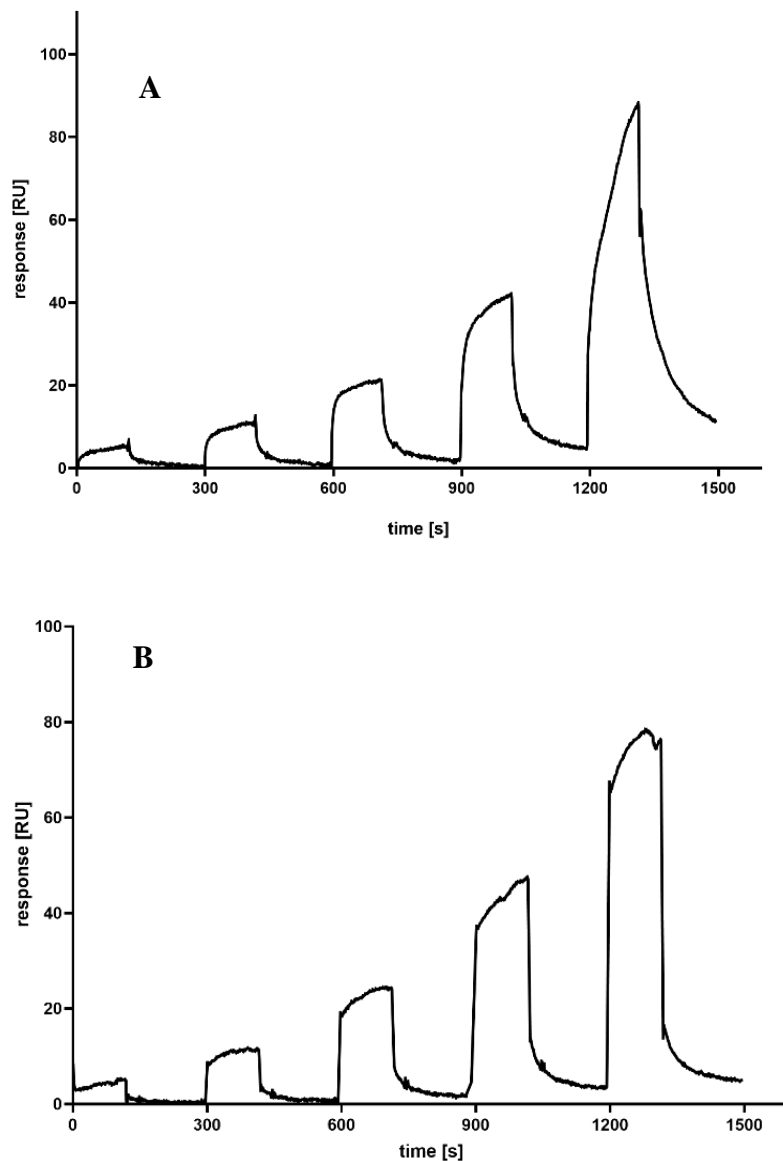
Elansolid A2 was shown to exert synergistic effects ( $\Sigma$  FICI = 0.5) with the 50S ribosomal subunit inhibitors erythromycin, chloramphenicol, and linezolid. No synergism ( $0.5 < \Sigma$  FICI < 4) with 30S ribosomal subunit inhibitors and the cell wall inhibitor vancomycin, which was used as a control. Elansolid A2 did not show antagonistic effects to any of the tested antibiotics indicating that it targets a distinct binding site. Data are summarized in **Table 4**.

**Table 4: Combination testing of elansolid A2 with different reference antibiotics. FICI: fractional inhibitory concentration index; I: indifference; S: synergism.**

	MIC [µg/mL]			$\Sigma$ FICI	Activity
	Antibiotic alone	Antibiotic in combination with Elansolid A2	Elansolid A2 in combination with antibiotic		
<b>Erythromycin</b>	0.5	0.125	1	0.5	<b>S</b>
<b>Chloramphenicol</b>	16	4	1	0.5	<b>S</b>
<b>Linezolid</b>	2	0.5	1	0.5	<b>S</b>
<b>Kanamycin</b>	8	1	2	0.625	<b>I</b>
<b>Vancomycin</b>	2	1	2	1	<b>I</b>
<b>Tetracycline</b>	0.5	0.25	2	1	<b>I</b>

### Surface Plasmon Resonance SPR

To confirm our genome-based findings that S7 and S11 ribosomal proteins are the target of elansolid A2, we used surface plasmon resonance (SPR) to characterize the binding of elansolid to each protein independently. SPR analysis demonstrated binding of elansolid A2 to *E. coli* ribosomal proteins with high affinity (equilibrium dissociation constant  $K_D$ :  $2.3 \times 10^{-9}$  M and  $1.3 \times 10^{-9}$  M for S7 and S11 proteins, respectively) and a fast recognition rate and slow dissociation from the protein (S7,  $k_a$ :  $1.5 \times 10^7$  M $^{-1}$  s $^{-1}$ , dissociation rate constant  $k_d$ :  $3 \times 10^{-2}$  s $^{-1}$ ; S11,  $k_a$ :  $7.8 \times 10^6$  M $^{-1}$  s $^{-1}$ ,  $k_d$ :  $10 \times 10^{-3}$  s $^{-1}$ ) (Figure 9). No binding was detected between the two ribosomal inhibitors, tetracycline, and erythromycin to S7 or S11.  $K_D$  values were calculated from the response data fitted to a model (the classical Langmuir binding model) using the Biacore X100 evaluation software 2.0.1.



Analyte	Ligand	$K_D$ [M]	$K_a$ [M $^{-1}$ s $^{-1}$ ]	$k_d$ [s $^{-1}$ ]
Elansolid A2	S7 protein	$2.3 \times 10^{-9}$	$1.5 \times 10^7$	$3 \times 10^{-2}$
	S11 protein	$1.3 \times 10^{-9}$	$7.8 \times 10^6$	$10 \times 10^{-3}$

**Figure 9: SPR-based kinetics of elansolid A2 binding to S7 and S11 ribosomal proteins.** Langmuir graph of elansolid A2 binding to (A) S7 and (B) S11 protein. Table showing values calculated from the response data fitted to a model (the classical Langmuir binding model) using the Biacore X100 evaluation software 2.0.1.  $K_D$ : equilibrium dissociation constant,  $k_a$ : association rate constant,  $k_d$ : dissociation constant.

## 2.5 Discussion

The elansolids represent a novel class of macrolide antibiotics with good activity against Gram-positive pathogens such as *S. aureus* and *S. pneumoniae* and a presumably unique ribosomal target. The *in vitro* frequency of resistance (FoR) of *S. aureus* was high ( $\sim 10^{-7}$ ) at 4-fold MIC of elansolid A2 and the mutation is stable and without any fitness cost as shown by metabolic activity measurement in the absence of antibiotic pressure. This suggests that the antibiotic development might be hindered by the fast development of a stable resistant population. Despite the high FoR of elansolid A2 *in vitro*, an important alternative should be taken into consideration; the mutant prevention concentration (MPC). The latter is defined as the lowest concentration of an antimicrobial agent that limits the occurrence of resistant mutants and is a measurement of concentration that has been used to prevent or minimize the selection of resistant strains during drug therapy<sup>33,34</sup>. In general, the *in vitro* determination of FoR depends on the standard MIC values, which do not completely correlate with *in vivo* results<sup>35</sup>. Thus, determination of the interval between the MIC and MPC, known as mutant selection window (MSW), is important to define the *in vitro* antimicrobial concentrations that favor the selection of resistant mutants<sup>33,36</sup>.

Although most of the ribosomal inhibitors exert their effect in a bacteriostatic mode of action (e.g., oxazolidinones, and streptogramins), elansolid A2 exerts a bactericidal killing effect against *S. aureus* as shown by time-kill curves. This is in line with aminoglycosides, that display a very rapid bactericidal effect at higher concentrations, especially in clinical practice, and macrolide (ketolide) family of antibiotics that include bactericidal (e.g., telithromycin or solithromycin) inhibitors<sup>37</sup>. The genes involved in resistance were identified by genome sequence analysis of several elansolid-resistant *S. aureus* mutants. Most *S. aureus* elansolid-resistant variants developed a point mutation in *rpsK* (encodes for 30S ribosomal protein S11, positioned in the platform) and one mutant showed a point mutation in *rpsG* (encodes for 30S ribosomal protein S7, positioned in the head). S7-S11 interaction has been identified as a crucial protein-protein interaction (PPI) for the ribosome function, allowing the formation of the exit

channel for mRNA passage. Further, the S7-S11 PPI induces a conformational change in the head and platform of the 30S ribosomal subunit during assembly, binding of translation factors (e.g. translational initiation factor IF3) or aminoacyl-tRNA (aatRNA) and during translocation<sup>23,29,30</sup>. Only one out of the eight analyzed mutants had a mutation in S7 protein and showed slow growth kinetics as monitored by optical density, and high metabolic activity as reflected by a peak in heat production compared to the other variants under antibiotic pressure. Unlike mutations in S11, the mutation in S7 is less efficient in conferring high-level resistance since mutant growth is only delayed in the presence of elansolid (and no cost without antibiotic pressure)

In *E. coli*, S7-S11 interaction involves S7 residues 148, 150, 152, 153 and 154, within 148–155 region, which is missing in eukaryotes and archaeabacteria and S11 residues 55, 58, 59, 60, and 63 which is less conserved in eukaryotes and archaeabacteria<sup>23</sup>. This region of interaction is highly conserved in bacteria as represented in **Figure 9**, showing the S7 and S11 sequence examples of four representative bacteria: *E. coli*, *T. thermophilus*, *S. aureus* and *S. pneumoniae* and *M. tuberculosis*<sup>23,38</sup>. Crystal structure studies of the bacterial 30S subunit based on site-directed mutagenesis to disrupt the interaction between S7 and S11, included either deletion of the 148-155 region in S7 or introduction of mutations in S7 and S11 interaction region. The results revealed that such mutations made the ribosomes error-prone and increased the capacity of the 30S to bind mRNA<sup>23</sup>. The disruption of contacts between S7 and S11, which are in the ribosome exit (E) site, presumably impairs the coupling between the E and A (aminoacyl) sites, which could contribute to decrease in the translational fidelity and make the ribosomes more susceptible to errors. Furthermore, disrupting the interaction might cause a disturbance in the exit channel, that is formed by the interaction of the two proteins, hindering it open, making it easier for the mRNA to bind and thus increasing the capacity of 30S to bind mRNA<sup>23</sup>. All elansolid variants with a mutation in *rpsK* that encodes for S11, show a replacement of proline by alanine in position 60 (P60A) which is among the residues involved in the binding to the S7,

affecting the assembly of the two ribosomal proteins and further impeding the ribosome function (**Figure 4 and 9**). Furthermore, proline residue in position 60 (P60) is highly conserved in bacteria (**Figure 9**) and given the importance of proline in polypeptide chain to reverse its direction, we hypothesize that such amino acid replacement prevents the interaction with the S7<sup>23,39</sup>. Genome analysis gives further evidence that elansolid A2 binds to S11 and prevents its interaction with S7 which impacts the dynamics of the ribosome and consequently inhibits protein synthesis.

Although the mutation observed in S7 protein occurred in position 88 (P88S) which is far from the 148-155 region that binds the S11, the proline residue 88 (P88) is conserved in most bacteria and its replacement might further impact the structure of the S7 and its binding to S11 or to translation factors in the small ribosomal subunit (**Figure 9**). In the same study, Robert et al., showed that when only S7, but not S11 protein, was mutated within the contact site, the capacity of association between the 30S ribosomal subunit to the 50S subunit decreased<sup>23</sup>. This shows that the mutation in S7 affects the ribosome in a more dramatic way than the mutation in S11. These findings relate to our observation with the variant harboring S7 mutation which showed a slower growth kinetics and consumed more energy to survive the antibiotic effect, which can be reflected as fitness loss. This can further explain that the predominance of S11 mutations, having a smaller impact on 30S-50S interaction than S7 mutations, may be preferred to hinder elansolid binding at the PPI site as the ribosome stays probably functional for the variant harboring S7 mutation. We hypothesize that elansolid binding to S7 blocks the interaction of the latter with S11 and/or other binders such as 16S rRNA and decreases the association between 30S and 50S subunits, leading to the failure in assembly of a functional ribosome and ultimately inhibiting protein synthesis. Given the importance of S7-S11 interaction in the

dynamics and functionality of the ribosomes, elansolid is the first reported antibiotic class that targets this site and inhibits protein synthesis.

Protein	Gene	Organism	Protein sequence
148 — 155			
S7	rpsG	<i>Escherichia coli</i>	...AEAN <u>KAFAHYR</u> W...LN
		<i>Staphylococcus aureus</i>	...AEAN <u>KAFAHYR</u> W
		<i>Mycobacterium tuberculosis</i>	...AEAN <u>RRAFAHYR</u> W
		<i>Streptococcus pneumoniae</i>	...AEAN <u>RRAFAHFR</u> W
		<i>Thermus thermophilus</i>	...AEAN <u>NRAYAHYR</u> W
Protein	Gene	Organism	Protein sequence
55 — 63			
S11	rpsK	<i>Escherichia coli</i>	...FRG <u>SRKSTPFAA</u> QV...RV
		<i>Staphylococcus aureus</i>	...FKG <u>SKKSTPFAA</u> QM...RV
		<i>Mycobacterium tuberculosis</i>	...FKG <u>SRKSTPFAA</u> QL...RV
		<i>Streptococcus pneumoniae</i>	...FKG <u>SRKSTPFAA</u> QA...RV
		<i>Thermus thermophilus</i>	...YKG <u>SRKGTPYAA</u> QL...AS
		<i>Staphylococcus aureus M1, M2, M4-M8</i>	...FKG <u>SKKSTAFAA</u> QM...RV

**Figure 9: Sequence of S7 (rpsG) and S11 (rpsK) ribosomal proteins.** A representative sequence of the 148-155 region of ribosomal protein S7 and of the region encompassing residues 55–63 of ribosomal protein S11 from different organisms. The highlighted, underlined sequences represent the region of interaction between S7 and S11. Marked in red is the alanine residue replacing proline in elansolid mutants M1, M2, M4-M8 in the region of S11 that interacts with the S7 protein in the 30S ribosomal subunit. *Escherichia coli* (strain K12), *Staphylococcus aureus* (strain NCTC 8325/PS47), *Mycobacterium tuberculosis* (strain ATCC25618/H37Rv), *Streptococcus pneumoniae* (strain ATCCBAA-255/R6), and *Thermus thermophilus* (strain ATCC27634/DSM 579/HB8). Sequences are obtained from Sequences from the Swiss-Prot protein data base ([us.expasy.org/sprot](http://us.expasy.org/sprot))

To confirm our genomic-based findings that S7 and S11 ribosomal proteins are the target of elansolid A2, we used surface plasmon resonance (SPR) to characterize the binding of elansolid A2. SPR analysis demonstrated binding of elansolid A2 to *E. coli* ribosomal proteins with high affinity with a fast recognition rate and slow dissociation from the protein. To further validate the ribosomal target of elansolid A2, we studied the efficiency of translation inhibition by *in vitro* *E. coli* lysate-based translation assay by monitoring luminescence induction resulting from expression of a firefly luciferase (Fluc) reporter protein. Elansolid A2 inhibits the *in vitro* translation with a half-inhibitory concentration (IC50) of ~6 µM (data not shown). Moreover,

we investigated by primer extension inhibition assays, toeprinting experiments, the position of the arrested ribosome on mRNA upon treatment with elansolid A2. We found out that elansolid A2 (at 5  $\mu$ M) traps the ribosome with the initiator tRNA in the P-site preventing the elongation step (data not shown). We suppose that elansolid blocks the first translocation is as it binds near the S7-S11 interface. These data further suggest that elansolid targets the ribosome not only in Gram-positive, but also in Gram-negative bacteria, but the activity against Gram-negative bacteria is hampered by the insufficient uptake and efflux<sup>40</sup>. This is in line with previous findings by Beckmann et al., where they showed than elansolid A2 exhibited an MIC of 2  $\mu$ g/mL against efflux-deficient *E. coli*  $\Delta tolC$  in combination with the membrane-permeabilizing peptide polymyxin B nonapeptide (PMBN)<sup>14</sup>.

To study the structure of the bacterial ribosomes, its subunits and functional complexes, cryo-Electron Microscopy (cryo-EM) reconstruction methods have offered high resolution views of the ribosome and explained a number of interactions<sup>29</sup>. The advances in high resolution X-ray structures of the bacterial ribosomes and the 30S and 50S subunits, has further facilitated the study of the molecular mechanism of action of ribosomal inhibitors. Nowadays, crystal structures of ribosomes complexed with almost all the major classes of ribosomal inhibitors, are available<sup>41</sup>. Crystal structures of isolated 30S and 50S subunits from *Thermus thermophilus* present an excellent atomic-resolution structures of the ribosome, and provided an insight on the interactions between tRNA, mRNA, antibiotics and translation factors and the ribosome in the A, P, and E sites<sup>29,42,43</sup>. Current work is focused on co-crystallizing elansolid A2 in complex with the *Thermus thermophilus* 70S ribosome. Initial data did not show a density in the empty ribosomes, 70S-PY crystals, when soaked with elansolid A2. However, current work is focused co-crystallizing elansolid A2 with 70S ribosomes in functional complexes with mRNA and A-, P-, and E-site tRNAs. This approach represents a more physiologically relevant type of complex and would allow us to study the interaction of elansolid A2 with the ribosome in the presence of mRNA and/or tRNA, that might be required for the drug to bind to the ribosome. In parallel to

X-ray crystallization efforts, cryo-EM imaging of elansolid A2 in complex with P-tRNA programmed *E. coli* ribosomes are ongoing. It is assumed that a P-tRNA programmed ribosomes rather than empty one and would give a better structure and provide further evidence for the presumed mode of inhibition.

## 2.6 Conclusion

The continuous increase in the emergence of threatening multidrug-resistant (MDR) pathogenic bacteria has been a major concern in the past decade<sup>44</sup>. The multidrug-resistant methicillin-resistant *Staphylococcus aureus* (MRSA) is of a great concern in hospitals and communities<sup>45</sup>. This alarming spread of MDR pathogens, demands the discovery of novel antibacterial agents with unique chemistry and novel mode of action. Natural products have been an important source for the discovery and development of antibiotics with new and complex chemical structures, and unique molecular targets. Challenging targets, such as the inhibition of protein-protein interactions that were considered for a long time as undruggable in the context of synthetic small molecule screening, can be addressed by natural product scaffolds<sup>46</sup>. Ribosomes represent a highly validated target for antibacterial drug discovery. Here, we presented elansolids, a group of secondary metabolites that exhibited a promising, bactericidal activity against several Gram-positive bacteria including drug-resistant *Staphylococcus aureus*. Mutant analysis by whole genome sequencing revealed the target being the 30S ribosomal proteins S7 and S11. *In vitro* proteins synthesis experiments further proved translation inhibition and toeprinting experiments further confirmed that elansolid A2 traps the ribosome with the initiator tRNA in the P-site preventing the elongation step. Biophysical assay (SPR) additionally validated at molecular level, the interaction of elansolid with S7 and S11 at high affinity. With the majority of ribosomal antibiotics targeting the RNA component of the ribosome, a few 30S ribosomal protein have been identified as targets for antibiotics<sup>44,47</sup>. S12 (*rpsL*) located in the A-site of the small ribosomal subunit, is a known target for streptomycin as shown in *E. coli*, *M. tuberculosis* and *L. biflexa*<sup>48</sup>. Additionally, streptomycin binding site is reported to be located

in the interface between the ribosomal subunits, close to proteins S5 (*rpsE*) in the 30S subunit, and moderate spectinomycin resistance was reported due to mutations in ribosomal protein S5 found in clinical *N. gonorrhoeae* strain<sup>49,50</sup>. Assuming that our findings can be confirmed in biochemical and structural biology studies, elansolids binding to S7-S11 would be the first antibiotic class targeting this site on the ribosome nicely explaining the lack of cross resistance with known antibiotic.

## 2.7 References

- (1) Harvey, A. L.; Edrada-Ebel, R.; Quinn, R. J. The Re-Emergence of Natural Products for Drug Discovery in the Genomics Era. *Nat Rev Drug Discov* **2015**, *14* (2), 111–129. <https://doi.org/10.1038/nrd4510>.
- (2) Atanasov, A. G.; Zotchev, S. B.; Dirsch, V. M.; Supuran, C. T. Natural Products in Drug Discovery: Advances and Opportunities. *Nat Rev Drug Discov* **2021**, *20* (3), 200–216. <https://doi.org/10.1038/s41573-020-00114-z>.
- (3) Katz, L.; Baltz, R. H. Natural Product Discovery: Past, Present, and Future. *Journal of Industrial Microbiology and Biotechnology* **2016**, *43* (2–3), 155–176. <https://doi.org/10.1007/s10295-015-1723-5>.
- (4) Bérdy, J. Bioactive Microbial Metabolites: A Personal View. *J Antibiot* **2005**, *58* (1), 1–26. <https://doi.org/10.1038/ja.2005.1>.
- (5) Antibiotic resistance in the environment: a link to the clinic? - ScienceDirect [https://www.sciencedirect.com/science/article/pii/S1369527410001190?casa\\_token=zSRTLzTPgmUAAAAA:bqQ4bgWpyr2h2SnIuhzjFZUECsV116DM0FHJ14y8PMQ-82ib5xroLzOaDks8LNHfAx4LPkIJVQ](https://www.sciencedirect.com/science/article/pii/S1369527410001190?casa_token=zSRTLzTPgmUAAAAA:bqQ4bgWpyr2h2SnIuhzjFZUECsV116DM0FHJ14y8PMQ-82ib5xroLzOaDks8LNHfAx4LPkIJVQ) (accessed 2021-12-14).
- (6) Steinmetz, H.; Gerth, K.; Jansen, R.; Schläger, N.; Dehn, R.; Reinecke, S.; Kirschning, A.; Müller, R. Elansolid A, a Unique Macrolide Antibiotic from Chitinophaga Sancti Isolated as Two Stable Atropisomers. *Angewandte Chemie International Edition* **2011**, *50* (2), 532–536. <https://doi.org/10.1002/anie.201005226>.
- (7) Kämpfer, P.; Young, C.-C.; Sridhar, K. R.; Arun, A. B.; Lai, W. A.; Shen, F. T.; Rekha, P. D. Y. 2006. Transfer of [Flexibacter] Sancti, [Flexibacter] Filiformis, [Flexibacter] Japonensis and [Cytophaga] Arvensicola to the Genus Chitinophaga and Description of Chitinophaga Skermanii Sp. Nov. *International Journal of Systematic and Evolutionary Microbiology* **56** (9), 2223–2228. <https://doi.org/10.1099/ijns.0.64359-0>.
- (8) Smyth, J. E.; Butler, N. M.; Keller, P. A. A Twist of Nature – the Significance of Atropisomers in Biological Systems. *Nat. Prod. Rep.* **2015**, *32* (11), 1562–1583. <https://doi.org/10.1039/C4NP00121D>.
- (9) LaPlante, S. R.; Edwards, P. J.; Fader, L. D.; Jakalian, A.; Hucke, O. Revealing Atropisomer Axial Chirality in Drug Discovery. *ChemMedChem* **2011**, *6* (3), 505–513. <https://doi.org/10.1002/cmdc.201000485>.
- (10) Toenjes, S. T.; Gustafson, J. L. Atropisomerism in Medicinal Chemistry: Challenges and Opportunities. *Future Med Chem* **2018**, *10* (4), 409–422. <https://doi.org/10.4155/fmc-2017-0152>.
- (11) Steinmetz, H.; Zander, W.; Shushni, M. A. M.; Jansen, R.; Gerth, K.; Dehn, R.; Dräger, G.; Kirschning, A.; Müller, R. Precursor-Directed Syntheses and Biological Evaluation of New Elansolid Derivatives. *ChemBioChem* **2012**, *13* (12), 1813–1817. <https://doi.org/10.1002/cbic.201200228>.
- (12) Jansen, R.; Gerth, K.; Steinmetz, H.; Reinecke, S.; Kessler, W.; Kirschning, A.; Müller, R. Elansolid A3, a Unique p-Quinone Methide Antibiotic from Chitinophaga Sancti. *Chemistry* **2011**, *17* (28), 7739–7744. <https://doi.org/10.1002/chem.201100457>.
- (13) Steinmetz, H.; Zander, W.; Shushni, M. A. M.; Jansen, R.; Gerth, K.; Dehn, R.; Dräger, G.; Kirschning, A.; Müller, R. Precursor-Directed Syntheses and Biological Evaluation of New Elansolid Derivatives. *ChemBioChem* **2012**, *13* (12), 1813–1817. <https://doi.org/10.1002/cbic.201200228>.
- (14) Beckmann, A.; Hüttel, S.; Schmitt, V.; Müller, R.; Stadler, M. Optimization of the Biotechnological Production of a Novel Class of Anti-MRSA Antibiotics from Chitinophaga Sancti. *Microb Cell Fact* **2017**, *16* (1), 143. <https://doi.org/10.1186/s12934-017-0756-z>.

(15) Yonath, A. ANTIBIOTICS TARGETING RIBOSOMES: Resistance, Selectivity, Synergism, and Cellular Regulation. *Annu. Rev. Biochem.* **2005**, *74* (1), 649–679. <https://doi.org/10.1146/annurev.biochem.74.082803.133130>.

(16) Wilson, D. N. Ribosome-Targeting Antibiotics and Mechanisms of Bacterial Resistance. *Nat Rev Microbiol* **2014**, *12* (1), 35–48. <https://doi.org/10.1038/nrmicro3155>.

(17) Brimacombe, R. The Ribosome: Function, Organization and Structure. In *Advances in Molecular and Cell Biology*; Bittar, E. E., Ed.; Advances in Molecular and Cell Biology; Elsevier, 1992; Vol. 4, pp 237–255. [https://doi.org/10.1016/S1569-2558\(08\)60181-2](https://doi.org/10.1016/S1569-2558(08)60181-2).

(18) Daptomycin versus linezolid for treatment of vancomycin-resistant enterococcal bacteremia: systematic review and meta-analysis | BMC Infectious Diseases | Full Text <https://bmccinfectdis.biomedcentral.com/articles/10.1186/s12879-014-0687-9> (accessed 2022-03-12).

(19) Müller, A.; Grein, F.; Otto, A.; Gries, K.; Orlov, D.; Zarubaev, V.; Girard, M.; Sher, X.; Shamova, O.; Roemer, T.; François, P.; Becher, D.; Schneider, T.; Sahl, H.-G. Differential Daptomycin Resistance Development in *Staphylococcus Aureus* Strains with Active and Mutated Gra Regulatory Systems. *International Journal of Medical Microbiology* **2018**, *308* (3), 335–348. <https://doi.org/10.1016/j.ijmm.2017.12.002>.

(20) Odds, F. C. Synergy, Antagonism, and What the Chequerboard Puts between Them. *Journal of Antimicrobial Chemotherapy* **2003**, *52* (1), 1. <https://doi.org/10.1093/jac/dkg301>.

(21) Andersson, D. I.; Hughes, D. Persistence of Antibiotic Resistance in Bacterial Populations. *FEMS Microbiology Reviews* **2011**, *35* (5), 901–911. <https://doi.org/10.1111/j.1574-6976.2011.00289.x>.

(22) rpsK - 30S ribosomal protein S11 - *Escherichia coli* (strain K12) - rpsK gene & protein <https://www.uniprot.org/uniprot/P0A7R9> (accessed 2021-12-20).

(23) Robert, F.; Brakier-Gingras, L. A Functional Interaction between Ribosomal Proteins S7 and S11 within the Bacterial Ribosome \*. *Journal of Biological Chemistry* **2003**, *278* (45), 44913–44920. <https://doi.org/10.1074/jbc.M306534200>.

(24) Kaminishi, T.; Wilson, D. N.; Takemoto, C.; Harms, J. M.; Kawazoe, M.; Schluenzen, F.; Hanawa-Suetsugu, K.; Shirouzu, M.; Fucini, P.; Yokoyama, S. A Snapshot of the 30S Ribosomal Subunit Capturing mRNA via the Shine-Dalgarno Interaction. *Structure* **2007**, *15* (3), 289–297. <https://doi.org/10.1016/j.str.2006.12.008>.

(25) Nowotny, V.; Nierhaus, K. H. Assembly of the 30S Subunit from *Escherichia Coli* Ribosomes Occurs via Two Assembly Domains Which Are Initiated by S4 and S7. *Biochemistry* **1988**, *27* (18), 7051–7055. <https://doi.org/10.1021/bi00418a057>.

(26) proline (CHEBI:26271) <https://www.ebi.ac.uk/chebi/searchId.do?chebiId=CHEBI:26271> (accessed 2021-12-20).

(27) Wower, J.; Scheffer, P.; Sylvers, L. A.; Wintermeyer, W.; Zimmermann, R. A. Topography of the E Site on the *Escherichia Coli* Ribosome. *The EMBO Journal* **1993**, *12* (2), 617–623. <https://doi.org/10.1002/j.1460-2075.1993.tb05694.x>.

(28) Greuer, B.; Thiede, B.; Brimacombe, R. The Cross-Link from the Upstream Region of mRNA to Ribosomal Protein S7 Is Located in the C-Terminal Peptide: Experimental Verification of a Prediction from Modeling Studies. *RNA* **1999**, *5* (12), 1521–1525. <https://doi.org/10.1017/S1355838299991550>.

(29) Yusupov, M. M.; Yusupova, G. Zh.; Baucom, A.; Lieberman, K.; Earnest, T. N.; Cate, J. H. D.; Noller, H. F. Crystal Structure of the Ribosome at 5.5 Å Resolution. *Science* **2001**, *292* (5518), 883–896. <https://doi.org/10.1126/science.1060089>.

(30) McCutcheon, J. P.; Agrawal, R. K.; Philips, S. M.; Grassucci, R. A.; Gerchman, S. E.; Clemons, W. M.; Ramakrishnan, V.; Frank, J. Location of Translational Initiation Factor

IF3 on the Small Ribosomal Subunit. *PNAS* **1999**, *96* (8), 4301–4306. <https://doi.org/10.1073/pnas.96.8.4301>.

(31) Stevens, D. A.; Vo, P. T. Synergistic Interaction of Trimethoprim and Sulfamethoxazole on *Paracoccidioides brasiliensis*. *Antimicrob Agents Chemother* **1982**, *21* (5), 852–854.

(32) Wormser, G. P.; Tang, Y.-W. Antibiotics in Laboratory Medicine, 5th Edition Edited by Victor Lorain Philadelphia: Lippincott Williams & Wilkins, 2005 832 Pp., Illustrated. \$199.00 (Cloth). *Clinical Infectious Diseases* **2005**, *41* (4), 577–577.

(33) Ferrari, R.; Magnani, M.; Souza, R. B.; Tognim, M. C. B.; Oliveira, T. C. R. M. Mutant Prevention Concentration (MPC) of Ciprofloxacin Against *Salmonella Enterica* of Epidemic and Poultry Origin. *Curr Microbiol* **2011**, *62* (2), 628–632. <https://doi.org/10.1007/s00284-010-9754-7>.

(34) Smith, H. J.; Nichol, K. A.; Hoban, D. J.; Zhanel, G. G. Stretching the Mutant Prevention Concentration (MPC) beyond Its Limits. *Journal of Antimicrobial Chemotherapy* **2003**, *51* (6), 1323–1325. <https://doi.org/10.1093/jac/dkg255>.

(35) Hesje, C. K.; Tillotson, G. S.; Blondeau, J. M. MICs, MPCs and PK/PDs: A Match (Sometimes) Made in Hosts. *Expert Review of Respiratory Medicine* **2007**, *1* (1), 7–16. <https://doi.org/10.1586/17476348.1.1.7>.

(36) Drlica, K. The Mutant Selection Window and Antimicrobial Resistance. *Journal of Antimicrobial Chemotherapy* **2003**, *52* (1), 11–17. <https://doi.org/10.1093/jac/dkg269>.

(37) Svetlov, M. S.; Vázquez-Laslop, N.; Mankin, A. S. Kinetics of Drug–Ribosome Interactions Defines the Cidality of Macrolide Antibiotics. *Proc Natl Acad Sci U S A* **2017**, *114* (52), 13673–13678. <https://doi.org/10.1073/pnas.1717168115>.

(38) Combet, C.; Blanchet, C.; Geourjon, C.; Deléage, G. NPS@: Network Protein Sequence Analysis. *Trends in Biochemical Sciences* **2000**, *25* (3), 147–150. [https://doi.org/10.1016/S0968-0004\(99\)01540-6](https://doi.org/10.1016/S0968-0004(99)01540-6).

(39) Hacke, M.; Gruber, T.; Schulenburg, C.; Balbach, J.; Arnold, U. Consequences of Proline-to-Alanine Substitutions for the Stability and Refolding of Onconase. *The FEBS Journal* **2013**, *280* (18), 4454–4462. <https://doi.org/10.1111/febs.12406>.

(40) Pagès, J.-M.; James, C. E.; Winterhalter, M. The Porin and the Permeating Antibiotic: A Selective Diffusion Barrier in Gram-Negative Bacteria. *Nat Rev Microbiol* **2008**, *6* (12), 893–903. <https://doi.org/10.1038/nrmicro1994>.

(41) Wilson, D. N. Ribosome-Targeting Antibiotics and Mechanisms of Bacterial Resistance. *Nat Rev Microbiol* **2014**, *12* (1), 35–48. <https://doi.org/10.1038/nrmicro3155>.

(42) Korostelev, A.; Trakhanov, S.; Laurberg, M.; Noller, H. F. Crystal Structure of a 70S Ribosome-TRNA Complex Reveals Functional Interactions and Rearrangements. *Cell* **2006**, *126* (6), 1065–1077. <https://doi.org/10.1016/j.cell.2006.08.032>.

(43) X-Ray Crystallography Study on Ribosome Recycling: The Mechanism of Binding and Action of RRF on the 50S Ribosomal Subunit. *The EMBO Journal* **2005**, *24* (2), 251–260. <https://doi.org/10.1038/sj.emboj.7600525>.

(44) Franceschi, F. Back to the Future: The Ribosome as an Antibiotic Target. *Future Microbiology* **2007**, *2* (6), 571–574. <https://doi.org/10.2217/17460913.2.6.571>.

(45) Invasive Methicillin-Resistant *Staphylococcus aureus* Infections in the United States | Infectious Diseases | JAMA | JAMA Network <https://jamanetwork.com/journals/jama/article-abstract/209197> (accessed 2022-03-14).

(46) Zinzalla, G.; Thurston, D. E. Targeting Protein–Protein Interactions for Therapeutic Intervention: A Challenge for the Future. *Future Medicinal Chemistry* **2009**, *1* (1), 65–93. <https://doi.org/10.4155/fmc.09.12>.

(47) Steitz, T. A.; Moore, P. B. RNA, the First Macromolecular Catalyst: The Ribosome Is a Ribozyme. *Trends in Biochemical Sciences* **2003**, *28* (8), 411–418. [https://doi.org/10.1016/S0968-0004\(03\)00169-5](https://doi.org/10.1016/S0968-0004(03)00169-5).

(48) Suriyanarayanan, B.; Lakshmi, P. P.; Santhosh, R. S.; Dhevendaran, K.; Priya, B.; Krishna, S. Streptomycin Affinity Depends on 13 Amino Acids Forming a Loop in Homology Modelled Ribosomal S12 Protein (RpsL Gene) of Lysinibacillus Sphaericus DSLS5 Associated with Marine Sponge (Tedania Anhelans). *Journal of Biomolecular Structure and Dynamics* **2016**, *34* (6), 1190–1200. <https://doi.org/10.1080/07391102.2015.1073633>.

(49) Ilina, E.; Malakhova, M.; Bodoev, I.; Filimonova, A.; Oparina, N.; Govorun, V. Mutation in Ribosomal Protein S5 Leads to Spectinomycin Resistance in *Neisseria Gonorrhoeae*. *Frontiers in Microbiology* **2013**, *4*.

(50) Agarwal, D.; O'Connor, M. Diverse Effects of Residues 74–78 in Ribosomal Protein S12 on Decoding and Antibiotic Sensitivity. *Biochemical and Biophysical Research Communications* **2014**, *445* (2), 475–479. <https://doi.org/10.1016/j.bbrc.2014.02.031>.

## Chapter 3

# Daptomycin-Peptide-Chimera are Active Against Multi-Resistant Pathogens and Acquire a Calcium-Independent Mechanism of Action

(Submitted manuscript with the title ‘One Step Ahead of Bacteria: Daptomycin-Peptide-Chimera Acquire a Calcium-Independent Mechanism of Action’)

Florian Umstätter <sup>†[a]</sup>, Sari Rasheed<sup>†[b,c]</sup>, Eric Mühlberg<sup>[a]</sup>, Tobias Hertlein<sup>[d]</sup>, Cornelius Domhan<sup>[e]</sup>, Karel D. Klika<sup>[f]</sup>, Christian Kleist<sup>[a]</sup>, Julia Werner<sup>[a]</sup>, Stefan Zimmermann<sup>[g]</sup>, Barbro Beijer<sup>[a]</sup>, Knut Ohlsen<sup>[d]</sup>, Uwe Haberkorn<sup>[a]</sup>, Marcus Koch<sup>[h]</sup>, Markus Bischoff<sup>[i]</sup>, Rolf Müller<sup>[b,c]</sup>, Jennifer Herrmann <sup>\*[b,c]</sup>, Walter Mier<sup>[a]</sup> and Philipp Uhl<sup>\*[a]</sup>

<sup>†</sup> These authors contributed equally.

---

[a] Dr. F. Umstätter, E. Mühlberg, Dr. C. Kleist, J. Werner, Dr. B. Beijer, Prof. Dr. U. Haberkorn, Prof. Dr. W. Mier, Dr. P. Uhl\*  
Department of Nuclear Medicine, Heidelberg University Hospital, 69120 Heidelberg, Germany

[b] S. Rasheed, Dr. J. Herrmann\*, Prof. Dr. R. Müller  
Helmholtz Institute for Pharmaceutical Research Saarland (HIPS), Helmholtz Centre for Infection Research (HZI), Saarland University, 66123 Saarbrücken, Germany

[c] S. Rasheed, Dr. J. Herrmann, Prof. Dr. R. Müller  
German Centre for Infection Research (DZIF), Braunschweig, Germany

[d] Dr. T. Hertlein, PD Dr. K. Ohlsen  
Institute for Molecular Infection Biology, University of Würzburg, 97080 Würzburg, Germany

[e] Dr. C. Domhan  
Institute of Pharmacy and Molecular Biotechnology, Heidelberg University, 69120 Heidelberg, Germany

[f] Dr. K. D. Klika  
German Cancer Research Center (DKFZ), NMR Spectroscopy Analysis Unit, 69120 Heidelberg, Germany

[g] Dr. S. Zimmermann  
Medical Microbiology and Hygiene, Heidelberg University Hospital, 69120 Heidelberg, Germany

[h] Dr. M. Koch  
INM-Leibniz-Institute for New Materials, Saarland University, 66123, Germany

[i] Prof. Dr. M. Bischoff  
Institute for Medical Microbiology and Hygiene, Saarland University, 66421 Homburg, Germany

---

## Contributions to the presented work

### Author's contribution

The author significantly contributed to the conception of this study, designed, and performed experiments, evaluated, and interpreted resulting data. The author performed the antibacterial testing for laboratory and clinical isolates, studied the time-kill kinetics, lysis experiments and quantification of ATP. Additionally, the author performed membrane potential studies and sample preparation for microscopy imaging and carried out *in vivo* infections in zebrafish larvae. The author contributed significantly to conceiving and writing this manuscript.

### Contribution by others

F. Umstätter significantly contributed to the conception of this study, designed, and performed experiments, evaluated, and interpreted resulting data. Additionally, he performed synthesis of peptide and conjugate, blocking experiment and cytotoxicity and hemolysis studies. He also contributed significantly to conceiving and writing this manuscript. E. Mühlberg and B. Beijer assisted in synthesis of peptide and conjugates. T. Hertlein and C. Domhan performed antimicrobial testing. K. D. Klika did the structural analysis and NMR studies. C Kleist carried out the hemolysis and cytotoxicity assays. J. Werner performed antimicrobial, hemolysis, and cytotoxicity testing. S. Zimmermann, K. Ohlsen, U. Haberkorn contributed to resourcing the manuscript. M. Koch performed scanning electron microscopy (SEM) images. M. Bischoff provided the daptomycin-resistant clinical isolates and and preformed the proofreading of the manuscript. J. Herrmann and P. Uhl contributed to the experimental design of the study and performed proofreading and conceptualization of this chapter. W. Mier and R. Müller contributed to the conceptualization and performed proofreading of the manuscript.

### 3 Daptomycin-Peptide-Chimera are Active Against Multi-Resistant Pathogens and Acquire a Calcium-Independent Mechanism of Action

#### 3.1 Abstract

Daptomycin is a lipopeptide antibiotic used to treat infections with vancomycin-resistant enterococci (VRE) and methicillin-resistant *Staphylococcus aureus* (MRSA). It interacts with the bacterial cell membrane in a calcium-dependent manner. Resistance to daptomycin has developed in VRE and MRSA clinical isolates after daptomycin treatment. Given the not-fully understood mode of action of daptomycin, the complexity of the structure regarding chemical modifications, its inactivation by lung surfactants, and the development of resistance, there is a necessity for strategies to reinforce the drug's activity. Herein, we show that conjugation of polycationic peptides highly increased the activity of daptomycin against resistant bacteria *in vitro* and *in vivo*, in zebrafish infected larvae. The most active conjugate consisted of a hexa-arginine peptide coupled to daptomycin. In contrast to daptomycin, these novel conjugates kill resistant pathogens *in vitro* in a calcium-independent manner resulting in cell lysis. Scanning electron microscopy further revealed the difference in cell membrane structure after treatment with the conjugate and daptomycin. Therefore, we propose a modified mode of action for this new class of antibacterial agents.

### 3.2 Introduction

According to the report of the Centers for Disease Control and Prevention's (CDC) National Healthcare Safety Network (NHSN) for antimicrobial-resistant pathogens associated with adult healthcare-associated infections (HAIs) between 2015 and 2017, *S. aureus* was the second most common pathogen across all HAIs constituting around 12% of reported pathogens. *E. faecalis* (7.9%) and *E. faecium* (3.8%) ranked 5<sup>th</sup> and 8<sup>th</sup>, respectively, in the most frequently isolated pathogens<sup>1</sup>.

Enterococci were originally included in the genus *Streptococcus*, however, based on genetic characterization in the 1980s, they were classified as an independent genus, *Enterococcus*<sup>2</sup>. *Enterococcus faecium* and *Enterococcus faecalis* are responsible for the majority of human infections in hospitalized patients<sup>3</sup>. Being the third most common nosocomial pathogen, enterococci cause urinary tract infections (UTIs), bacteremia, intra-abdominal infections, and endocarditis<sup>4</sup>. They are also responsible for up to 20% of community-acquired endocarditis<sup>5</sup>. Enterococci survive hospital settings due to their intrinsic resistance and tolerance to most commonly used antibiotics such as  $\beta$ -lactams, aminoglycosides, cephalosporins, fluoroquinolones, streptogramins and trimethoprim-sulfamethoxazole<sup>4,6</sup>. Furthermore, they can acquire resistance and overcome treatment with chloramphenicol, aminoglycosides, erythromycin, tetracycline, rifampin, and glycopeptides<sup>4</sup>. In 1988, isolation of vancomycin-resistant *E. faecalis* and *E. faecium* was first reported in England<sup>7</sup>. Then, Vancomycin resistant enterococci (VRE) have rapidly spread worldwide. Vancomycin resistance is widely common in *E. faecium*, and relatively rare in *E. faecalis*<sup>4,8</sup>. In a recent executive summary for the surveillance of antimicrobial resistance in Europe in 2020, a 'particular concern' in the increase of vancomycin-resistant isolates of *E. faecium*, from 11.6% in 2016 to 16.8% in 2020 was reported<sup>9</sup>. The VRE situation nowadays in Germany is also alarming, where the Antibiotic Resistance Surveillance system (ARS), hosted by the Robert Koch Institute (RKI), showed that the number of *E. faecium* isolates with resistance to vancomycin increased from 11.2% in 2014

to 26.1% in 2017<sup>10</sup>. Similarly, data from 'Krankenhaus-Infektions-Surveillance-System' (KISS) focusing on Intensive Care Unit (ICU-KISS) reported a 282% increase in VRE cases between 2007 and 2012, and likewise, data from the Paul Ehrlich Society revealed a continuous increase in VRE isolates from 12.6 %, 16,6% to 24,4% in 2010, 2013 and 2016<sup>11-13</sup>.

Staphylococci are bacteria of the human skin microbiota and they are opportunistic pathogens<sup>14,15</sup>. *Staphylococcus aureus* and *Staphylococcus epidermidis* account for about two third of implant infections<sup>16</sup>. *S. aureus* is a major human pathogen and the causative agent of infections including bacteremia, infective endocarditis (IE), skin and soft tissue infections (SSTIs), osteomyelitis, device-related infections, pulmonary infections, toxic shock syndrome (TSS), and urinary tract infections<sup>17,18</sup>. Soon after the discovery of methicillin in 1960s, methicillin-resistant *S. aureus* (MRSA) isolates have been isolated from patients in the United Kingdom<sup>19</sup>. Vancomycin and teicoplanin were the last resort antibiotics for the treatment of MRSA, however, in 1996, the first MRSA strain with reduced susceptibility to vancomycin (Minimum Inhibitory Concentration, MIC: 8 mg/L), termed vancomycin intermediate-resistant *S. aureus* (VISA), was isolated from a surgical wound infection in Japan<sup>20,21</sup>. In 2002, MRSA-vancomycin-resistant *S. aureus* (VRSA) strains were reported in the United States. The strains harbored the *vanA* operon, transmitted by *Tn1546* transposon, by conjugation from a glycopeptide-resistant *Enterococcus faecalis*<sup>22</sup>. In Germany, data from KISS surveillance for the period between 2007 and 2016 showed that there is a major reduction in nosocomial *S. aureus* infections due to MRSA from 37.1% to 21.8% for blood stream infections (BSI), from 38.7% to 19.2% for lower respiratory tract infections (LRTI) and from 21.1% to 7.4% in surgical site infections (SSI)<sup>23</sup>. Although there was a decrease in the percentage of MRSA isolates in Europe between 2016 and 2020, MRSA remains a critical pathogen, with high incidence among certain age groups and in several countries<sup>9,24</sup>.

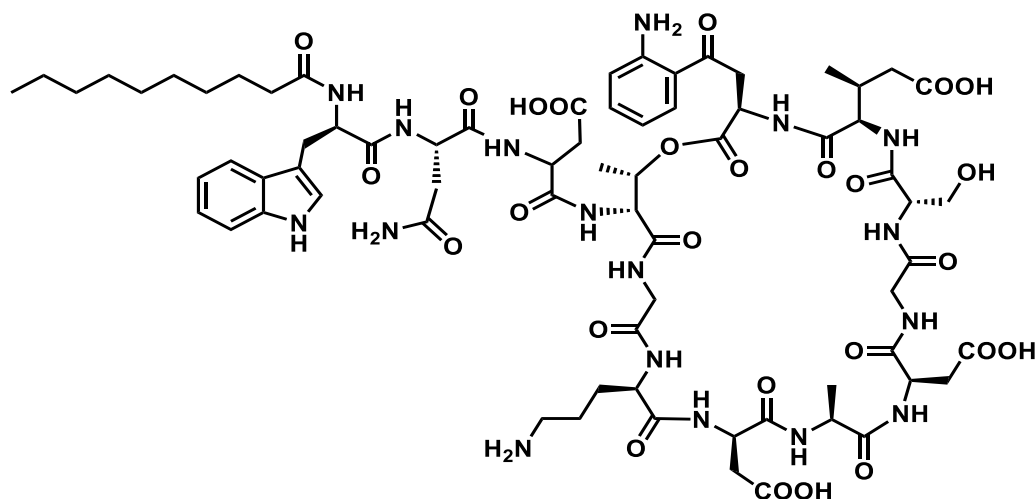


**Figure 1: Chemical structure of daptomycin**

The scarce of antibiotic arsenal and the spread of antimicrobial resistance, led to the use of last-resort antibiotics such as daptomycin to manage VRE and MRSA infections<sup>25,26</sup>. Daptomycin (**Figure 1**) is a novel antimicrobial agent used for the treatment of multidrug-resistant, Gram-positive pathogens, such as MRSA, VRE, and glycopeptide-intermediate and -resistant *S. aureus*<sup>27</sup>. Daptomycin has been shown to induce skeletal muscle myopathy, however, dosing alterations minimized such effects<sup>28</sup>. In 2003, daptomycin, was approved by the Food and Drug Administration (FDA) for the treatment of complicated skin and skin-structure infection (SSSIs) and in 2006, it was approved in the United States for the treatment of *S. aureus* bacteremia<sup>29</sup>. Until today, daptomycin is the last approved and marketed novel antibiotic class<sup>30</sup>.

Daptomycin is a cyclic lipopeptide discovered in the 1980s, produced by the soil bacterium, *Streptomyces roseosporus*<sup>31</sup>. Daptomycin exerts a potent bactericidal activity among most clinically important pathogens, and its mode of action is not yet fully understood. Studies showed that daptomycin binds to the bacterial membrane lipid phosphatidylglycerol (PG), and it inserts itself in the cell membrane in a calcium-dependent manner, resulting in membrane depolarization and subsequent loss of intracellular components, including K<sup>+</sup>, Mg<sup>2+</sup> and ATP<sup>32–36</sup>. Calcium ions reduce the overall negative charge of the peptide and induces structural

changes that permit the antibiotic to interact with the bacterial cell membrane<sup>35</sup>. Further studies demonstrated that daptomycin induces lipid aggregates (patches) on the surface of bacterial membranes which redirects the localization of proteins involved in cell division and cell wall synthesis and may ultimately lead to a breach in the cell membrane and cell death<sup>37</sup>. A similar study shows that the membrane lipid-aggregates induced by the daptomycin-calcium complex, causes the removal of lipid molecules from the bilayers (lipid-extracting phenomenon) leading to cell death<sup>38</sup>. Further studies showed that daptomycin inhibits cell wall synthesis, leading to rearrangement of fluid lipid domains, thus, affecting overall membrane fluidity, causing proton leakage and a gradual decrease in membrane potential, but does not lead to the formation of membrane pores<sup>38,39</sup>. Most recently, the  $\text{Ca}^{2+}$ -daptomycin complex was shown to interact with bacterial cell envelope precursors in the presence of the anionic phospholipid phosphatidylglycerol (PG), forming a tripartite complex at the staphylococcal septum and interrupting cell wall biosynthesis, resulting in massive membrane rearrangements, followed by membrane leakage and cell death<sup>40</sup>. The same study further hypothesized the lack of activity of daptomycin against streptomycetes-producer strain, and Gram-negative pathogens due to the reduced PG content<sup>41,42</sup>. Furthermore, the inactivation of daptomycin by pulmonary surfactant *in vitro* might be attributed to the relatively high PG content in lung surfactant<sup>43</sup>. In **Figure 2**, few proposed mechanisms of action of daptomycin are summarized.

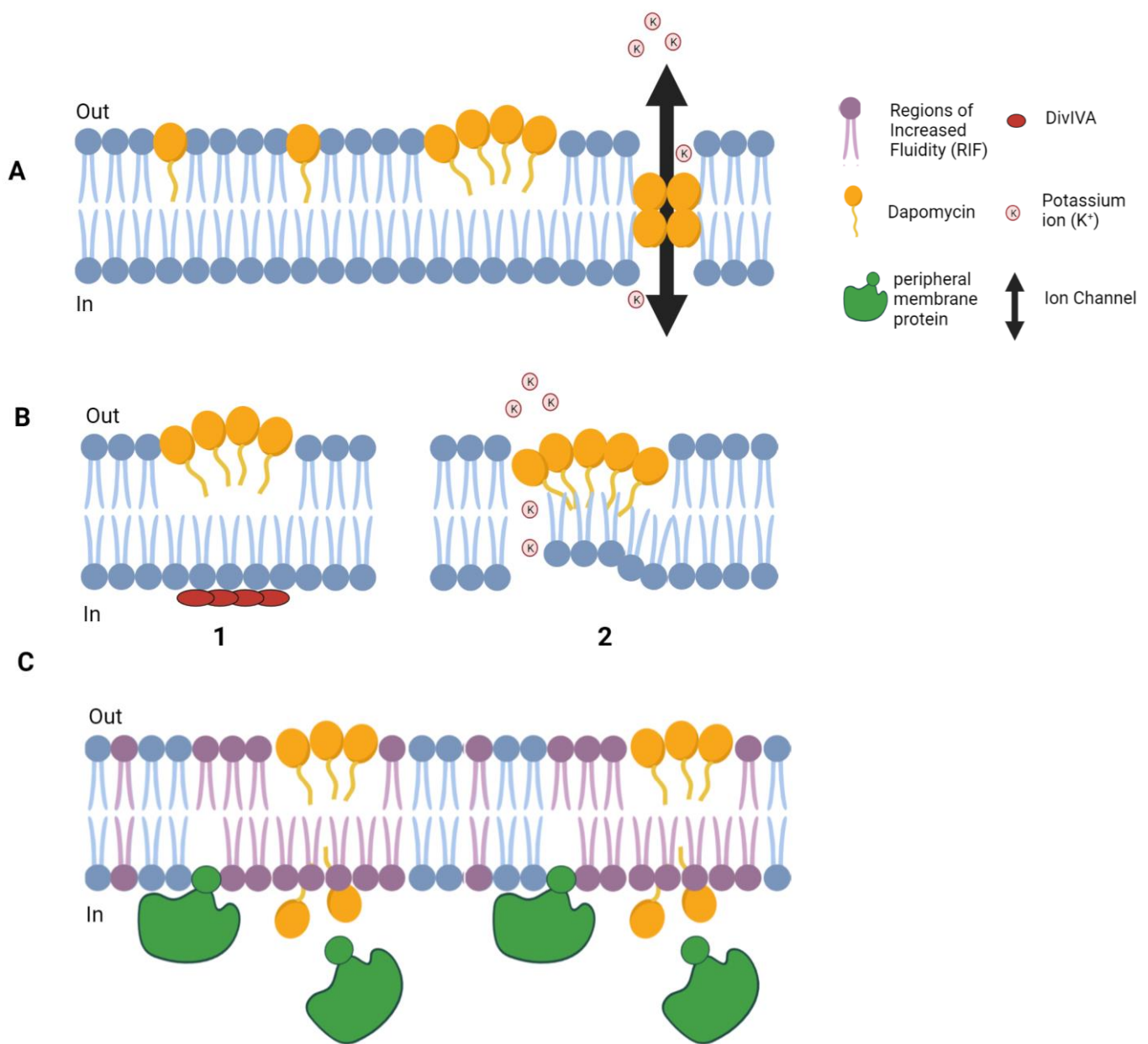


**Figure 3: Proposed mechanisms of action of  $Ca^{2+}$ -daptomycin complex.** (A) The complex inserts into the cell membrane and oligomerizes in the outer leaflet. Daptomycin oligomers translocate into the inner leaflet of the membrane, resulting in the formation of a functional pore-like structure. Ions such as  $K^+$  leaks out of the bacterial cell, causing membrane depolarization<sup>36</sup>. (B) (1) At sub-MIC, alterations of outer-leaflet curvature recruit the essential cell division protein (DivIVA), leading the cell to incorrectly identify the location as a site of potential cell division. This leads to local changes in peptidoglycan biogenesis, affecting cell wall morphology and septation. (2) At supra-MIC, sites of local membrane curvature are induced, leading to discontinuities in the membrane at the site of complex insertion which causes slow leakage of ions and loss of membrane potential<sup>37</sup>. (C) Peripheral membrane proteins involved in cell wall and lipid synthesis localize to RIFs indicated by a high concentration of fluid lipids. Following insertion, redistribution of lipids in the outer and inner leaflet leads to the flipping of daptomycin through the bilayer to the inner leaflet. Peripheral membrane proteins are displaced from RIFs. As a result, access to fluid lipids in the inner leaflet is blocked, resulting in the withdrawal of fluid lipids from the bulk and increased membrane rigidity<sup>39</sup>. *Figures adopted from [36, 37 and 39].*

Despite its therapeutic effectiveness, there is an increasing number of reports of daptomycin clinical failures due to emergence of resistance among patients infected with VRE and MRSA<sup>44-49</sup>. *S. aureus* and *E. faecium* resistance breakpoints are  $\geq 1$   $\mu\text{g}/\text{mL}$  and  $\geq 8$   $\mu\text{g}/\text{mL}$ , respectively, according to the European Committee on Antimicrobial Susceptibility Testing (EUCAST) (**Figure 3**) and the Clinical and Laboratory Standards Institute (CLSI)<sup>50,51</sup>. The development of resistance to daptomycin in MRSA and VRE is associated with modifications of the cell envelope and reduced drug binding to cell membrane proteins<sup>52-54</sup>. Although several resistant mutants were isolated, resistance development to daptomycin is still slow compared to other drugs<sup>55</sup>.

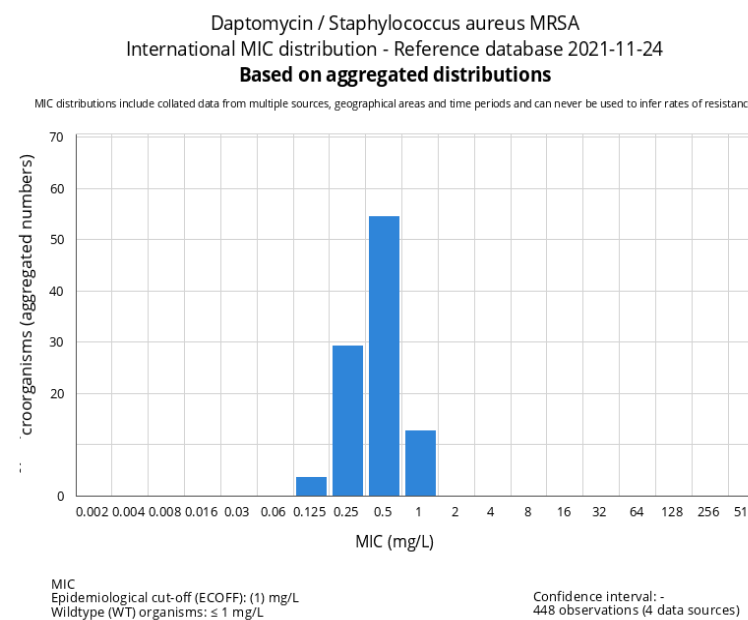
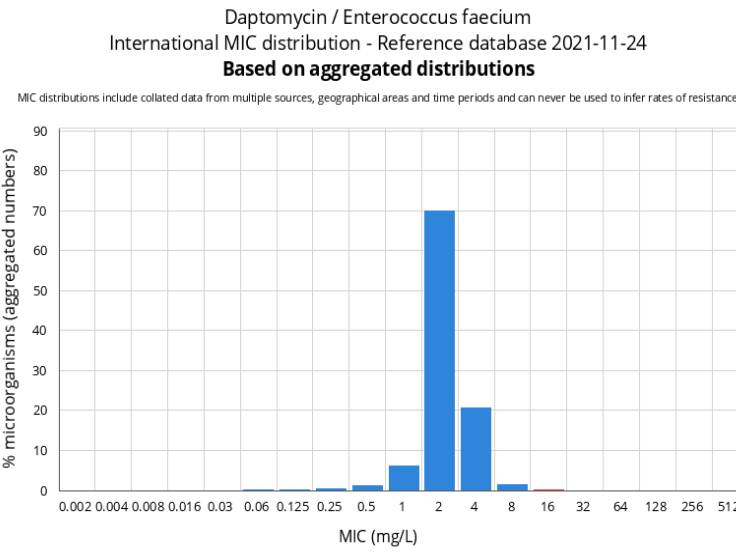
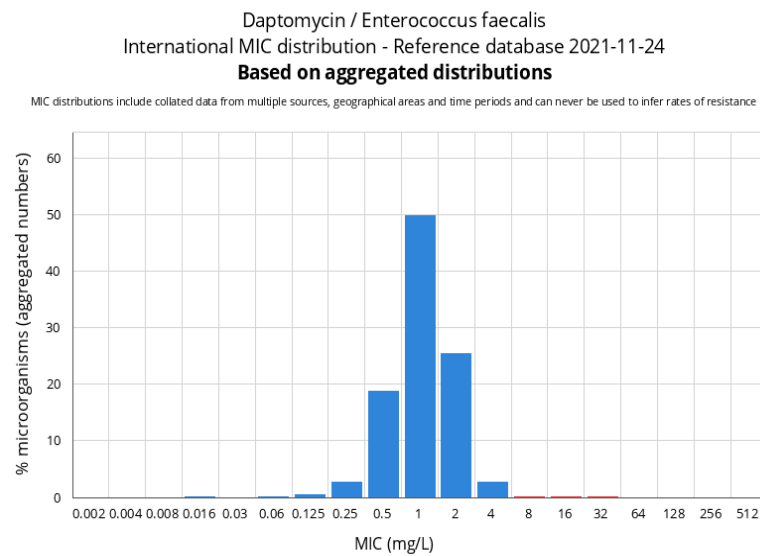


**Figure 3: International daptomycin MIC (mg/L) distributions for (A) *E. faecalis*, (B) *E. faecium* and (C) *S. aureus* MRSA.** Data from the European Committee on Antimicrobial Susceptibility Testing (EUCAST) (<https://mic.eucast.org/search/>). Daptomycin breakpoint for *E. faecalis* and *E. faecium*  $\geq 8$   $\mu$ g/mL and for *S. aureus*  $> 1$   $\mu$ g/mL.

Due to the complexity of derivatization of daptomycin, and to preserve the effectiveness of such a last-resort antibiotic, the demand for fast and financially rewarding strategies of antibiotic development is crucial. The modification of established drugs represents an example of such strategies to shorten the drug development process, and thereby also to reduce costs. Previous studies with vancomycin revealed that polycationic peptide conjugation is a viable approach to obtain highly active derivatives<sup>56</sup>. Herein, we aim at demonstrating the feasibility of the approach for daptomycin. We showed that conjugation of polycationic peptides significantly increased the activity of daptomycin against a laboratory generated daptomycin-resistant *S. aureus* isolate. Intriguingly, and in contrast to daptomycin, the lead conjugate DAP-R6, acts independently from the prevalent calcium concentration and can kill daptomycin-resistant pathogens. DAP-R6 was found to increase the survival of zebrafish larvae infected with daptomycin-resistant *S. aureus*. Scanning electron microscopy further revealed differences in cell membrane structure after treatment with the conjugate and daptomycin. Thus, we propose a modified mode of action of this new class of antibacterial agents.

### 3.3 Materials and Methods

#### 3.3.1 Peptide synthesis

The peptide moiety was synthesized by solid phase peptide synthesis using the Fmoc strategy as described previously. Briefly, a rink amid resin (loading 0.67 mmol/g) was preloaded with cysteine. Further amino acids were coupled using a standard protocol on an Applied Biosystems 433A synthesizer with HBTU activation strategy. The final cleavage of the peptide was performed in TFA/H<sub>2</sub>O/TIS (90/5/5) for at least two hours. The cleaved peptide was precipitated in diethyl ether and dried. Purification of the peptide was performed by preparative HPLC.

#### 3.3.2 Daptomycin-conjugate synthesis

For the synthesis of daptomycin polycationic peptide conjugates, the previously described coupling strategy was used (Umstätter et al., 2020)<sup>56</sup>. For this, daptomycin was mixed with 0.5 eq of a heterobifunctional crosslinker (Sulfo-SMCC) DMSO stock solution in PBS (pH 8.16) and shaken at room temperature for one hour. The product was purified by preparative HPLC and lyophilized. For peptide coupling, the daptomycin-SMCC conjugate was dissolved in PBS (pH 5.5) and mixed with the peptide solution in DMSO. Purification by preparative HPLC was performed after two hours reaction at room temperature.

#### 3.3.3 NMR studies

NMR spectra were acquired using a Bruker Avance II NMR spectrometer equipped with a 5-mm, inverse-configuration probe with triple-axis gradient capability at a field strength of 14.1 T operating at 600 and 150 MHz for <sup>1</sup>H and <sup>13</sup>C nuclei, respectively, in *d*<sub>6</sub>-DMSO or D<sub>2</sub>O at 24.9 °C. Pulse widths were calibrated following the described protocol.<sup>[3]</sup> The chemical shifts of <sup>1</sup>H nuclei are reported relative to the internal reference TMS ( $\delta$  H = 0 ppm). General NMR experimental and acquisition details for 1D 1H and selective 1D NOESY ( $\tau_m$ , 0.3 s) and

standard, gradient-selected 2D COSY and  $^1\text{H}\{^{13}\text{C}\}$ -HSQC have been previously described for routine spectral assignment and structural analysis<sup>57</sup>.

### 3.3.4 $\text{Ca}^{2+}$ ion-induced micelle formation by NMR

Solutions of DAP-R6 and daptomycin were prepared in  $\text{D}_2\text{O}$  at 24.9 °C and at a concentration of 1 mM together with 0, 1, 2 and 5 equivalents of  $\text{CaCl}_2$ . The samples with 5 equivalents of  $\text{CaCl}_2$  were subsequently diluted by  $\frac{1}{2}$ ,  $\frac{1}{4}$  and 1/20. Micelle formation was ascertained by signal line broadening as per literature<sup>58</sup>.

### 3.3.5 Bacterial strains and growth conditions

Daptomycin-resistant *S. aureus* (DRSA) clinical isolates (n=26) as well as vancomycin-resistant *E. faecium* (VRE) clinical isolates (n=34), were provided by the Institute of Medical Microbiology and Hygiene at University Hospital Saarland. *S. aureus* HG001 and the corresponding HG001 DAP<sup>R</sup> mutant (Müller et al., 2017)<sup>59</sup> were grown on Trypticase<sup>TM</sup> Soy Broth (TSA) and kept at 37°C.

*S. aureus* strains Newman, Mu50 and N315 were obtained from the stock collection of the Institute of Medical Microbiology, Zurich, Switzerland, and kindly provided by Brigitte Berger-Bächi. Experiments were conducted in Mueller Hinton Broth (MHB), Mueller Hinton II Broth (Cation-Adjusted) (BD BBL) (MHBII) and Mueller Hinton II Broth supplemented to 50 mg/L  $\text{Ca}^{2+}$  (MHBII- $\text{Ca}^{2+}$ ) according to the guidelines of Clinical and Laboratory Standards Institute (CLSI).

### 3.3.6 Antimicrobial susceptibility testing

Minimal inhibitory concentrations (MIC) for laboratory and clinical isolates were determined in MHBII- $\text{Ca}^{2+}$  unless otherwise stated, by standard broth microdilution. Briefly, 75 µl/well of bacterial suspension at  $\sim 4 \times 10^5$  CFU/mL were added to a 96-well plate, along with 75 µl of compounds in serial dilution (0.03-64 µg/mL). The plates were then incubated for 24 h at 37°C,

and the lowest concentration at which no growth was observed by visual observation was considered as the MIC.

### 3.3.7 Maximum tolerated concentration (MTC) in zebrafish embryos/larvae

MTC assays were performed to determine developmental and acute toxicity of DAP-R6 and daptomycin on different embryonic developmental stages of zebrafish. Briefly, embryos were sorted at 0 dpf (day post fertilization) in a 96-well plate (1 embryo/well). The embryos were then immersed in different concentrations of DAP-R6 and daptomycin (6.25-50  $\mu$ g/mL) in 0.3x Danieau's solution (0.05 M NaCl, 0.01 M KCl, Ca(NO<sub>3</sub>)<sub>2</sub>, MgSO<sub>4</sub>, Hepes buffer; pH 7.3) (n=20). The embryos/larvae were observed microscopically every 24 h to monitor embryonic development, anomalies, pigmentation, heartbeat, and locomotor responses. An embryo/larva was considered dead if there was no heartbeat recorded.

### 3.3.8 Time-kill curves (TKC) and cell lysis monitoring

TKCs were performed using log-phase *S. aureus* HG001 (daptomycin-susceptible). Bacteria were cultured in MHBII overnight, and then diluted 1:100, two hours prior to the start of the experiment. Briefly, the bacterial suspension was adjusted to 10<sup>7</sup> CFU/mL in MHBII-Ca<sup>2+</sup> and cultured at 37°C in the presence of 2-and 4-fold MIC of DAP-R6 (MIC 2  $\mu$ g/mL) and of daptomycin (MIC 1  $\mu$ g/mL), respectively. Samples were taken at different time points (0, 15, 30, 60, 120, 180, 240 and 360 min) and were cultured on solid medium (Trypticase<sup>TM</sup> Soy agar, TSA). Following 24 h incubation at 37°C, colony forming unit (CFU) were counted and a bactericidal effect was defined as > 3 log decrease in CFU/mL.

Cell lysis was monitored by measuring optical density of treated *S. aureus* HG001 (wt) during log-phase growth in MHBII-Ca<sup>2+</sup>. OD<sub>600</sub> was adjusted to 0.5 and bacterial cultures were treated with 2.5 and/or 5  $\mu$ g/mL of DAP-R6 and/or daptomycin. OD<sub>600</sub> was monitored at different time points (0, 15, 30, 60, 90, and 120 min).

### 3.3.9 Measurement of total ATP over time

ATP concentrations in treated and untreated samples were measured. Briefly, *S. aureus* HG001 (wt) bacterial suspensions were adjusted to  $10^7$  CFU/mL in MHBII- $\text{Ca}^{2+}$  and cultured in the presence of 4-fold MIC of DAP-R6 (MIC 2  $\mu\text{g}/\text{mL}$ ) and daptomycin (MIC 1 $\mu\text{g}/\text{mL}$ ). At each time point (15, 30, 60 and 120 min), 50  $\mu\text{L}$  of the sample were taken and 50  $\mu\text{L}$  BacTiter-Glo<sup>TM</sup> microbial cell viability reagent was added. Luminescence as a measure of ATP content and bacterial viability was measured using Tecan Infinite M200Pro with an integration time of 500 ms.

### 3.3.10 Scanning Electron Microscopy (SEM)

#### Sample preparation and fixation

*S. aureus* HG001 and the HG001 DAP<sup>R</sup> mutant were cultured in MHBII overnight, and then diluted 1:100 2 hours prior to the start of the experiment. Briefly, OD<sub>600</sub> was adjusted to 0.5 in MHBII- $\text{Ca}^{2+}$  and cultured at 37°C with 10  $\mu\text{g}/\text{mL}$  DAP-R6 and daptomycin for 2 hours. Cells were washed twice with Phosphate buffered saline (PBS) and fixed with 4% Paraformaldehyde (PFA 16% aqueous solution EM grade) for 30 mins at room temperature. Cells were washed twice with Milli-Q<sup>®</sup> water for imaging.

#### Imaging

Imaging was performed at the laboratories of Leibniz Institute for New Materials GmbH (INM) at Saarland University. Briefly, Fixed samples (1  $\mu\text{L}$ ) were carefully dried on a silicon wafer before depositing a thin gold layer by sputter deposition (20 mA, 45 sec). Secondary electron images were captured in high vacuum mode using an FEI Quanta<sup>TM</sup> 400 FEG SEM equipped with an Everhart-Thornley Detector (ETD) at 10 kV accelerating voltage (spot size 3, 10  $\mu\text{s}$  dwell time).

### 3.3.11 Bacterial membrane potential

Membrane depolarization was measured using the *BacLight*™ bacterial membrane potential kit (Invitrogen™). Briefly, an overnight culture of *S. aureus* was adjusted to an OD<sub>600</sub> of 0.1 and cells were treated with varying concentrations of DAP-R6 and daptomycin (2- and 4-fold MIC). the samples were stained with the fluorescent membrane potential indicator dye DiOC<sub>2</sub>(3) (3,3'-diethyloxacarbocyanine iodide) for 35 minutes. DiOC<sub>2</sub>(3) shows green fluorescence in all bacterial cells at low concentrations, but the fluorescence shifts toward red emission as the dye molecules self-associate at higher cytosolic concentrations caused by increased membrane potentials. The stained samples were measured using Tecan Infinite M200Pro plate reader at varying time points (Emission Wavelength 675 and 525 nm for red and green fluorescence, respectively). The proton ionophore CCCP (carbonyl cyanide 3-chlorophenylhydrazone) and nisin were used as positive control.

### 3.3.12 *In-vivo* efficacy in zebrafish-DRSA model

All zebrafish studies have been performed with larvae younger than 120 hours post-fertilization (hpf). *The use of self-feeding ZF embryos and larvae that are younger than 120 hpf are not considered as animal experiments according to European legislation (EU directive 2010/63/EU)*<sup>60</sup>.

The zebrafish-DRSA model was used to study the *in vivo* efficacy of DAP-R6. Briefly, zebrafish embryos at 1 dpf (day post fertilization) were sorted and anesthetized by incubating them in 0.0002% tricaine (3-amino benzoic acid ethyl ester) pH 7.0, during the injection process. OD<sub>600</sub> of HG001 DAP<sup>R</sup> mutant strain in exponential phase was adjusted to 0.25 and mixed with 0.5% phenol red (1:1 dilution). The microinjection needle was loaded with the DRSA using a microloader tip, and the needle was loaded onto a micromanipulator. The embryo was positioned so that the yolk is directly below the tip of the needle. The needle was then lowered until it contacted the yolk sac of the embryo. The embryo was gently pushed into the tip of needle until it just pierces the yolk, and the required volume (~2 nL) was injected, yielding

~120-150 CFU/embryo. The larvae were removed afterwards and incubated at 28 °C for 30 minutes prior to treatment. Following infection, the larvae were treated via yolk injection with ~2 nL of (i) DMSO control (vehicle), (ii) daptomycin and (iii) DAP-R6, yielding ~20 ng/larva of tested antibiotics. The larvae were incubated at 28 °C for 4 dpi (days post infection) and survival was monitored and reported daily. For this experiment, a total of 100 zebrafish embryos of the wild AB line were used. The samples (n=25) were divided into (i) uninfected-untreated control, (ii) infected-treated with DMSO control, (iii) infected-treated with daptomycin, and (iv) infected-treated with DAP-R6.

### 3.4 Results

#### 3.4.1 Peptide and daptomycin-conjugate synthesis

The conjugates consist of a peptide moiety and the daptomycin-core conjugated by the SMCC linker. Conjugates were obtained by solid phase peptide synthesis, followed by conjugation to daptomycin via a stable thioether bond. The active ester moiety of Sulfo-SMCC was linked to the primary amine function of the ornithine residue. Consequently, the peptide was added to the maleimide function of the heterobifunctional crosslinker (**Figure 4**). The approach we were focusing on, was to change the net charge of this peptide moiety. For this reason, various peptide sequences differing in net charge were synthesized.

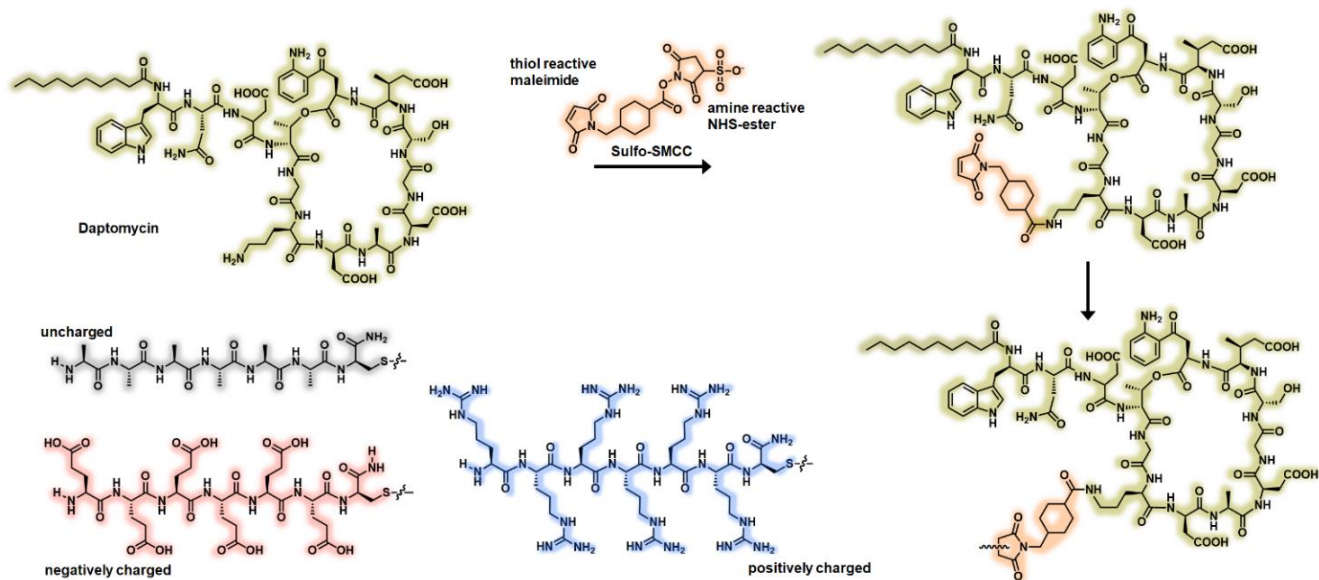


**Figure 4: Structure and synthesis of the novel daptomycin derivatives.** The respective peptide moiety is linked to daptomycin using the heterobifunctional linker Sulfo-SMCC. The first step is the site-specific derivatization at the ornithine residue of daptomycin. Subsequently, the thiol group of the peptide is bound by Michael addition to the maleimide moiety of the linker Sulfo-SMCC.

### 3.4.2 Antimicrobial susceptibility testing

To gain insight into the structure-activity relationship (SAR) of the novel conjugates, various peptide sequences differing in net charge were synthesized, and the activity (minimum inhibitory concentrations; MIC) of the conjugates was determined by broth microdilution assays using daptomycin sensitive and resistant *S. aureus* strains. The results imply that a positive net charge of the peptide sequence is crucial. Screening revealed an optimum of six positive charges per molecule. The most effective, in terms of activity against the daptomycin-resistant strain, was conjugate ‘DAP-R6’ harboring arginine as the basic amino acid, outperforming both the conjugates containing the natural amino acids lysine as well as those based on the unnatural amino acid ornithine (**Table 1**). The promising activity of the conjugate DAP-R6 to overcome daptomycin resistance led us to further characterize this compound. Complete MIC data of the conjugates against few *S. aureus* strains are summarized in supplementary data-**Table S1**.

**Table 1: MIC determination of daptomycin conjugates differing in net charge on a daptomycin sensitive and resistant *S. aureus* strain.**

Compound (peptide moiety)	Net Charge peptide moiety	MIC (µg/mL) <i>S. aureus</i> HG001 (wt)	MIC (µg/mL) <i>S. aureus</i> HG001 (DRSA)
<b>Daptomycin</b>	-	<b>0.5</b>	<b>32</b>
DAP-D6 (D6C)	-6	> 64	> 64
DAP-G6 (G6C)	0	32	> 64
DAP-A6 (A6C)	0	> 64	> 64
DAP-R3E3 (R3E3C)	0	> 64	> 64
DAP-R1 (R1C)	+1	4	> 64
DAP-R3 (R3C)	+3	0.5	16
<b>DAP-R6 (R6C)</b>	<b>+6</b>	<b>1-2</b>	<b>4</b>
DAP-K6 (K6C)	+6	0.5	16
DAP-Orn6 (Orn6C)	+6	2	8
DAP-R9 (R9C)	+9	8	8

To ensure that the effect of DAP-R6 was solely due to the antibiotic moiety, and not due the conjugated peptide or linker, MIC was determined for R6C (peptide) and R6C-SMCC (Peptide + linker) with *S. aureus* HG001 (wt), and vancomycin-resistant *E. faecium* VRE (ATCC 51559). Peptide R6C alone did not have any inhibitory effect on either bacterial isolate (MIC of  $> 64 \mu\text{g/mL}$  for *S. aureus* HG001 (wt) and  $64 \mu\text{g/mL}$  for *E. faecium* VRE strain (ATCC 51559)). Similarly, MIC was high for the peptide and linker together (MIC of  $64 \mu\text{g/mL}$  for HG001 (wt) and  $32 \mu\text{g/mL}$  for VRE, *E. faecium* strain (ATCC51559)). These data show that neither the linker, nor the peptide alone have a potent antibacterial inhibitory effect, compared to the complete conjugate DAP-R6 (Table 1 and Table 2).

**Table 2: MIC determination of peptide (R6C) and peptide linker (R6C-SMCC) on *S. aureus* and *E. faecium* strains.**

Substance	MIC ( $\mu\text{g/mL}$ ) <i>S. aureus</i> HG001 (wt)	MIC ( $\mu\text{g/mL}$ ) <i>E. faecium</i> VRE (ATCC51559)
<b>Peptide (R6C)</b>	$> 64$	64
<b>Peptide+linker (R6C-SMCC)</b>	64	32

### 3.4.3 MIC determination at different calcium concentrations

The influence of calcium on micelle formation, the initial step of daptomycin's mode of action, was studied by NMR spectroscopy. The calcium-induced micelle formation known for daptomycin was also observed for DAP-R6. Comprehensive analysis of the calcium-promoted effects revealed even greater stability of the DAP-R6 micelles as reflected by their resistance against dilution. Therefore, a significant calcium dependence on the antimicrobial activity of DAP-R6 was expected. Surprisingly, the antibacterial activity of DAP-R6 was found completely independent from the anticipated effects of calcium supplementation. For this reason, we studied the MIC of the conjugate and daptomycin in different media with different concentration of calcium supplements. The activity of DAP-R6 against sensitive as well as resistant *S. aureus* strains in the absence of calcium, pointed towards significant differences in modes of action of daptomycin and DAP-R6 (Table 3).

**Table 3: MIC comparison of daptomycin and its derivative DAP-R6 in microdilution testing in different media with varying calcium composition against the laboratory-acquired daptomycin resistant strain HG001**

Medium	MIC (µg/mL)		MIC (µg/mL)	
	<i>S. aureus</i> HG001 (wt)	Daptomycin	<i>S. aureus</i> HG001 (DRSA)	Daptomycin
DAP-R6	Daptomycin	DAP-R6	Daptomycin	
Mueller Hinton Broth (3-6 mg/L calcium)	2	64	4	> 128
Mueller Hinton II Broth (20-25 mg/L calcium)	2	8	4	64-128
Ca <sup>2+</sup> supplemented				
Mueller Hinton II Broth (50 mg/L calcium)	1	0.5	4	32

Furthermore, we assessed the MIC of daptomycin and its conjugate DAP-R6 on several clinical DRSA strains (n=26) (EUCAST breakpoint > 1 µg/mL). Like the daptomycin-resistant laboratory strain, DAP-R6 exhibited an effect against daptomycin-resistant clinical isolates with narrow MIC distribution (MIC<sub>50/90</sub> of 4 µg/mL). Furthermore, DAP-R6 is also highly active against vancomycin-resistant *E. faecium* (VRE) clinical isolates with an MIC<sub>50</sub> of 2 µg/mL and MIC<sub>90</sub> of 4 µg/mL, respectively. Data are summarized in **Table 4**.

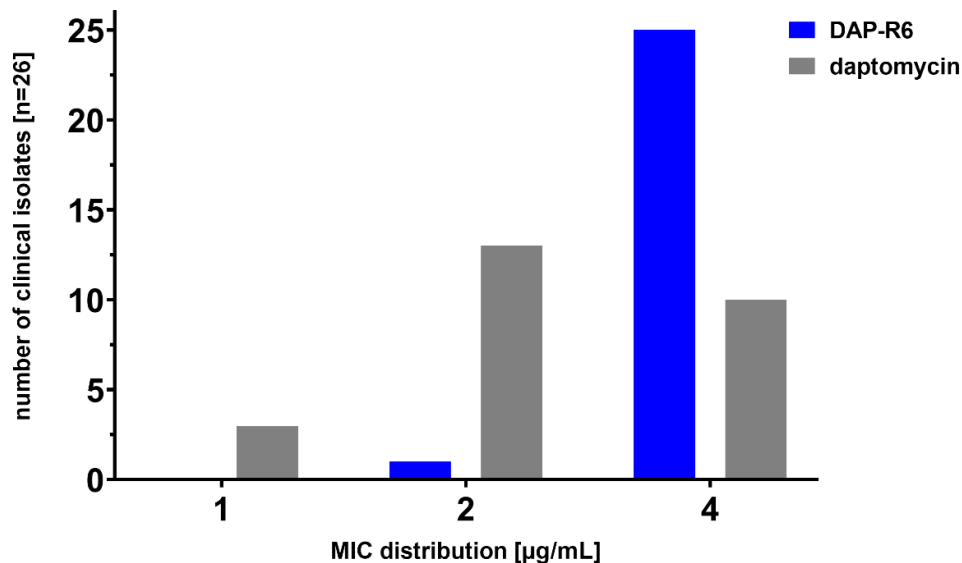
**Table 4: MIC determination of DAP-R6 and daptomycin on daptomycin-resistant *S. aureus* (DRSA) clinical isolates (n = 26) in the presence and absence of calcium, and on vancomycin-resistant on vancomycin-resistant *E. faecium* (VRE) clinical isolates (n=34)**

Medium	MIC <sub>50</sub> (µg/mL)		MIC <sub>90</sub> (µg/mL)	
	DAP-R6	Daptomycin	DAP-R6	Daptomycin
Mueller Hinton Broth (3-6 mg/L calcium)	4	32	8	32
Ca <sup>2+</sup> supplemented Mueller Hinton II Broth (50 mg/L calcium)	4	2	4	4

Medium	MIC <sub>50</sub> (µg/mL)		MIC <sub>90</sub> (µg/mL)	
	DAP-R6	Vancomycin	DAP-R6	Vancomycin
Mueller Hinton Broth (3-6 mg/L calcium)	2	> 64	4	> 64

To further validate the independency of the daptomycin-conjugate on calcium ions, we examined the MIC of clinical DRSA isolates in the absence and presence of calcium ions. As expected, and in line with laboratory strains, the minimum inhibitory concentration of daptomycin was affected by the presence of  $\text{Ca}^{2+}$  in the testing media ( $\text{MIC}_{50}$  shifted from 32 to 2  $\mu\text{g}/\text{mL}$  and  $\text{MIC}_{90}$  shifted from 32 to 4  $\mu\text{g}/\text{mL}$  in the presence of  $\text{Ca}^{2+}$ ). In the contrary, the minimum inhibitory concentration of daptomycin-conjugate was not affected by the absence of  $\text{Ca}^{2+}$  in the testing media and the values remained the same. The data are summarized in **Table 4**. It is useful to note that the DAP-R6 did not overcome the daptomycin resistance in clinical isolates since they are resistant to daptomycin with a low MIC, close to the EUCAST breakpoint ( $\geq 1 \mu\text{g}/\text{mL}$ ), which is even below the scope of activity of the conjugate against the wild type strain (2  $\mu\text{g}/\text{mL}$ ). Thus, the activity of DAP-R6 is to be further assessed with additional clinical isolates with a higher MIC to daptomycin (in the scope of activity of the conjugate), or the usage of *E. faecium* daptomycin resistant strains, that have a EUCAST breakpoints of  $\geq 8 \mu\text{g}/\text{mL}$ . However, MIC distribution shows no resistance correlation between daptomycin and DAP-R6 (correlation coefficient 0.3). MIC distribution of clinical isolates is summarized in **Figure 5**.



**Figure 5: MIC distribution of clinical isolates.** The distribution of MIC for DRSA clinical isolates differs between daptomycin and DAP-R6.

### 3.4.4 *In vitro* and *in vivo* toxicity assessment

Potential *in vitro* toxicity of DAP-R6 was assessed using a hepatocellular carcinoma cell line (HepG2). Encouragingly, the compound did not exert any cytotoxic effects at the tested concentrations (up to 100 µg/mL). *In vivo* tolerability was assessed in a zebrafish embryo/larvae toxicity model. As suspected from *in vitro* cytotoxicity screening, we did not observe toxic effects on continuously exposed larvae at five days post-fertilization (dpf) when DAP-R6 was added at concentrations up to 50 µg/mL into the fish water (0.3x Danieau's solution) at 1 dpf (supplement data-Figure S4). Based on these insights, molecular imaging and biodistribution studies in Wistar rats were performed. In contrast to daptomycin, which rapidly accumulates in the kidneys followed by renal elimination, DAP-R6 showed a notable change in pharmacokinetics: the main amount of the conjugate is targeted to the liver (Figure 6A). A second fraction reaches the kidneys, which is accompanied by renal elimination resulting in a significantly changed liver to kidney ratio (Figure 6B).

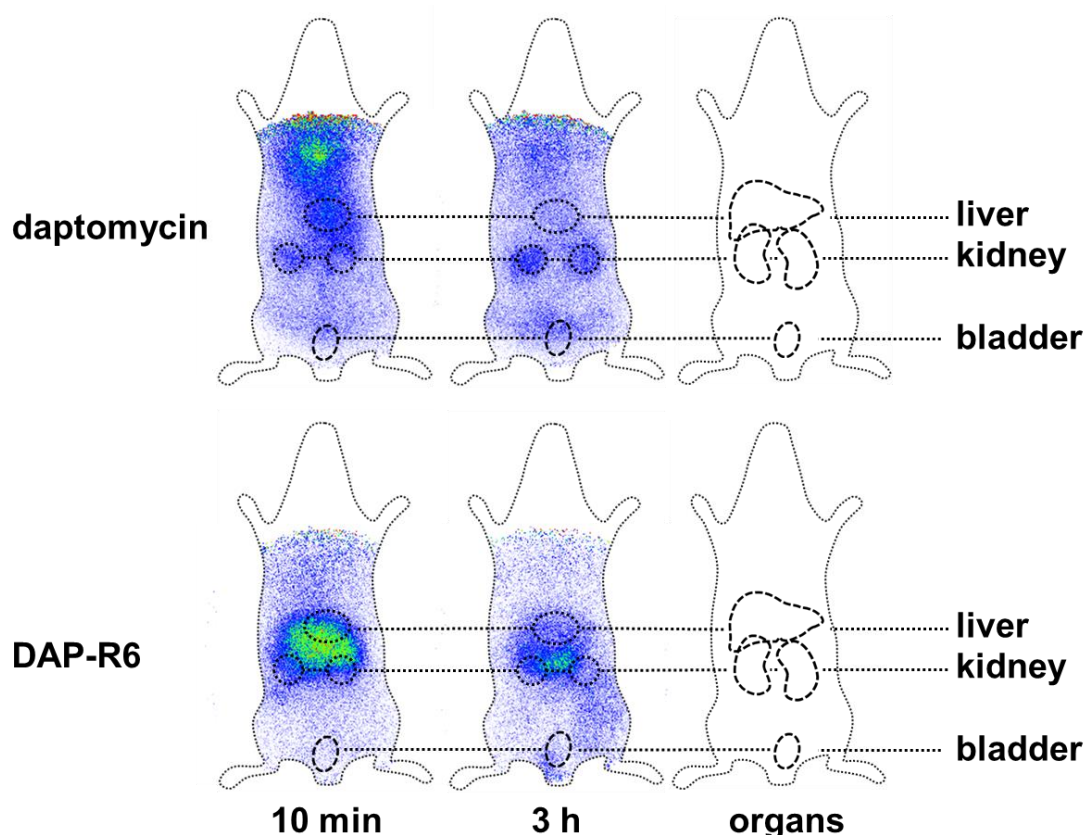


**Figure 6: Biodistribution of daptomycin and its derivative DAP-R6 in rat.** (A) Scintigraphic imaging of  $^{125}\text{I}$ -labelled daptomycin in comparison to  $^{125}\text{I}$ -labelled DAP-R6. (B) The changed organ distribution profile is confirmed by the biodistribution study of daptomycin and DAP-R6. %D/g: Percentage daptomycin per gram tissue.

### 3.4.5 Time-kill curves (TKC) and cell lysis monitoring

Comprehensive analysis of the kinetics of time-kill studies revealed an accelerated onset of the activity of DAP-R6 compared to daptomycin. This difference in bacterial elimination provided a further proof for the existence of a potential additional mode of action (Figure 7). Treatment with DAP-R6 (4-fold MIC) reduced bacterial count as early as 15 minutes, and after 2 hours, the bacterial count was at its minimal. On the other hand, the bactericidal effect of daptomycin was slower than that of DAP-R6. The increased activity of DAP-R6 against daptomycin-resistant strains points to an enhanced *in vitro* activity.

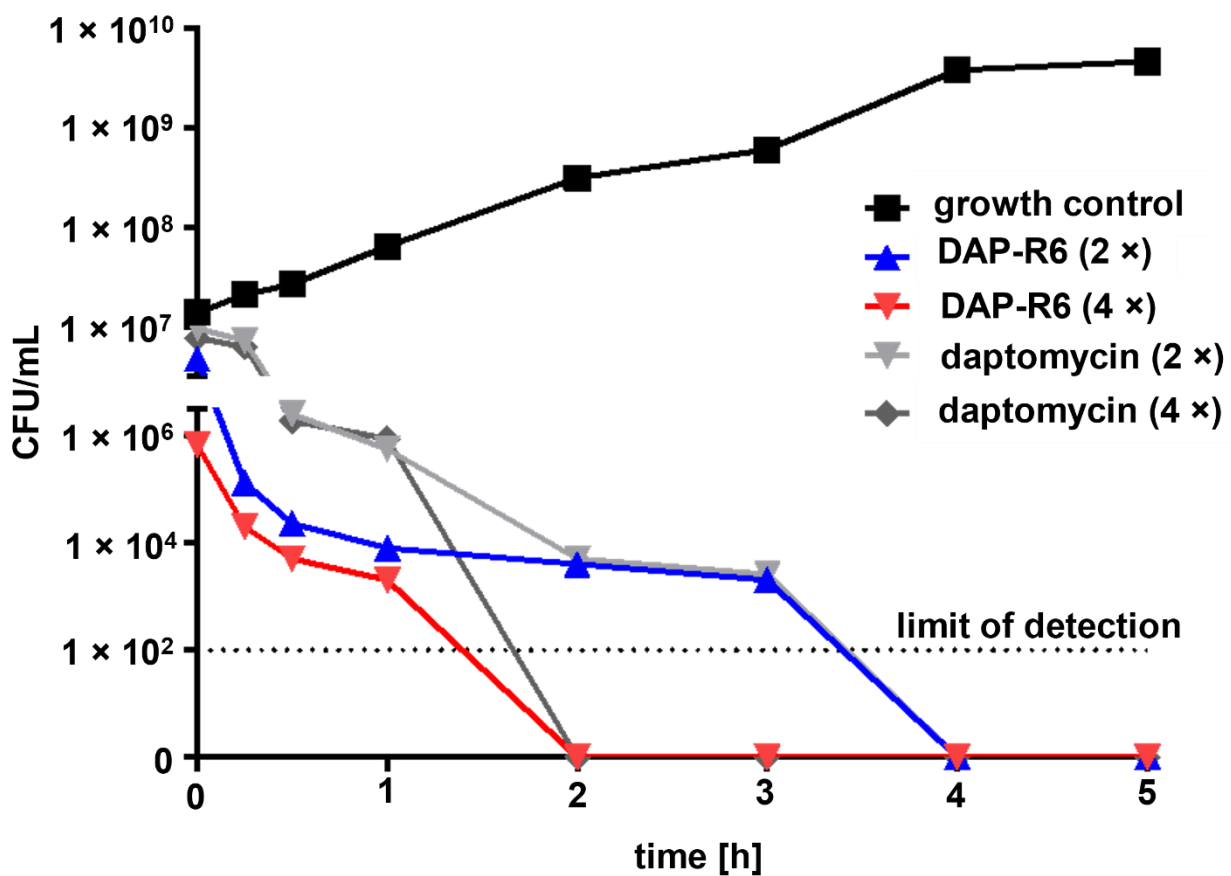


**Figure 7. Time-kill curves (TKCs) of DAP-R6 and daptomycin against *S. aureus* HG001 (wt).** Exponential phase cultures of *S. aureus* wild type HG001 were grown and treated with 2x and 4x MIC of DAP-R6 (MIC 2 $\mu$ g/mL) and daptomycin (MIC 1  $\mu$ g/mL), and CFU were enumerated by plating appropriate sample dilutions on solid agar. DAP-R6 exerted a fast bactericidal effect within 15 minutes, while daptomycin had a delayed bactericidal effect. Dotted blue line represents limit of detection (LoD = 100)

It has been reported that daptomycin's bactericidal activity does not result in cell lysis<sup>26,34</sup>. To assess whether DAP-R6 exerts its activity against *S. aureus* in a similar manner, we monitored cell lysis by measuring optical density (OD<sub>600</sub>) during log-phase growth of bacteria after treatment with 2.5 and 5  $\mu$ g/mL DAP-R6 (MIC 2  $\mu$ g/mL) or daptomycin (MIC 1  $\mu$ g/mL). (Figure 8). Unlike daptomycin, DAP-R6 induced a rapid drop in OD<sub>600</sub> as fast as 15 minutes post treatment. This drop in optical density implies that the conjugate exerts its bactericidal activity through lysis. This activity was observed to a much lower extent after treatment with daptomycin. Thus, we suggest that the conjugate has a different mode of action than daptomycin. Although several reports support that daptomycin does not induce lysis, this effect is observed at higher concentrations of the drug where it interferes with cell membrane lipid organization and initiates cell wall breaches that disrupt the membrane, potentially leading to cell lysis<sup>39</sup>.

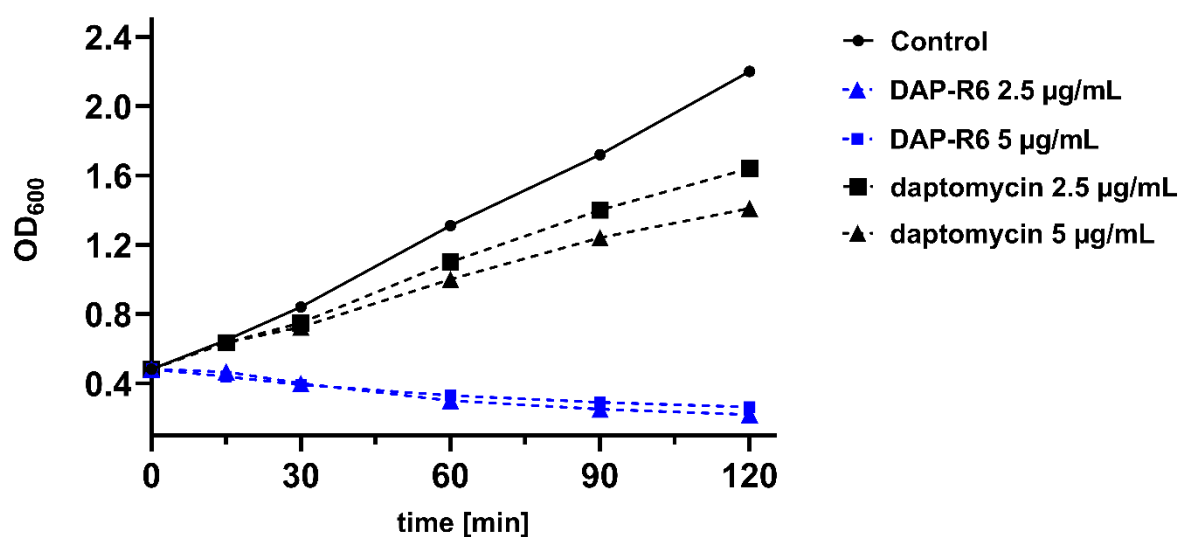


**Figure 8. Bacterial lysis assessment.** Optical density OD<sub>600</sub> of *S. aureus* HG001 wt strain was monitored during log-phase following exposure to 2.5 and 5  $\mu$ g/mL DAP-R6 or daptomycin for 2 hours. This drop in optical density implies a lysis effect for DAP-R6 which was not observed for daptomycin for up to 2 h post treatment.

### 3.4.6 Measurement of total ATP over time

The rapid antibacterial effect of DAP-R6 was further confirmed by an orthogonal assay that relies on the quantification of ATP as a measure of cell viability. The level of ATP in *S. aureus* decreased rapidly after treatment with DAP-R6 compared to a slower reduction with daptomycin (Table 5). These data are in line with time-kill curves that show a more rapid onset of DAP-R6 action compared to daptomycin.

**Table 5: ATP concentration in *S. aureus* following exposure to DAP-R6 and daptomycin.** Level of ATP decreased rapidly upon treatment with 4-fold MIC of DAP-R6 compared to that of daptomycin for 2 hours.

Time (min)	Luminescence as a measure of ATP content (Ratio to untreated control)	
	4X MIC DAP-R6	4X MIC Daptomycin
15	0.9	1.1
30	0.6	1.1
60	0.3	0.9
120	0.07	0.3

### 3.4.7 Scanning Electron Microscopy (SEM)

To confirm the lytic effect of the daptomycin-conjugate, we imaged *S. aureus* HG001 (wt) strain using Scanning Electron Microscopy (SEM). Samples were treated with 10 µg/mL DAP-R6 (5-fold MIC) and daptomycin (10-fold MIC) for 2 hours at 37°C. After fixation with 4% paraformaldehyde, secondary electron images were captured in high vacuum mode. Daptomycin treated sample showed membrane-lipid aggregates at the septum of cell-division arrested cells. This effect of daptomycin was also observed in other recent studies <sup>37,38</sup>. For this, we confirmed that daptomycin exerts its effect on the septum of dividing cells by forming membrane patches that lead to rupture of the cell membrane<sup>40</sup>. DAP-R6 showed a total membrane rupture, confirming our ‘lysis’ theory, thus, daptomycin and the conjugate alters the bacterial membrane in diverse ways. SEM images are shown in Figure 9.

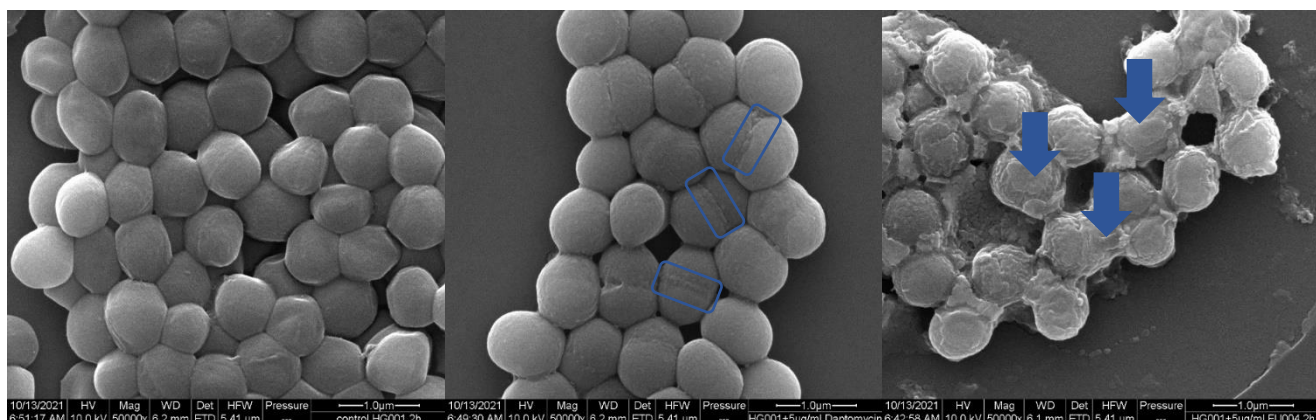


**Figure 9:** Scanning electron microscopy images of *S. aureus* HG001. After 2 h incubation, (A) untreated samples, (B) daptomycin induced membrane aggregates at the division-arrested cells without lysis, in contrast to (C), the antimicrobial effects of DAP-R6 reflected by rupture and a prevalent release of cell wall blocks with a strongly accelerated onset of bactericidal effects.

### 3.4.8 Bacterial membrane potential

To assess and compare the effect of DAP-R6 and daptomycin on membrane depolarization, we studied the bacterial membrane potential using the fluorescent membrane potential indicator dye DiOC<sub>2</sub>(3). Our data, summarized in **Figure 10**, showed that DAP-R6 at 2-and 4-fold MIC (4 and 8  $\mu$ g/mL) caused membrane depolarization as fast as 5 minutes and continued dropping gradually in concentration-dependent manner to reach low values after 35 minutes. This fast membrane depolarization is in line with the fast lytic effect observed as fast as 15 minutes post treatment, and further validate the mode of action of the conjugate via membrane disruption which leads to the leakage of cellular ions, interrupting the membrane potential. The membrane depolarization effect of DAP-R6 at 4-fold MIC is like that of nisin, which exerts its antibacterial effects through interacting with cytoplasmic membrane causing pore formation, leading to efflux of ions<sup>61</sup>. On the other hand, daptomycin did not exert any membrane depolarization for 35 minutes, which is line with our time-kill experiments which show that daptomycin did not exert its bactericidal effect until after 1 hour (**Figure 7**). Similar data showed that daptomycin does not induce depolarization until 30-60 minutes post treatment<sup>39,62</sup>. The proton ionophore CCCP (1  $\mu$ g/mL) induced full membrane depolarization as early as 5 minutes.

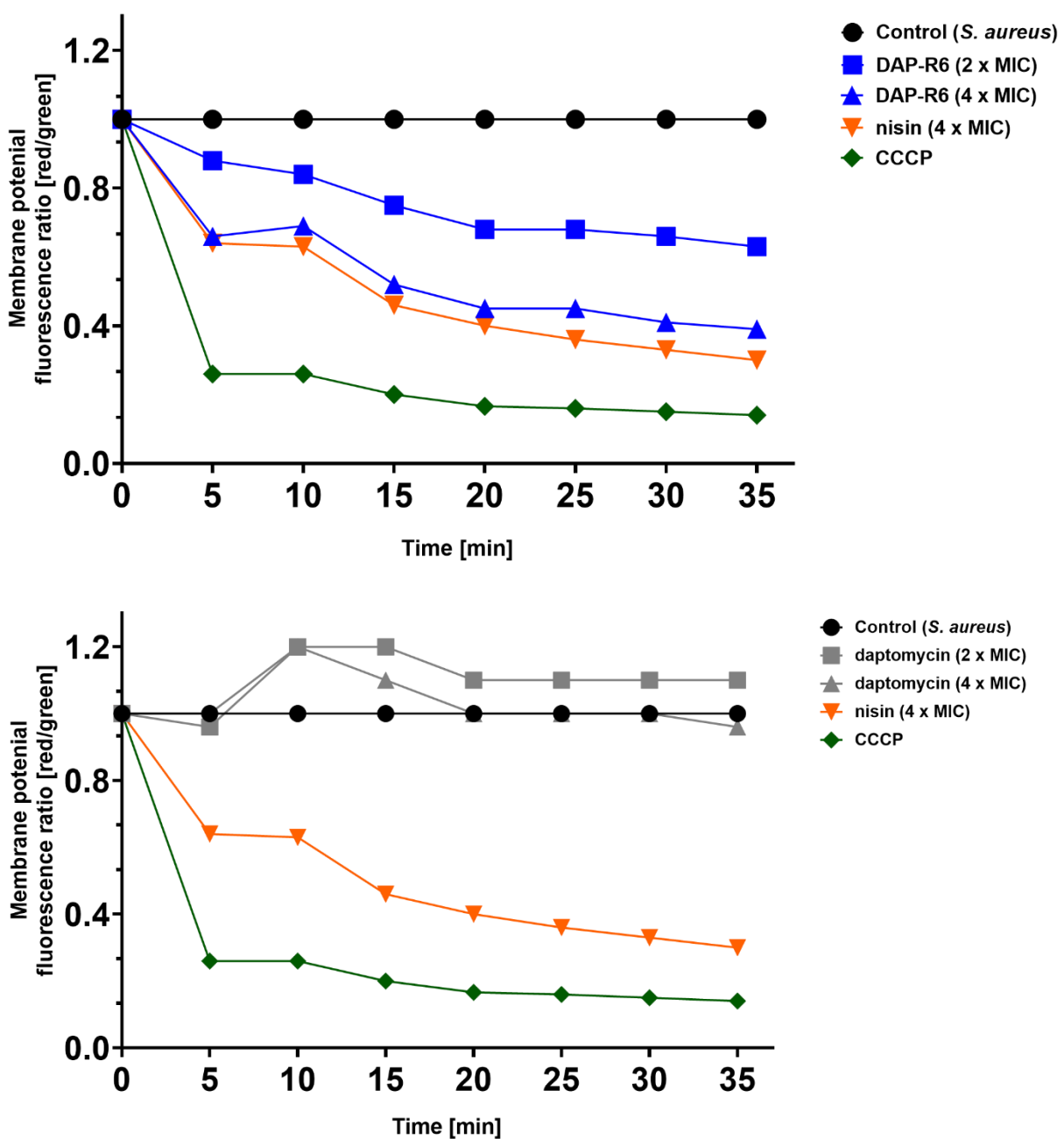


**Figure 10: Membrane potential in *S. aureus*.** Red/green ratios were calculated using mean fluorescence intensities of samples incubated with DiOC<sub>2</sub>(3) in the presence of 2- and 4-fold MIC DAP-R6 (4 and 8 µg/mL) and daptomycin (2 and 4 µg/mL), 4-fold nisin (16 µg/mL) and 1 µg/mL CCCP. DAP-R6 induced membrane depolarization as early as 5 minutes and gradually decreased. Daptomycin did not cause depolarization during the first 35 minutes of treatment. Nisin and CCCP induced depolarization as fast as 5 minutes.

### 3.4.9 *In vivo* efficacy in zebrafish-DRSA model

DRSA-infected zebrafish embryos were treated via yolk injection with ~2 nL of (i) DMSO control (vehicle), (ii) daptomycin and (iii) DAP-R6, yielding ~20 ng/larva of tested antibiotics, and the embryos/larvae were incubated at 28 °C for 4 dpi (days post infection) and survival as a measure of compound efficacy was monitored and reported daily. The data summarized in **Figure 11**, show that the infected-untreated embryos could not survive DRSA infection for more than 3 days where most of the untreated larvae (80%) died at 3 dpi. Daptomycin treatment did not overcome the bacterial infection, where 64% of the infected larvae did not survive after 3 dpi. In contrast, treatment with the conjugate saved more than 85% of the infected larvae at 3 dpi. At the end of the experiment (4 dpi), treatment with the conjugate saved 48% of the larvae, compared to the 16% of those that were treated with daptomycin and 8% able to naturally overcome the infection. These data suggest that the conjugate can overcome daptomycin resistance, not only *in vitro*, but also *in vivo* in the zebrafish larvae model of DRSA infection.

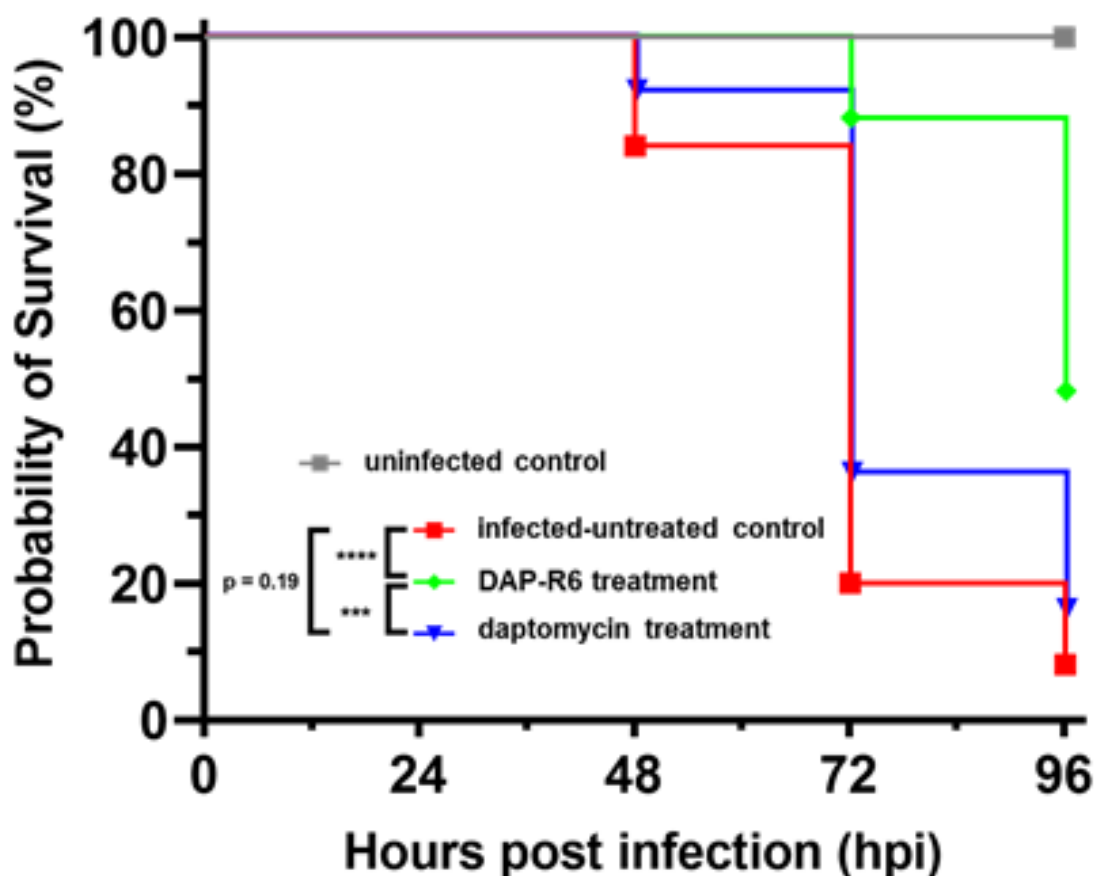


Figure 11: Kaplan Meier graph of DRSA-infected zebrafish embryos after treatment with daptomycin and DAP-R6. Treatment with DAP-R6 led to a prolonged survival of DRSA-infected larvae compared to daptomycin. Significance calculation using log-rank (Mantel-Cox) test. (\*\*\*\* =  $<0.0001$ ; \*\*\* = 0.0007)

### 3.5 Discussion

With the prevalent resistance to several antibiotics and the declining antibiotic development, last-resort antibiotics such as daptomycin, are used to manage vancomycin-resistant *E. faecium* (VRE) and methicillin-resistant *S. aureus* (MRSA) infections especially among critically ill hospitalized patients<sup>25,63</sup>. Until today, there is a low proportion of daptomycin resistance in VRE and MRSA in Europe, however, there are increasing reports worldwide of daptomycin resistance, due to prolonged treatment courses and infections with high bacterial burdens<sup>25,26</sup>. The linkage of antibiotics to a polycationic peptide represents a promising and effective approach for the development of highly potent substances by structural modification of already existing drugs to combat multidrug-resistant.

Previous study by Umstätter et al., showed that site-specific conjugation of short polycationic peptide to glycopeptide antibiotic, vancomycin exhibited ~1000-fold increased antimicrobial activity and was able to overcome vancomycin resistance<sup>56</sup>. The lead conjugate (FU002) consisting of vancomycin, linked to Hexa-arginine peptide by heterobifunctional cross linker SMCC (succinimidyl 4-(N-maleimidomethyl)cyclohexane-1-carboxylate), demonstrated low MIC values (< 4 µg/mL) and overcomes important types of vancomycin resistance (*vanA*, *vanB* and *vanC*) in *E. faecium*, *E. faecalis* and *E. casseliflavus* strains<sup>56</sup>. Additionally, FU002 displayed good safety profile in tested cell lines (blood, kidney, and liver cells) by *in vitro* cytotoxicity studies and did not show hemolysis of human blood cells. We have further carried out biological assessment for vancomycin-conjugate (FU002) in house and confirmed its good activity against several vancomycin-resistant enterococci strains (VRE) and vancomycin-intermediate resistant *S. aureus* strain (VISA) as well as clinical-VRE isolates (data not shown). Surprisingly, the peptide and the peptide-linker alone exhibited only a very weak antibacterial effect. The promising conjugation of vancomycin to polycationic peptide opened the door for the development of other conjugates with the last resort lipopeptide antibiotic, daptomycin.

Herein, we studied several daptomycin-conjugates consisting of various peptide sequences differing in net charge linked to the daptomycin-core by the SMCC linker. The structure-activity relationship (SAR) of the novel conjugates was determined by MIC determination of daptomycin-sensitive and -resistant *S. aureus* strains. The results showed that a positive net charge, with an optimum of six positive charges per molecule of the peptide sequence is essential for the enhanced activity of the conjugate. Surpassing both conjugates containing either lysine or ornithine, DAP-R6 harboring arginine as the basic amino acid exhibited the most effective activity against the daptomycin-resistant strain HG001 (DRSA). The lead conjugate DAP-R6 demonstrated a promising activity with an MIC of 2  $\mu$ g/mL and overcame daptomycin resistance in a resistant laboratory strain-HG001 (MIC of 32  $\mu$ g/mL against daptomycin)<sup>59</sup>. The peptide and/or linker separately showed a very weak inhibitory effect against several tested strains, which shows that the full conjugate is needed to exert a killing effect. Furthermore, this indicates that the conjugate remains intact and that the positively charged peptide might offer better binding affinity against the negatively charged cell membrane. These important findings led us to further investigate the importance of conjugating a cationic peptide to the anionic daptomycin in overcoming resistance. Since the *in vitro* activity of daptomycin is dependent on calcium ions that reduce the overall negative charge of the antibiotic and induces conformational changes that permit the antibiotic to interact with the bacterial cell membrane, we tested whether the conjugate is less dependant on calcium than daptomycin alone<sup>35</sup>. As expected, and unlike daptomycin, the conjugate retained its inhibitory effect against the DRSA strain and several DRSA clinical isolates when tested in media with different calcium concentrations. We hypothesize that the polycationic peptide substitutes the need of calcium in reducing the negative charge of daptomycin and bridges it to the cell membrane thereby boosting the activity of the “warhead” daptomycin in inducing its bactericidal effect<sup>35,53,62</sup>.

Unlike most antibiotics, the mechanisms of resistance to daptomycin are distinct and include structural and functional membrane modifications, as well as alterations of the cell wall<sup>59</sup>. Two main resistance mechanisms have been reported in *S. aureus* and include electrostatic repulsion of the positively charged daptomycin-calcium complex by increase in the positive charge of the cell membrane which results in a decreased binding of daptomycin, and a thickened cell wall, which have been found in clinical MRSA and VISA strains<sup>36</sup>. Other factors such as membrane phospholipid metabolism, changes in membrane fluidity and carotenoid pigment content have also been associated with daptomycin resistance in *S. aureus*<sup>64–66</sup>. For the positively charged DAP-R6 to overcome daptomycin resistance in HG001, we speculated that the mode of resistance in this strain is due to a thickened cell wall, rather than ‘charge repulsion’. As described by Müller et al., the HG001 DRSA strain exhibited only modest changes in cell surface charge, but showed a significantly thickened cell wall and are surrounded by additional alterations of the membrane and the cell wall material as observed by transmission electron microscopy<sup>59</sup>.

$\text{MIC}_{50/90}$  of DAP-R6 against DRSA clinical isolates in clinical isolates is in the range of 4  $\mu\text{g}/\text{mL}$ . This value is above the EUCAST clinical breakpoint for daptomycin resistance for *S. aureus*. Thus, although DAP-R6 kept its activity against clinical isolates but did not overcome resistance. This might be attributed to either the close MIC values of the isolates to the breakpoint of EUCAST for daptomycin resistance, which is even lower than the activity of the conjugate on the wild type of strain (MIC 2  $\mu\text{g}/\text{mL}$ ), or the mutants’ mode of resistance is different from that of the laboratory strain. Genome sequence analysis and characterization of the clinical isolates is to be further explored to explain the resistance phenotype.

Since the polycationic peptide is not active alone, the fact that the conjugate is calcium-independent and that it overcomes daptomycin resistance in DRSA, we hypothesize that DAP-R6 facilitates membrane interaction and achieves its effect in a distinct mode of action than daptomycin. To compare the mode of action of DAP-R6 to daptomycin- $\text{Ca}^{2+}$  complex, we

observed that the conjugate exerts a faster onset of cidal activity of *S. aureus* than daptomycin, and that the mode of action is through lysis, which is not the case with daptomycin<sup>67</sup>. We further examined disruption of membrane potential upon treatment with DAP-R6 and noticed that it induced membrane depolarization faster than daptomycin. Scanning electron microscopy additionally revealed that the conjugate caused disruption of the cell membrane and changed its morphology, whereas daptomycin induced membrane blebs at the septum of division-arrested cells. We hypothesize that the conjugate exerts its bactericidal effect in a distinct mode of action than daptomycin through lysis of bacterial cells causing a fast efflux of intracellular components and ultimately leading to cell death. Further investigations will include mutant generation of DAP-R6 to study the mechanism of action of the conjugate and examine the genes involved in resistance as well as the underlying transcriptomic and proteomic changes. Additionally, characterising the mutants for phenotypic characteristics such as cell wall thickness, autolysis, pigmentation, biofilm formation, membrane phospholipid metabolism, and changes in membrane fluidity are to be carried out. Such approach might give a better hint on the mode of action of daptomycin as well. Further approaches include fluorescently labeling DAP-R6 and monitor its binding site in the cell membrane with fluorescence microscopy.

### 3.6 Conclusion

Antimicrobial resistance necessitates the development of new antibiotics with “resistance-breaking” properties. In this study, daptomycin, an antibiotic of last resort, was coupled to polycationic peptides. Conjugation of polycationic peptides was proven to represent a versatile strategy for the fast and affordable reactivation of daptomycin. The conjugate antibiotic demonstrated *in vitro* and *in vivo* activity against a highly daptomycin-resistant strain. The lead conjugate DAP-R6 exerted a fast and more potent effect than daptomycin. It exerted its effect in a calcium-independent manner, as the conjugated polycationic peptide was able to replace the need for calcium ions. This suggests that adding a positive charge to the anionic antibiotic leads to a better attachment and oligomerization of daptomycin to bacterial membrane. Results from the DRSA-zebrafish model showed that treatment with the conjugate prolonged the survival of the larvae. This early model is encouraging as it shows that DAP-R6 might be also effective in higher organism models.

### 3.7 Acknowledgements

We acknowledge K. Leotta for support with the animal experiments, L. Pätzold for supplying the clinical isolates and F. Fries for support with MIC testing. We also thank the “Deutsche Forschungsgemeinschaft”, grant number 436573923; MI 684/7-1 and the DZIF unit TTU9 for financial support. In addition, the authors acknowledge Prof. Dr. Tanja Schneider (University Hospital Bonn) for providing *S. aureus* strains.

### 3.8 Supplementary information

#### 3.8.1 Antimicrobial susceptibility testing

**Table S1:** Antimicrobial susceptibility testing of different daptomycin conjugates against *S. aureus* strains

Compound	Conjugated peptide moiety	MIC [mg/L] on <i>S. aureus</i> Newman (VSSA)	MIC [mg/L] on <i>S. aureus</i> N315 (MRSA/V SSA)	MIC [mg/L] on <i>S. aureus</i> Mu50 (VISA)	MIC [mg/L] on <i>S. aureus</i> HG001 (wild type)	MIC [mg/L] on <i>S. aureus</i> HG001 (DRSA)
Daptomycin	-	0.5	0.5	2	0.5	32
DAP-R6	R6C	1	0.5-1	2	1-2	4
DAP-R3	R3C	0.5-1	2	4	0.5	16
DAP-R9	R9C	4	8	8	8	8
DAP-K6	K6C	1	4	4	0.5	16
DAP-R3K3	R3K3C	2	2	4	2	8
DAP-R3A3	R3A3C	2	2	16	8	> 64
DAP-R3G3	R3G3C	1	1	8	1	64
DAP-R3E3	R3E3C	> 64	> 64	> 64	> 64	> 64
DAP-(RE)3	(RE)3C	> 64	> 64	> 64	> 64	> 64
DAP-H6	H6C	16	16	> 64	64	> 64
DAP-R1	RC	1	2	16	4	> 64
DAP-A6	A6C	32	32	> 64	> 64	> 64
DAP-K1	KC	2	2	16	8	> 64
DAP-G6	G6C	8	8	> 64	32	> 64
DAP-K3	K3C	0.5	0.5	8	1	64
DAP-K9	K9C	1	1	4	4	16
DAP-F6	F6C	> 64	> 64	> 64	> 64	> 64
DAP-D6	D6C	> 64	> 64	> 64	> 64	> 64
DAP-Orn6	Orn6C	0.25	0.5	2	2	8
DAP-CapR3	C6-R3C	4	2	8	8	> 64
DAP-CapryR3	C8-R3C	4	4	8	8	> 64
DAP-CarR3	C10-R3C	8	4	16	4	> 64
DAP-MyrR3	C14-R3C	> 64	4-8	> 64	> 64	> 64
DAP-PalmR3	C16-R3C	> 64	> 64	> 64	> 64	> 64
DAP-SteaR3	C18-R3C	> 64	> 64	> 64	> 64	> 64
DAP-CapK3	C6-K3C	2	2	16	4	> 64
DAP-CapryK3	C8-K3C	4	4	16	8	> 64
DAP-CarK3	C10-K3C	8	8	8	16	64
DAP-LauK3	C12-K3C	8	4	> 64	32	> 64
DAP-MyrK3	C14-K3C	> 64	32	> 64	> 64	> 64
DAP-PalmK3	C16-K3C	> 64	> 64	> 64	> 64	> 64
DAP-SteaK3	C18-K3C	> 64	> 64	> 64	> 64	> 64

### 3.8.2 In-vivo toxicity in zebrafish

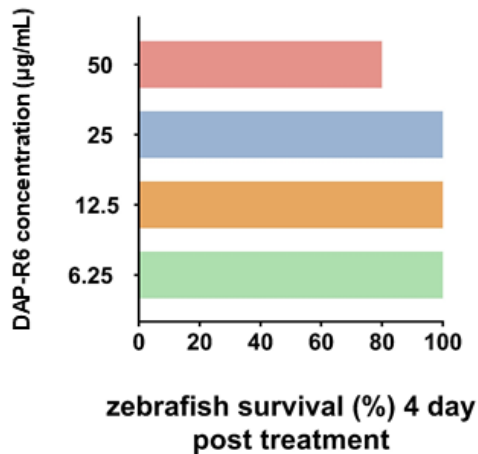


**Figure S4.** The maximum tolerated concentration of DAP-R6 in zebrafish embryos/larvae. 80% of zebrafish embryos/larvae survived a concentration of 50  $\mu\text{g/mL}$  of DAP-R6.

### 3.9 References

- (1) Weiner-Lastinger, L. M.; Abner, S.; Edwards, J. R.; Kallen, A. J.; Karlsson, M.; Magill, S. S.; Pollock, D.; See, I.; Soe, M. M.; Walters, M. S.; Dudeck, M. A. Antimicrobial-Resistant Pathogens Associated with Adult Healthcare-Associated Infections: Summary of Data Reported to the National Healthcare Safety Network, 2015–2017. *Infection Control & Hospital Epidemiology* **2020**, *41* (1), 1–18. <https://doi.org/10.1017/ice.2019.296>.
- (2) Schleifer, K. H.; Kilpper-Bälz, R. 1984. Transfer of *Streptococcus Faecalis* and *Streptococcus Faecium* to the Genus *Enterococcus* Nom. Rev. as *Enterococcus Faecalis* Comb. Nov. and *Enterococcus Faecium* Comb. Nov. *International Journal of Systematic and Evolutionary Microbiology* **34** (1), 31–34. <https://doi.org/10.1099/00207713-34-1-31>.
- (3) Ruoff, K. L.; de la Maza, L.; Murtagh, M. J.; Spargo, J. D.; Ferraro, M. J. Species Identities of *Enterococci* Isolated from Clinical Specimens. *Journal of Clinical Microbiology* **1990**, *28* (3), 435–437. <https://doi.org/10.1128/jcm.28.3.435-437.1990>.
- (4) Kristich, C. J.; Rice, L. B.; Arias, C. A. Enterococcal Infection—Treatment and Antibiotic Resistance. In *Enterococci: From Commensals to Leading Causes of Drug Resistant Infection*; Gilmore, M. S., Clewell, D. B., Ike, Y., Shankar, N., Eds.; Massachusetts Eye and Ear Infirmary: Boston, 2014.
- (5) Megran, D. W. Enterococcal Endocarditis. *Clinical Infectious Diseases* **1992**, *15* (1), 63–71. <https://doi.org/10.1093/clinids/15.1.63>.
- (6) Gold, H. S.; Moellering, R. C. Antimicrobial-Drug Resistance. *New England Journal of Medicine* **1996**, *335* (19), 1445–1453. <https://doi.org/10.1056/NEJM199611073351907>.
- (7) Uttley, A. H.; Collins, C. H.; Naidoo, J.; George, R. C. Vancomycin-Resistant Enterococci. *Lancet* **1988**, *1* (8575–6), 57–58. [https://doi.org/10.1016/s0140-6736\(88\)91037-9](https://doi.org/10.1016/s0140-6736(88)91037-9).
- (8) Rybak, J. M.; Barber, K. E.; Rybak, M. J. Current and Prospective Treatments for Multidrug-Resistant Gram-Positive Infections. *Expert Opinion on Pharmacotherapy* **2013**, *14* (14), 1919–1932. <https://doi.org/10.1517/14656566.2013.820276>.
- (9) Surveillance of antimicrobial resistance in Europe, 2020 data <https://www.ecdc.europa.eu/en/publications-data/surveillance-antimicrobial-resistance-europe-2020> (accessed 2021-11-23).
- (10) Markwart, R.; Willrich, N.; Haller, S.; Noll, I.; Koppe, U.; Werner, G.; Eckmanns, T.; Reuss, A. The Rise in Vancomycin-Resistant *Enterococcus Faecium* in Germany: Data from the German Antimicrobial Resistance Surveillance (ARS). *Antimicrob Resist Infect Control* **2019**, *8* (1), 147. <https://doi.org/10.1186/s13756-019-0594-3>.
- (11) Gastmeier, P.; Schröder, C.; Behnke, M.; Meyer, E.; Geffers, C. Dramatic Increase in Vancomycin-Resistant Enterococci in Germany. *Journal of Antimicrobial Chemotherapy* **2014**, *69* (6), 1660–1664. <https://doi.org/10.1093/jac/dku035>.
- (12) Liese, J.; Schüle, L.; Oberhettinger, P.; Tschörner, L.; Nguyen, T.; Dörfel, D.; Vogel, W.; Marschal, M.; Autenrieth, I.; Willmann, M.; Peter, S. Expansion of Vancomycin-Resistant *Enterococcus Faecium* in an Academic Tertiary Hospital in Southwest Germany: A Large-Scale Whole-Genome-Based Outbreak Investigation. *Antimicrob Agents Chemother* **2019**, *63* (5), e01978-18. <https://doi.org/10.1128/AAC.01978-18>.
- (13) Werner, G.; Neumann, B.; Weber, R. E.; Kresken, M.; Wendt, C.; Bender, J. K.; Becker, K.; Borgmann, S.; Diefenbach, A.; Hamprecht, A.; Hogardt, M.; Wichelhaus, T.; Kemp, V.; Huebner, N.-O.; Kaasch, A.; Geginat, G.; Kohnen, W.; Menzer, A.; Krause, T.; Miethke, T.; Pranada, F.; Radojn, F.; Tobisch, S.; Jansen, V.; Regnath, T.; Bührlen, U.; Schneider-Brachert, W.; Schwarz, R.; Luemen, M.; Skov, R.; Thuermer, A.; Baum, H. von; Weig, M.; Uwe, G.; Zabel, L.; Wulffen, H. von; Döring, S. Thirty Years of VRE in

Germany – “Expect the Unexpected”: The View from the National Reference Centre for Staphylococci and Enterococci. *Drug Resistance Updates* **2020**, *53*, 100732. <https://doi.org/10.1016/j.drup.2020.100732>.

(14) Cogen, A. I.; Nizet, V.; Gallo, R. I. Skin Microbiota: A Source of Disease or Defence? *British Journal of Dermatology* **2008**, *158* (3), 442–455. <https://doi.org/10.1111/j.1365-2133.2008.08437.x>.

(15) Stefani, S.; Chung, D. R.; Lindsay, J. A.; Friedrich, A. W.; Kearns, A. M.; Westh, H.; MacKenzie, F. M. Meticillin-Resistant *Staphylococcus Aureus* (MRSA): Global Epidemiology and Harmonisation of Typing Methods. *International Journal of Antimicrobial Agents* **2012**, *39* (4), 273–282. <https://doi.org/10.1016/j.ijantimicag.2011.09.030>.

(16) Oliveira, W. F.; Silva, P. M. S.; Silva, R. C. S.; Silva, G. M. M.; Machado, G.; Coelho, L. C. B. B.; Correia, M. T. S. *Staphylococcus Aureus* and *Staphylococcus Epidermidis* Infections on Implants. *Journal of Hospital Infection* **2018**, *98* (2), 111–117. <https://doi.org/10.1016/j.jhin.2017.11.008>.

(17) Tong, S. Y. C.; Davis, J. S.; Eichenberger, E.; Holland, T. L.; Fowler, V. G. *Staphylococcus Aureus* Infections: Epidemiology, Pathophysiology, Clinical Manifestations, and Management. *Clinical Microbiology Reviews* **2015**, *28* (3), 603–661. <https://doi.org/10.1128/CMR.00134-14>.

(18) Taylor, T. A.; Unakal, C. G. *Staphylococcus Aureus*. In *StatPearls*; StatPearls Publishing: Treasure Island (FL), 2021.

(19) Jevons, M. P. “Celbenin” - Resistant *Staphylococci*. *Br Med J* **1961**, *1* (5219), 124–125.

(20) Enright, M. C.; Robinson, D. A.; Randle, G.; Feil, E. J.; Grundmann, H.; Spratt, B. G. The Evolutionary History of Meticillin-Resistant *Staphylococcus Aureus* (MRSA). *Proc Natl Acad Sci U S A* **2002**, *99* (11), 7687–7692. <https://doi.org/10.1073/pnas.122108599>.

(21) Hiramatsu, K.; Hanakia, H.; Inob, T.; Yabutab, K.; Ogoric, T.; Tenoverd, F. C. Journal of Antimicrobial Chemotherapy (1997) *40*, 135–146 Methicillin-Resistant *Staphylococcus Aureus*.

(22) Périchon, B.; Courvalin, P. VanA-Type Vancomycin-Resistant *Staphylococcus Aureus*. *Antimicrobial Agents and Chemotherapy* **2009**, *53* (11), 4580–4587. <https://doi.org/10.1128/AAC.00346-09>.

(23) Kramer, T. S.; Schröder, C.; Behnke, M.; Aghdassi, S. J.; Geffers, C.; Gastmeier, P.; Remschmidt, C. Decrease of Meticillin Resistance in *Staphylococcus Aureus* in Nosocomial Infections in Germany—a Prospective Analysis over 10 Years. *Journal of Infection* **2019**, *78* (3), 215–219. <https://doi.org/10.1016/j.jinf.2018.12.005>.

(24) World Health Organization; Nations, F. and A. O. of the U.; Health, W. O. for A. *Monitoring Global Progress on Antimicrobial Resistance: Tripartite AMR Country Self-Assessment Survey (TrACSS) 2019–2020: Global Analysis Report*; World Health Organization, 2021.

(25) Heidary, M.; Khosravi, A. D.; Khoshnood, S.; Nasiri, M. J.; Soleimani, S.; Goudarzi, M. Daptomycin. *Journal of Antimicrobial Chemotherapy* **2018**, *73* (1), 1–11. <https://doi.org/10.1093/jac/dkx349>.

(26) Markwart, R.; Willrich, N.; Eckmanns, T.; Werner, G.; Ayobami, O. Low Proportion of Linezolid and Daptomycin Resistance Among Bloodborne Vancomycin-Resistant *Enterococcus Faecium* and Meticillin-Resistant *Staphylococcus Aureus* Infections in Europe. *Frontiers in Microbiology* **2021**, *12*, 1379. <https://doi.org/10.3389/fmicb.2021.664199>.

(27) Tedesco, K. L.; Rybak, M. J. Daptomycin. *Pharmacotherapy: The Journal of Human Pharmacology and Drug Therapy* **2004**, *24* (1), 41–57. <https://doi.org/10.1592/phco.24.1.41.34802>.

(28) Oleson, F. B.; Berman, C. L.; Kirkpatrick, J. B.; Regan, K. S.; Lai, J. J.; Tally, F. P. Once-Daily Dosing in Dogs Optimizes Daptomycin Safety. *Antimicrob Agents Chemother* **2000**, *44* (11), 2948–2953. <https://doi.org/10.1128/AAC.44.11.2948-2953.2000>.

(29) Eisenstein, B. I.; Oleson, F. B., Jr; Baltz, R. H. Daptomycin: From the Mountain to the Clinic, with Essential Help from Francis Tally, MD. *Clinical Infectious Diseases* **2010**, *50* (Supplement\_1), S10–S15. <https://doi.org/10.1086/647938>.

(30) Gray, D. A.; Wenzel, M. More Than a Pore: A Current Perspective on the In Vivo Mode of Action of the Lipopeptide Antibiotic Daptomycin. *Antibiotics* **2020**, *9* (1), 17. <https://doi.org/10.3390/antibiotics9010017>.

(31) Debono, M.; Barnhart, M.; Carrell, C. B.; Hoffmann, J. A.; Occolowitz, J. L.; Abbott, B. J.; Fukuda, D. S.; Hamill, R. L.; Biemann, K.; Herlihy, W. C. A21978C, A COMPLEX OF NEW ACIDIC PEPTIDE ANTIBIOTICS: ISOLATION, CHEMISTRY, AND MASS SPECTRAL STRUCTURE ELUCIDATION. *J. Antibiot.* **1987**, *40* (6), 761–777. <https://doi.org/10.7164/antibiotics.40.761>.

(32) Muraih, J. K.; Harris, J.; Taylor, S. D.; Palmer, M. Characterization of Daptomycin Oligomerization with Perylene Excimer Fluorescence: Stoichiometric Binding of Phosphatidylglycerol Triggers Oligomer Formation. *Biochimica et Biophysica Acta (BBA) - Biomembranes* **2012**, *1818* (3), 673–678. <https://doi.org/10.1016/j.bbamem.2011.10.027>.

(33) Ho, S. W.; Jung, D.; Calhoun, J. R.; Lear, J. D.; Okon, M.; Scott, W. R. P.; Hancock, R. E. W.; Straus, S. K. Effect of Divalent Cations on the Structure of the Antibiotic Daptomycin. *Eur Biophys J* **2008**, *37* (4), 421–433. <https://doi.org/10.1007/s00249-007-0227-2>.

(34) Hobbs, J. K.; Miller, K.; O'Neill, A. J.; Chopra, I. Consequences of Daptomycin-Mediated Membrane Damage in *Staphylococcus Aureus*. *Journal of Antimicrobial Chemotherapy* **2008**, *62* (5), 1003–1008. <https://doi.org/10.1093/jac/dkn321>.

(35) Jung, D.; Rozek, A.; Okon, M.; Hancock, R. E. W. Structural Transitions as Determinants of the Action of the Calcium-Dependent Antibiotic Daptomycin. *Chemistry & Biology* **2004**, *11* (7), 949–957. <https://doi.org/10.1016/j.chembiol.2004.04.020>.

(36) Tran, T. T.; Munita, J. M.; Arias, C. A. Mechanisms of Drug Resistance: Daptomycin Resistance. *Ann N Y Acad Sci* **2015**, *1354*, 32–53. <https://doi.org/10.1111/nyas.12948>.

(37) Pogliano, J.; Pogliano, N.; Silverman, J. A. Daptomycin-Mediated Reorganization of Membrane Architecture Causes Mislocalization of Essential Cell Division Proteins. *Journal of Bacteriology* **2012**, *194* (17), 4494–4504. <https://doi.org/10.1128/JB.00011-12>.

(38) Chen, Y.-F.; Sun, T.-L.; Sun, Y.; Huang, H. W. Interaction of Daptomycin with Lipid Bilayers: A Lipid Extracting Effect. *Biochemistry* **2014**, *53* (33), 5384–5392. <https://doi.org/10.1021/bi500779g>.

(39) Müller, A.; Wenzel, M.; Strahl, H.; Grein, F.; Saaki, T. N. V.; Kohl, B.; Siersma, T.; Bandow, J. E.; Sahl, H.-G.; Schneider, T.; Hamoen, L. W. Daptomycin Inhibits Cell Envelope Synthesis by Interfering with Fluid Membrane Microdomains. *PNAS* **2016**, *113* (45), E7077–E7086. <https://doi.org/10.1073/pnas.1611173113>.

(40) Grein, F.; Müller, A.; Scherer, K. M.; Liu, X.; Ludwig, K. C.; Klöckner, A.; Strach, M.; Sahl, H.-G.; Kubitscheck, U.; Schneider, T. Ca<sup>2+</sup>-Daptomycin Targets Cell Wall Biosynthesis by Forming a Tripartite Complex with Undecaprenyl-Coupled Intermediates and Membrane Lipids. *Nat Commun* **2020**, *11* (1), 1455. <https://doi.org/10.1038/s41467-020-15257-1>.

(41) Sandoval-Calderón, M.; Nguyen, D. D.; Kapono, C. A.; Herron, P.; Dorrestein, P. C.; Sohlenkamp, C. Plasticity of Streptomyces Coelicolor Membrane Composition Under

Different Growth Conditions and During Development. *Frontiers in Microbiology* **2015**, *6*, 1465. <https://doi.org/10.3389/fmicb.2015.01465>.

(42) Randall, C. P.; Mariner, K. R.; Chopra, I.; O'Neill, A. J. The Target of Daptomycin Is Absent from *Escherichia Coli* and Other Gram-Negative Pathogens. *Antimicrobial Agents and Chemotherapy* **2012**.

(43) Silverman, J. A.; Mortin, L. I.; VanPraagh, A. D. G.; Li, T.; Alder, J. Inhibition of Daptomycin by Pulmonary Surfactant: In Vitro Modeling and Clinical Impact. *The Journal of Infectious Diseases* **2005**, *191* (12), 2149–2152. <https://doi.org/10.1086/430352>.

(44) Miller, W. R.; Bayer, A. S.; Arias, C. A. Mechanism of Action and Resistance to Daptomycin in *Staphylococcus Aureus* and *Enterococci*. *Cold Spring Harb Perspect Med* **2016**, *6* (11), a026997. <https://doi.org/10.1101/cshperspect.a026997>.

(45) Bender, J. K.; Cattoir, V.; Hegstad, K.; Sadowy, E.; Coque, T. M.; Westh, H.; Hammerum, A. M.; Schaffer, K.; Burns, K.; Murchan, S.; Novais, C.; Freitas, A. R.; Peixe, L.; Del Grosso, M.; Pantosti, A.; Werner, G. Update on Prevalence and Mechanisms of Resistance to Linezolid, Tigecycline and Daptomycin in Enterococci in Europe: Towards a Common Nomenclature. *Drug Resistance Updates* **2018**, *40*, 25–39. <https://doi.org/10.1016/j.drup.2018.10.002>.

(46) Mangili, A.; Bica, I.; Snydman, D. R.; Hamer, D. H. Daptomycin-Resistant, Methicillin-Resistant *Staphylococcus Aureus* Bacteremia. *Clinical Infectious Diseases* **2005**, *40* (7), 1058–1060. <https://doi.org/10.1086/428616>.

(47) Lellek, H.; Franke, G. C.; Ruckert, C.; Wolters, M.; Wolschke, C.; Christner, M.; Büttner, H.; Alawi, M.; Kröger, N.; Rohde, H. Emergence of Daptomycin Non-Susceptibility in Colonizing Vancomycin-Resistant *Enterococcus Faecium* Isolates during Daptomycin Therapy. *International Journal of Medical Microbiology* **2015**, *305* (8), 902–909. <https://doi.org/10.1016/j.ijmm.2015.09.005>.

(48) Munoz-Price, L. S.; Lolans, K.; Quinn, J. P. Emergence of Resistance to Daptomycin during Treatment of Vancomycin-Resistant *Enterococcus Faecalis* Infection. *Clinical Infectious Diseases* **2005**, *41* (4), 565–566. <https://doi.org/10.1086/432121>.

(49) Green, M. R.; Anasetti, C.; Sandin, R. L.; Rolfe, N. E.; Greene, J. N. Development of Daptomycin Resistance in a Bone Marrow Transplant Patient with Vancomycin-Resistant *Enterococcus Durans*. *J Oncol Pharm Pract* **2006**, *12* (3), 179–181. <https://doi.org/10.1177/1078155206069165>.

(50) EM100 Connect - CLSI M100 ED31:2021 <http://em100.edaptivedocs.net/GetDoc.aspx?doc=CLSI%20M100%20ED31:2021&sbsok=CLSI%20M100%20ED31:2021%20SECTION%20CLSI%20BREAKPOINT%20ADDITIONS/REVISIONS%20SINCE%20202010&format=HTML&hl=daptomycin> (accessed 2021-11-24).

(51) EUCAST: Clinical breakpoints and dosing of antibiotics [https://eucast.org/clinical\\_breakpoints/](https://eucast.org/clinical_breakpoints/) (accessed 2021-11-24).

(52) van Hal, S. J.; Paterson, D. L.; Gosbell, I. B. Emergence of Daptomycin Resistance Following Vancomycin-Unresponsive *Staphylococcus Aureus* Bacteraemia in a Daptomycin-Naïve Patient—a Review of the Literature. *Eur J Clin Microbiol Infect Dis* **2011**, *30* (5), 603–610. <https://doi.org/10.1007/s10096-010-1128-3>.

(53) Kaatz, G. W.; Lundstrom, T. S.; Seo, S. M. Mechanisms of Daptomycin Resistance in *Staphylococcus Aureus*. *International Journal of Antimicrobial Agents* **2006**, *28* (4), 280–287. <https://doi.org/10.1016/j.ijantimicag.2006.05.030>.

(54) Arias, C. A.; Panesso, D.; McGrath, D. M.; Qin, X.; Mojica, M. F.; Miller, C.; Diaz, L.; Tran, T. T.; Rincon, S.; Barbu, E. M.; Reyes, J.; Roh, J. H.; Lobos, E.; Sodergren, E.; Pasqualini, R.; Arap, W.; Quinn, J. P.; Shamoo, Y.; Murray, B. E.; Weinstock, G. M.

Genetic Basis for In Vivo Daptomycin Resistance in Enterococci. *New England Journal of Medicine* **2011**, 365 (10), 892–900. <https://doi.org/10.1056/NEJMoa1011138>.

(55) Brötz-Oesterhelt, H.; Brunner, N. A. How Many Modes of Action Should an Antibiotic Have? *Current Opinion in Pharmacology* **2008**, 8 (5), 564–573. <https://doi.org/10.1016/j.coph.2008.06.008>.

(56) Umstätter, F.; Domhan, C.; Hertlein, T.; Ohlsen, K.; Mühlberg, E.; Kleist, C.; Zimmermann, S.; Beijer, B.; Klika, K. D.; Haberkorn, U.; Mier, W.; Uhl, P. Vancomycin Resistance Is Overcome by Conjugation of Polycationic Peptides. *Angewandte Chemie International Edition* **2020**, 59 (23), 8823–8827. <https://doi.org/10.1002/anie.202002727>.

(57) Virta, P.; Koch, A.; Roslund, M. U.; Mattjus, P.; Kleinpeter, E.; Kronberg, L.; Sjöholm, R.; Klika, K. D. Synthesis, Characterisation and Theoretical Calculations of 2,6-Diaminopurine Etheno Derivatives. *Org. Biomol. Chem.* **2005**, 3 (16), 2924–2929. <https://doi.org/10.1039/B505508C>.

(58) Ball, L.-J.; Goult, C. M.; Donarski, J. A.; Micklefield, J.; Ramesh, V. NMR Structure Determination and Calcium Binding Effects of Lipopeptide Antibiotic Daptomycin. *Org. Biomol. Chem.* **2004**, 2 (13), 1872–1878. <https://doi.org/10.1039/B402722A>.

(59) Müller, A.; Grein, F.; Otto, A.; Gries, K.; Orlov, D.; Zarubaev, V.; Girard, M.; Sher, X.; Shamova, O.; Roemer, T.; François, P.; Becher, D.; Schneider, T.; Sahl, H.-G. Differential Daptomycin Resistance Development in *Staphylococcus aureus* Strains with Active and Mutated Gra Regulatory Systems. *International Journal of Medical Microbiology* **2018**, 308 (3), 335–348. <https://doi.org/10.1016/j.ijmm.2017.12.002>.

(60) Directive 2010/63/EU of the European Parliament and of the Council of 22 September 2010 on the Protection of Animals Used for Scientific PurposesText with EEA Relevance. 47.

(61) Alves, F. C. B.; Albano, M.; Andrade, B. F. M. T.; Chechi, J. L.; Pereira, A. F. M.; Furlanetto, A.; Rall, V. L. M.; Fernandes, A. A. H.; dos Santos, L. D.; Barbosa, L. N.; Fernandes Junior, A. Comparative Proteomics of Methicillin-Resistant *Staphylococcus aureus* Subjected to Synergistic Effects of the Lantibiotic Nisin and Oxacillin. *Microbial Drug Resistance* **2020**, 26 (3), 179–189. <https://doi.org/10.1089/mdr.2019.0038>.

(62) Silverman, J. A.; Perlmutter, N. G.; Shapiro, H. M. Correlation of Daptomycin Bactericidal Activity and Membrane Depolarization in *Staphylococcus aureus*. *Antimicrobial Agents and Chemotherapy* **2003**, 47 (8), 2538–2544. <https://doi.org/10.1128/AAC.47.8.2538-2544.2003>.

(63) Rodvold, K. A.; McConeghy, K. W. Methicillin-Resistant *Staphylococcus aureus* Therapy: Past, Present, and Future. *Clinical Infectious Diseases* **2014**, 58 (suppl\_1), S20–S27. <https://doi.org/10.1093/cid/cit614>.

(64) Peleg, A. Y.; Miyakis, S.; Ward, D. V.; Earl, A. M.; Rubio, A.; Cameron, D. R.; Pillai, S.; Jr, R. C. M.; Eliopoulos, G. M. Whole Genome Characterization of the Mechanisms of Daptomycin Resistance in Clinical and Laboratory Derived Isolates of *Staphylococcus aureus*. *PLOS ONE* **2012**, 7 (1), e28316. <https://doi.org/10.1371/journal.pone.0028316>.

(65) In Vitro Cross-Resistance to Daptomycin and Host Defense Cationic Antimicrobial Peptides in Clinical Methicillin-Resistant *Staphylococcus aureus* Isolates <https://www.ncbi.nlm.nih.gov/pmc/articles/PMC3165344/> (accessed 2022 -03 -14).

(66) Mishra, N. N.; Bayer, A. S. Correlation of Cell Membrane Lipid Profiles with Daptomycin Resistance in Methicillin-Resistant *Staphylococcus aureus*. *Antimicrob Agents Chemother* **2013**, 57 (2), 1082–1085. <https://doi.org/10.1128/AAC.02182-12>.

(67) Cotroneo, N.; Harris, R.; Perlmutter, N.; Beveridge, T.; Silverman, J. A. Daptomycin Exerts Bactericidal Activity without Lysis of *Staphylococcus aureus*. *Antimicrob Agents Chemother* **2008**, 52 (6), 2223–2225. <https://doi.org/10.1128/AAC.01410-07>.

## Chapter 4

### 4 General Discussion and Conclusion

The major aim of the thesis was the characterization of two antibiotic classes with the potential to overcome antimicrobial resistance employing different strategies. The first approach discussed in **chapter 1** is natural product-guided, where elansolid A2 isolated from the gliding bacterium *Chitinophaga sancti* was characterized for its antibacterial activity, time-kill kinetics, cross resistance, as well as the mode of resistance and mode of action. In line with the general notion that natural products often exhibit innovative modes of action, elansolid A2 was found to inhibit protein synthesis by targeting a presumably unique site on the bacterial ribosome. The second approach discussed in **chapter 2** is based on chemically modifying the clinically used antibiotic daptomycin through conjugation with a polycationic peptide moiety generating a resistance-breaking antibiotic. The antibacterial activity was studied, killing kinetics were investigated, and the mode of action of the frontrunner conjugate DAP-R6 was compared to that of daptomycin. Indeed, there is evidence for DAP-R6 overcoming daptomycin resistance in *Staphylococcus aureus*.

#### 4.1 Natural product antibiotics addressing unique targets

Microbial natural products are the origin of most classes of antibiotics in clinical use, and they continue to be a rich source of unique and complex structural scaffolds that act on new targets and can overcome the resistance<sup>1</sup>. Owing to their fundamental role, bacterial ribosome and protein synthesis represent an attractive target for the discovery and development of novel antibacterial agents<sup>2</sup>. The bacterial ribosome is composed of 16S, 23S and 5S ribosomal RNAs (rRNAs) dominating the main functional sites and around 54 ribosomal proteins<sup>3</sup>. Few common sites are targeted by ribosomal inhibitors including the path of the mRNA and tRNAs on the

30S subunit or at or near the peptidyl-transferase center (PTC), that catalyzes peptide bond formation<sup>2,3</sup>.

Bacteria have developed several mechanisms to counteract the antibiotics targeting the ribosome such as decreased permeability of drugs, or by active efflux, drug modification or degradation, increased expression of the target or of a mimic of the target that confiscates the drug, and factor-assisted protection of the drug target to dislocate the drug from its binding site<sup>4-8</sup>. Target mutation or modification of rRNA and/or ribosomal proteins is the most common resistance mechanism for ribosomal inhibitors, and includes for example, mutation of ribosomal proteins L3, L11 and L22 that confers resistance to tiamulin, thiostrepton-like antibiotics and macrolides respectively<sup>9-11</sup>. Linezolid resistance in *S. aureus* is due to the combination of both rRNA C2534U mutation and ribosomal protein mutations in L3 and L4<sup>12</sup>. In elansolids mutants, the only mutations explored by whole genome sequencing involve S7 (*rpsG*) and S11 (*rpsK*) ribosomal proteins, so we speculate that they are the direct target of elansolid A2. This is to be further confirmed by X-ray crystallography and Cryo-electron microscopy (Cryo-EM) to explain how elansolids bind to the ribosome and inhibit protein synthesis. This resistance involves a unique protein-protein interaction site that is not reported to be the target of any drug, which opens the door to further study PPIs in ribosomes as possible and unique targets for antimicrobial drugs.

Elansolid A2 can become an important antibiotic in the protein synthesis inhibitors arsenal, due to its rapid bactericidal activity against multidrug-resistant *S. aureus* pathogens, and its unique 30S ribosomal target. The S7-S11 interface represents an important site that connect the head of the 30 S subunit to the platform and is involved in the formation of the exit channel through which passes the messenger RNA. However, this site was never reported in literature as a target for antibacterial agents. Understanding the specific interaction of elansolid with S7-S11 by structure-based approaches such as crystal structure analysis and Cryo-EM imaging might fuel

a chemistry discovery program making use of the structural information regarding this important, un- or under-exploited site, that might not be recognized by existing resistance mechanisms. Furthermore, this study shows that natural products can offer a novel binding site and new modes of action that can serve as starting points for antibiotic drug development. The interaction between S7 and S11 proteins is not the only characterized protein-protein interaction (PPI) that display ribosomal functionality. Ribosomal proteins S4 and S5 have been shown to participate in the decoding and assembly on the ribosome and the interaction with antibiotics, such as spectinomycin<sup>13,14</sup>. Thus, beside rRNA, PPI interactions play an important part in the dynamics of the ribosome, and present promising un- or under-exploited targets for the development of ribosomal inhibitors. Several compounds that target novel sites on the 30S subunit have been identified, such as Furvina<sup>®</sup> that is shown to inhibits protein synthesis by blocking translation initiation, through binding to the 30S ribosomal subunit and inhibiting P-site decoding<sup>15</sup>. In addition to Cryo-EM imaging and co-crystallization of elansolids with 70S ribosomes, further approaches will focus on co-crystallization of elansolid A2 with S7 and/or S11 and studying the neutralization effect of elansolid on the binding of the two ribosomal proteins by biophysical assays.

#### 4.2 Modification of existing antibiotic classes to overcome AMR

The outer membrane (OM) permeability barrier of Gram-negative pathogens is a vital resistance factor and hinders the penetration of antibiotics<sup>16</sup>. Several approaches to circumvent this permeability mediated resistance have been developed. These strategies include either the conjugation of drugs with components to destabilize the bacterial OM such as polycationic peptides, or to make use of the bacterial nutrient uptake by a Trojan Horse strategy.

Conjugation of existing antibiotics to either a peptide, antibody, or iron-chelating agent, proved to be a successful, cost-efficient, and fast strategy to enhance ADME (adsorption, distribution, metabolism, excretion) properties and reduce toxicity of antibiotics. Furthermore, such modifications can help to overcome resistance and address difficult-to-treat bacterial infections, such as intracellular and persistent infections<sup>17,18</sup>. Among the successful examples nature has developed are sideromycins, which are antibiotics covalently linked to the iron-chelating molecules, siderophores<sup>19</sup>. Iron is essential for bacteria as a cofactor in many metabolic processes, but due to its low solubility in aerobic environments, many bacteria produce and excrete low-molecular-weight (500–1500 D) siderophores into their environment to chelate iron, and then recognize and actively import them<sup>20,21</sup>. Bacteria have evolved uptake systems to allow them to utilize siderophores made by other bacteria (xenosiderophores)<sup>22,23</sup>. To counter this iron ‘thievery’, some bacteria developed sideromycins, known as ‘Trojan horse’, which are conjugates of a siderophore and a lethal component<sup>20</sup>. Only few naturally occurring sideromycins have been discovered, including albomycin, a derivative of ferrichrome with a bound thioribosyl-pyrimidine moiety and Salmycin, a ferrioxamine derivative with a bound aminodisaccharide<sup>24</sup>. A wide spectrum of siderophore–antibiotic conjugates have been chemically synthesized, among which is the recently FDA-approved drug cefiderocol. The latter is a novel siderophore-cephalosporin conjugate antibiotic that exhibited structural stability against hydrolysis by serine- and metallo-β-lactamases, including clinically relevant

carbapenemases, and is used for the treatment of cUTIs, including kidney infections caused by Gram-negative pathogens<sup>25,26</sup>. However, recent studies have reported the development of resistance to cefiderocol in *P. aeruginosa*, *E. coli*, *K. pneumoniae*, *E. cloacae* and *A. baumannii*. The resistance mechanisms include alterations of the iron uptake pathways (*P. aeruginosa*), production of metallo-β-lactamases (*E. coli*), production of β-lactamases (*K. pneumoniae* and *E. cloacae*) and reduced expression of the siderophore receptor and mutations in Penicillin Binding Protein (*A. baumannii*)<sup>27-30</sup>. It is useful to note that no acquired β-lactamases were found in *P. aeruginosa* and *A. baumannii* strains<sup>27,28</sup>. Since the import of antibiotic-siderophore depends on the bacterial membrane receptor proteins, it is expected that the development of resistance in clinical isolates would emerge rapidly<sup>28</sup>. In comparison, enhancing antibiotic activity by conjugation of antibiotics to elements such as peptides such as our lead daptomycin conjugate DAP-R6 that bind with adapted membrane composition should show a decreased propensity to resistance development as further alterations of the membrane composition are unlikely to occur as this would pose a significant burden to the bacteria. In a preliminary study done with resistance development with DAP-R6 mutants, we were not able to generate mutants after several passages, but this must be further assessed. Future steps will include generation of resistant mutants to DAP-R6 to investigate the genetic, transcriptomic and proteomic changes, which will allow us to further study and understand the mechanism behind the action of the promising conjugate.

#### 4.3 Conclusion

The rapid rise in infections caused by bacteria that are resistant to almost all available antibiotics is alarming and necessitates global strategic plans to tackle it. Natural products represent a rich source for the discovery and development of new chemical compounds with a unique mechanism of action to fight pathogenic bacteria and to overcome severe and hard-to-treat infections. The search for new chemical matter with promising antibacterial efficiency is supported by advances in the field including new tools and techniques such as, high-throughput screening (HTS) of compound libraries, fragment-based design, next-generation sequencing (NGS) technologies and genome mining, and CRISPR/Cas9-mediated genome editing<sup>31,32</sup>. The conventional antibiotic discovery and development is time-consuming, costly and has led to a very small pipeline of truly new therapeutic options. For this reason, a number of strategies and alternatives to antibiotics have been developed, including conjugation of already existing antibiotics, combination therapy, bacteriophage therapy, vaccines, antibodies, probiotics, lysins, immune stimulation and suppression, host defense peptides and innate defense peptides, toxin sequestration using liposomes, and alphamers<sup>33</sup>.

There is an indispensable need for the development of antimicrobials that directly affect pathogens and interfere with key components of cell processes and functions, however, additional alternative approaches to clear bacterial infections and overcome AMR are also urgently needed. Several novel strategies including host-directed therapy (HDT) and anti-virulence therapies have been investigated. HDT interferes with host mechanisms that are required by the pathogen to replicate and persist, boost the immune responses against it and further reduce inflammation at the site of infection<sup>34</sup>. Among the promising HDT examples are those addressed for treatment of intracellular *M. tuberculosis* (Mtb)<sup>35</sup>. Mtb replicates within early phagosomes, persists in macrophages, and escapes the host immune responses. Several HDTs have been directed at each stage of the macrophage life cycle of Mtb, and include trigger of autophagy, activation of cytokines, promote phagosome maturation, induce antimicrobial

peptides, and inhibit lipid body formation<sup>36-38</sup>. Anti-virulence therapies interfere with the ability of the bacteria to activate their virulence traits to establish an infection, preventing them from colonizing the host<sup>39</sup>. Additionally, these anti-virulence drugs could be used in combination with antimicrobials. A number of anti-virulence therapies has been developed that target adhesins and biofilms, toxins, and specialized secretion systems<sup>39</sup>. The advantages of such strategies present are that there is weaker pressure for the development of resistance, and since they target the immune system or virulence pathways that exist exclusively in pathogens, they are less likely to have severe side effects.

The rapidly evolving crisis of bacterial resistance requires a great awareness and fast response plans to tackle this alarming health hazard. Promising strategies to combat resistance should focus on preventing infections from occurring in the first place, discovering new tactics to directly attack pathogens without developing resistance, or to target host-pathogen interactions without directly affecting the pathogen, to slow the spread of resistance to prolong the effectiveness of last resort antibiotics, and to encourage investments in the field of drug discovery and development. The two approaches presented in this work, highlight important aspects to combat the alarming spread of bacterial resistance. Elansolids proved that natural products are an important and rich niche for the development of novel antibiotics with new mode of action, and they might offer a promising platform for drug development and design programs. Conjugation of already existing antibiotics such as daptomycin to polycationic peptides offer a faster and cheaper approach to overcome resistance and enhance the activity and delivery of the drugs and might bypass the potential side-effects and toxicity of the antibiotic.

#### 4.4 References

- (1) Genilloud, O. Natural Products Discovery and Potential for New Antibiotics. *Current Opinion in Microbiology* **2019**, *51*, 81–87. <https://doi.org/10.1016/j.mib.2019.10.012>.
- (2) Hermann, T. Drugs Targeting the Ribosome. *Current Opinion in Structural Biology* **2005**, *15* (3), 355–366. <https://doi.org/10.1016/j.sbi.2005.05.001>.
- (3) Wilson, D. N. Ribosome-Targeting Antibiotics and Mechanisms of Bacterial Resistance. *Nat Rev Microbiol* **2014**, *12* (1), 35–48. <https://doi.org/10.1038/nrmicro3155>.
- (4) Wright, G. D. Bacterial Resistance to Antibiotics: Enzymatic Degradation and Modification. *Advanced Drug Delivery Reviews* **2005**, *57* (10), 1451–1470. <https://doi.org/10.1016/j.addr.2005.04.002>.
- (5) Ramirez, M. S.; Tolmasky, M. E. Aminoglycoside Modifying Enzymes. *Drug Resistance Updates* **2010**, *13* (6), 151–171. <https://doi.org/10.1016/j.drup.2010.08.003>.
- (6) The selection in vivo and characterization of an RNA recognition motif for spectinomycin - ScienceDirect <https://www.sciencedirect.com/science/article/abs/pii/S0968089697000606> (accessed 2022-03-14).
- (7) Connell, S. R.; Tracz, D. M.; Nierhaus, K. H.; Taylor, D. E. Ribosomal Protection Proteins and Their Mechanism of Tetracycline Resistance. *Antimicrob Agents Chemother* **2003**, *47* (12), 3675–3681. <https://doi.org/10.1128/AAC.47.12.3675-3681.2003>.
- (8) Dönhöfer, A.; Franckenberg, S.; Wickles, S.; Berninghausen, O.; Beckmann, R.; Wilson, D. N. Structural Basis for TetM-Mediated Tetracycline Resistance. *Proceedings of the National Academy of Sciences* **2012**, *109* (42), 16900–16905. <https://doi.org/10.1073/pnas.1208037109>.
- (9) Tu, D.; Blaha, G.; Moore, P. B.; Steitz, T. A. Structures of MLSBK Antibiotics Bound to Mutated Large Ribosomal Subunits Provide a Structural Explanation for Resistance. *Cell* **2005**, *121* (2), 257–270. <https://doi.org/10.1016/j.cell.2005.02.005>.
- (10) Davidovich, C.; Bashan, A.; Auerbach-Nevo, T.; Yaggie, R. D.; Gontarek, R. R.; Yonath, A. Induced-Fit Tightens Pleuromutilins Binding to Ribosomes and Remote Interactions Enable Their Selectivity. *Proceedings of the National Academy of Sciences* **2007**, *104* (11), 4291–4296. <https://doi.org/10.1073/pnas.0700041104>.
- (11) Translational Regulation via L11: Molecular Switches on the Ribosome Turned On and Off by Thiomodulin and Micrococcin - ScienceDirect <https://www.sciencedirect.com/science/article/pii/S1097276508000440> (accessed 2022-03-14).
- (12) Inactivation of the Indigenous Methyltransferase RlmN in *Staphylococcus aureus* Increases Linezolid Resistance | Antimicrobial Agents and Chemotherapy <https://journals.asm.org/doi/full/10.1128/AAC.00183-11> (accessed 2022-03-14).
- (13) Agarwal, D.; Kamath, D.; Gregory, S. T.; O'Connor, M. Modulation of Decoding Fidelity by Ribosomal Proteins S4 and S5. *J Bacteriol* **2015**, *197* (6), 1017–1025. <https://doi.org/10.1128/JB.02485-14>.
- (14) Ribosomal Protein Conferring Sensitivity to the Antibiotic Spectinomycin in *Escherichia coli* [https://www.science.org/doi/abs/10.1126/science.165.3888.85?casa\\_token=UQCW4nwTuScAAAAA:OLGWEGYD4ftS9MJIQa1um0WmBjlpztK0FceqUhu8ztEL-C1AM9-7UpyiLe1Ti8lh1AIdsXViR14LImo](https://www.science.org/doi/abs/10.1126/science.165.3888.85?casa_token=UQCW4nwTuScAAAAA:OLGWEGYD4ftS9MJIQa1um0WmBjlpztK0FceqUhu8ztEL-C1AM9-7UpyiLe1Ti8lh1AIdsXViR14LImo) (accessed 2022-03-14).
- (15) Fabbretti, A.; Brandi, L.; Petrelli, D.; Pon, C. L.; Castañedo, N. R.; Medina, R.; Gualerzi, C. O. The Antibiotic Furvina® Targets the P-Site of 30S Ribosomal Subunits and Inhibits

Translation Initiation Displaying Start Codon Bias. *Nucleic Acids Research* **2012**, *40* (20), 10366–10374. <https://doi.org/10.1093/nar/gks822>.

(16) Möllmann, U.; Heinisch, L.; Bauernfeind, A.; Köhler, T.; Ankel-Fuchs, D. Siderophores as Drug Delivery Agents: Application of the “Trojan Horse” Strategy. *Biometals* **2009**, *22* (4), 615–624. <https://doi.org/10.1007/s10534-009-9219-2>.

(17) David, A. A.; Park, S. E.; Parang, K.; Tiwari, R. K. Antibiotics-Peptide Conjugates Against Multidrug-Resistant Bacterial Pathogens. *Current Topics in Medicinal Chemistry* **2018**, *18* (22), 1926–1936. <https://doi.org/10.2174/1568026619666181129141524>.

(18) Mariathasan, S.; Tan, M.-W. Antibody–Antibiotic Conjugates: A Novel Therapeutic Platform against Bacterial Infections. *Trends in Molecular Medicine* **2017**, *23* (2), 135–149. <https://doi.org/10.1016/j.molmed.2016.12.008>.

(19) Negash, K. H.; Norris, J. K. S.; Hodgkinson, J. T. Siderophore–Antibiotic Conjugate Design: New Drugs for Bad Bugs? *Molecules* **2019**, *24* (18), 3314. <https://doi.org/10.3390/molecules24183314>.

(20) Miller, M. J.; Liu, R. Design and Syntheses of New Antibiotics Inspired by Nature’s Quest for Iron in an Oxidative Climate. *Acc. Chem. Res.* **2021**, *54* (7), 1646–1661. <https://doi.org/10.1021/acs.accounts.1c00004>.

(21) C. Hider, R.; Kong, X. Chemistry and Biology of Siderophores. *Natural Product Reports* **2010**, *27* (5), 637–657. <https://doi.org/10.1039/B906679A>.

(22) Species selectivity of new siderophore-drug conjugates that use specific iron uptake for entry into bacteria | Antimicrobial Agents and Chemotherapy <https://journals.asm.org/doi/10.1128/AAC.40.11.2610> (accessed 2022-01-24).

(23) Miethke, M.; Kraushaar, T.; Marahiel, M. A. Uptake of Xenosiderophores in *Bacillus Subtilis* Occurs with High Affinity and Enhances the Folding Stabilities of Substrate Binding Proteins. *FEBS Letters* **2013**, *587* (2), 206–213. <https://doi.org/10.1016/j.febslet.2012.11.027>.

(24) Braun, V.; Pramanik, A.; Gwinner, T.; Köberle, M.; Bohn, E. Sideromycins: Tools and Antibiotics. *Biometals* **2009**, *22* (1), 3–13. <https://doi.org/10.1007/s10534-008-9199-7>.

(25) McCarthy, M. W. Cefiderocol to Treat Complicated Urinary Tract Infection. *Drugs Today (Barc)* **2020**, *56* (3), 177–184. <https://doi.org/10.1358/dot.2020.56.3.3118466>.

(26) Sato, T.; Yamawaki, K. Cefiderocol: Discovery, Chemistry, and In Vivo Profiles of a Novel Siderophore Cephalosporin. *Clinical Infectious Diseases* **2019**, *69* (Supplement\_7), S538–S543. <https://doi.org/10.1093/cid/ciz826>.

(27) Streling, A. P.; Al Obaidi, M. M.; Lainhart, W. D.; Zangeneh, T.; Khan, A.; Dinh, A. Q.; Hanson, B.; Arias, C. A.; Miller, W. R. Evolution of Cefiderocol Non-Susceptibility in *Pseudomonas Aeruginosa* in a Patient Without Previous Exposure to the Antibiotic. *Clinical Infectious Diseases* **2021**, *73* (11), e4472–e4474. <https://doi.org/10.1093/cid/ciaa1909>.

(28) Malik, S.; Kaminski, M.; Landman, D.; Quale, J. Cefiderocol Resistance in *Acinetobacter Baumannii*: Roles of  $\beta$ -Lactamases, Siderophore Receptors, and Penicillin Binding Protein 3. *Antimicrobial Agents and Chemotherapy* **64** (11), e01221-20. <https://doi.org/10.1128/AAC.01221-20>.

(29) Simner, P. J.; Mostafa, H. H.; Bergman, Y.; Ante, M.; Tekle, T.; Adebayo, A.; Beiskin, S.; Dzintars, K.; Tamma, P. D. Progressive Development of Cefiderocol Resistance in *Escherichia Coli* During Therapy Is Associated With an Increase in BlaNDM-5 Copy Number and Gene Expression. *Clinical Infectious Diseases* **2021**, ciab888. <https://doi.org/10.1093/cid/ciab888>.

(30) Simner, P. J.; Beiskin, S.; Bergman, Y.; Ante, M.; Posch, A. E.; Tamma, P. D. Defining Baseline Mechanisms of Cefiderocol Resistance in the Enterobacteriales. *Microbial Drug Resistance* **2022**, *28* (2), 161–170. <https://doi.org/10.1089/mdr.2021.0095>.

(31) Hutchings, M. I.; Truman, A. W.; Wilkinson, B. Antibiotics: Past, Present and Future. *Current Opinion in Microbiology* **2019**, *51*, 72–80. <https://doi.org/10.1016/j.mib.2019.10.008>.

(32) Discovery of microbial natural products by activation of silent biosynthetic gene clusters | Nature Reviews Microbiology <https://www.nature.com/articles/nrmicro3496> (accessed 2022-01-25).

(33) Czaplewski, L.; Bax, R.; Clokie, M.; Dawson, M.; Fairhead, H.; Fischetti, V. A.; Foster, S.; Gilmore, B. F.; Hancock, R. E. W.; Harper, D.; Henderson, I. R.; Hilpert, K.; Jones, B. V.; Kadioglu, A.; Knowles, D.; Ólafsdóttir, S.; Payne, D.; Projan, S.; Shaunak, S.; Silverman, J.; Thomas, C. M.; Trust, T. J.; Warn, P.; Rex, J. H. Alternatives to Antibiotics—a Pipeline Portfolio Review. *The Lancet Infectious Diseases* **2016**, *16* (2), 239–251. [https://doi.org/10.1016/S1473-3099\(15\)00466-1](https://doi.org/10.1016/S1473-3099(15)00466-1).

(34) Kaufmann, S. H. E.; Dorhoi, A.; Hotchkiss, R. S.; Bartenschlager, R. Host-Directed Therapies for Bacterial and Viral Infections. *Nat Rev Drug Discov* **2018**, *17* (1), 35–56. <https://doi.org/10.1038/nrd.2017.162>.

(35) Lugo-Villarino, G.; Neyrolles, O. Manipulation of the Mononuclear Phagocyte System by Mycobacterium Tuberculosis. *Cold Spring Harb Perspect Med* **2014**, *4* (11), a018549. <https://doi.org/10.1101/cshperspect.a018549>.

(36) Gutierrez, M. G.; Master, S. S.; Singh, S. B.; Taylor, G. A.; Colombo, M. I.; Deretic, V. Autophagy Is a Defense Mechanism Inhibiting BCG and Mycobacterium Tuberculosis Survival in Infected Macrophages. *Cell* **2004**, *119* (6), 753–766. <https://doi.org/10.1016/j.cell.2004.11.038>.

(37) Gurk-Turner, C.; Manitpisitkul, W.; Cooper, M. A Comprehensive Review of Everolimus Clinical Reports: A New Mammalian Target of Rapamycin Inhibitor. *Transplantation* **2012**, *94* (7), 659–668. <https://doi.org/10.1097/TP.0b013e31825b411c>.

(38) Bruns, H.; Stegelmann, F.; Fabri, M.; Döhner, K.; Zandbergen, G. van; Wagner, M.; Skinner, M.; Modlin, R. L.; Stenger, S. Abelson Tyrosine Kinase Controls Phagosomal Acidification Required for Killing of Mycobacterium Tuberculosis in Human Macrophages. *The Journal of Immunology* **2012**, *189* (8), 4069–4078. <https://doi.org/10.4049/jimmunol.1201538>.

(39) Rasko, D. A.; Sperandio, V. Anti-Virulence Strategies to Combat Bacteria-Mediated Disease. *Nat Rev Drug Discov* **2010**, *9* (2), 117–128. <https://doi.org/10.1038/nrd3013>.